STORM SEDIMENTATION ON THE SURF ZONE AND INNER CONTINENTAL SHELF, DUCK, NORTH CAROLINA

by

Rebecca Lenel Beavers

Department of Geology
Duke University

Dissertation submitted in partial fulfillment of
the requirements for the degree of Doctor
of Philosophy in the Department of
Geology in the Graduate School of
Duke University

1999

ABSTRACT

Nearshore storm sedimentation on the surf zone and inner continental shelf has previously been documented by beach profiles and cores, but these methods usually provide only pre- and post-storm measurements. By connecting these discrete measurements with continuous sonar altimetry, seabed elevation changes during storms were used to interpret the stratigraphic signature of modern nearshore storm deposits and assess the seabed elevation variability documented by fairweather profiles.

Time series of seabed elevation and co-located measures of wave and current characteristics at 3 water depths (5.5, 8, and 13 m) were collected offshore of Duck, North Carolina. Detailed analyses of seabed elevation changes were conducted for hurricanes and northeaster storms during 1994-1997. Maximum values of net seabed accretion occurred at locations within the outer surf zone, but maximum values of net seabed erosion occurred at locations offshore of the surf zone. At outer surf zone and inner shelf locations, northeaster storms were more likely to cause net accretion than either no net change or net deposition, but hurricanes were as likely to cause net erosion as net deposition.

For a northeaster storm that occurred during the October 1997 SandyDuck experiment, sonar altimeter measurements of seabed elevation were used to establish the chronology of storm sediments collected with diver-operated boxcores. Downcore depths to basal erosion contacts in post-storm cores corresponded remarkably well with erosion maxima measured by sonar altimeters during storm events. Rapid deposition of sediments

occurred in the few hours preceding and initial 4-20 hours following maximum wave heights, when gradients in wave height, mean currents, and associated bed shear stresses were relatively large. Nearshore storm deposits consisted of up to 20 cm of parallel to sub-parallel laminated sediments, with occasional ripple cross-stratification and lag deposits composed of gravel and shell fragments.

Continuous sonar altimeter measurements during storm events were compared with nearby pre- and post-storm beach profile data. Sonar altimeters at 5.5, 8, and 13 m depths measured a range of seabed elevations of approximately 40 cm. Smaller ranges of seabed elevations were measured by profiles at 5.5 and 8 m depths, because fairweather beach profiles only document net seabed elevation changes resulting from storm events.

ACKNOWLEDGMENTS

To complete this dissertation, I have been assisted by numerous people. Kent Hathaway and the staff at the USACE Field Research Facility in Duck, NC, have shouldered the responsibility for collecting the bipod data since 1994. These long-term data represent a tremendous accomplishment in nearshore science and comprise the backbone of this dissertation. Bill Birkemeier and Kent Hathaway have unfailingly answered questions, critiqued drafts, and offered encouragement with this dissertation. J. Bailey Smith provided my initial instruction on boxcore processing. I thank all participants of the SandyDuck'97 experiment, particularly Dr. Alex Hay, Dr. Dan Hanes, Dr. Steve Elgar, Dr. Edie Gallagher, and Grace Battisto, for providing additional pieces to the puzzle of storm sediment dynamics at Duck.

My dissertation advisor, Dr. Peter Howd, has provided a strong back for pulling cores from the seafloor and wisdom for pulling hesitant thoughts from my brain. Peter gave me the opportunity to explore new ocean 'depths' and supplied examples of excellent field skills and information gathering. I thank my Ph.D. committee members: Drs. Orrin Pilkey, Tom Drake, Peter Haff, and Lincoln Pratson, for introducing me to many nuances of the North Carolina coast and making my first forays into fluid mechanics so much fun that I continue to revisit the sediment-water interface.

Tim Boynton knew when to restrict my activities as a scientific diver and when to allow me the freedom to safely pursue the science I enjoy. Numerous scientific divers, particularly Dr. Rob Thieler, Dr. Tracy Andacht, Carolyn Smyth, Dr. David Brown, and Eddie Roggenstein, volunteered their time, which could have been otherwise focused on

their graduate studies and jobs *or* spent diving in warm, clear waters, to help me collect cores at Duck. Scott Taylor spent endless hours transforming my inconsistent core xrays into photographic images of scientific merit.

The Duke University Marine Laboratory faithfully provided my stipend for 5 years. I thank the US Army Corps of Engineers and the Office of Naval Research for grants to Dr. Howd to fund bipod instrumentation and data analyses. Dr. Ed Thornton graciously provided the current meters initially deployed on the bipods. I received grants from the Geological Society of America, American Association of Petroleum Geologists, Sigma Xi, and the American Academy of Underwater Sciences to support core collection and processing expenses. Additional funds from various sources at Duke University and the Southeastern Section of the Geological Society of America provided conference travel funds to present portions of this research at numerous meetings.

Drs. Bill Fox, Bud Wobus, and Al Curran have encouraged my research and teaching efforts ever since I was an undergraduate at Williams College. Many graduate students, undergraduate students, faculty, staff, and friends have made my work in Durham, NC, Beaufort, NC, Duck, NC, and St. Petersburg, FL enjoyable. The unconditional support of my family, my dog Brandy, and friends, particularly Eddie, Rachel, and Hilary, have made this degree possible.

I dedicate this dissertation to Dr. Elizabeth Stalvey. Thank you for reminding me that anything is possible with enough determination.

TABLE OF CONTENTS

LIST OF FIGURES

LIST OF TABLES

LIST OF ABBREVIATIONS

ADV	Acoustic Doppler Velocimeter
D_c	Closure depth
EST	Eastern Standard Time
FRF	Field Research Facility
h	Local water depth
h_b	Water depth at breaking
h_r	Dimensionless 'depth' relative to surf zone position
H_{mo}	Wave height
H_{rms}	Root-mean-square wave height
K	von Karmon's constant
T_p	Peak spectral wave period
$u_c(z)$	Elevation-dependent mean current velocity
u_{*c}	Shear velocity related to mean current
z	Vertical axis
z_o	Bed roughness
γ	Ratio of rms wave height to local water depth
ρ	Water density
τ_o	Bed shear stress
ϕ	Grain size: $-\log_2$ (grain size in mm)

CHAPTER 1

INTRODUCTION

Ever since geologists realized that migrating bedforms deposit layered sediments like those preserved in rocks, they have attempted to relate the evolution of seabed morphology to internal sedimentary structures and external flow conditions. Along most coastlines, flows near the seabed are greatest during storms. Storm winds generate surface gravity waves that shoal in shallow water depths and undergo a series of nonlinear interactions when they break in the surf zone (Elgar et al., 1990). Within surf zones, the region of active breaking waves, forces that result from the dissipation of breaking waves dominate circulation (Wright et al., 1991). These forces can increase bottom friction and sediment transport (Thornton and Guza, 1983), alter seabed morphology (Hay and Wilson, 1994), and create storm deposits (Smith et al., 1995) where these transported sediments accumulate.

Due to the difficulty of monitoring the evolution of the seabed during storms, laboratory flumes have been the only previous setting where it was feasible to continuously monitor bed configuration and sample shallow stratigraphy created during simulated high-energy events (Arnott and Southard, 1990). This study presents some of the first field results of nearshore cores collected where the seabed elevation and hydrodynamic forcing are continuously measured by instrumentation during storms. The data were collected offshore of the US Army Corps of Engineers Field Research Facility

in Duck, NC from 1994-1997. Continuous measurements of seabed elevation changes were made at 3 locations in 5.5, 8, and 13 m water depth and encompass a wide range of hydrodynamic conditions. Previous deployments on the inner continental shelf and the surf zone only lasted up to a few months (Wright et al., 1994a).

Many scales of morphologic and dynamic integration are required to assess the fate of sediments during storms. In Chapter 2, seabed elevation changes during hurricanes and northeaster storms are evaluated to determine if either type of storm results in identifiable patterns of net erosion or net deposition on the surf zone and inner continental shelf. In Chapter 3, sediments deposited at 3 locations during a northeaster storm are linked (at cm scale) with overlying physical processes. In Chapter 4, 5 months of continuous measurements of seabed elevation changes are compared with less frequent beach profile data to evaluate the aspects of seabed response to storm events captured by beach profile data. The following sections describe the variability in the morphology (geologic setting) and fluid dynamics (waves and mean currents) which exist at Duck, NC.

Geologic Setting

The Field Research Facility (FRF) of the US Army Engineer Waterways Experiment Station is located on the Atlantic Ocean near the middle of Currituck Spit. Currituck Spit forms the northern end of the Outer Banks and extends over 100 km southeast from Cape Henry, Virginia, to Oregon Inlet, North Carolina. Currituck Sound,

the northernmost of a series of extensive shallow sounds behind the Outer Banks, is connected to the Atlantic Ocean at Oregon Inlet.

The Outer Banks form the seaward margin of the Coastal Plain province. West of the sounds, the coastal plain is low-lying and covered by extensive swamps and lakes. The main topographic features are a series of north-south trending terraces which rise in a stepwise manner westward and mark former shorelines corresponding to higher sea level stands during the Pleistocene (Meisburger and Judge, 1989).

The eastern half of the coastal plain is underlain by Quaternary sediments that fill a depositional basin known as the Albemarle Embayment and unconformably overlie late Tertiary sediments (Meisburger and Judge, 1989; Riggs et al., 1995). Superimposed on this regional stratigraphy is an ancient drainage system resulting in series of fluvial valleys filled with younger sediment separated by interfluve areas of older stratigraphic units (Riggs et al., 1995). In northeastern North Carolina, Riggs et al. (1992) documented portions of as many as 18 Quaternary sea-level highstands within 60 m of these Quaternary deposits. Quaternary sea-level fluctuations have produced an extremely complex sediment record reflecting migration of depositional regimes and associated erosional events (Riggs et al., 1992). During lowered sea level of glacial periods, fluvial sediments were distributed across the continental shelf, and evidence of extensive fluvial channeling remains (Rice et al., 1998). Fluvial sand and gravel deposits remain in cored sections of channel deposits (Riggs et al., 1992), and fluvial and estuarine sediments remain in backfilled paleochannels (Rice et al., 1998).

Field and Duane (1976) presented evidence that most barrier islands in the mid-Atlantic region formed seaward of the present coast during the Holocene transgression and migrated to their present position in response to rising sea level. Thus, the northern Outer Banks barrier system is perched on underlying pre-modern sediments. Offshore contours are relatively straight to 13 m depth with some irregularities adjacent to the research pier. One or two nearshore sandbars are usually present (Lippmann and Holman, 1990). The shoreface is covered by a sand sheet (Schwartz et al., 1997) which thins to less than 1 m at about 11-12 m depth (Rice et al., 1998). At approximately 18 m water depth, the bathymetry portrays significant (> 3 m) variability and is accompanied by an increase in the number of paleofluvial channels that crop out on the seafloor (Rice et al., 1998). Older sediments are exposed on the inner shelf as bathymetric highs and influence modern shoreface dynamics and composition (Cox et al., 1995; Riggs et al., 1995).

Sediments become finer offshore to 13 m depth (Schwartz et al., 1997) and are well-sorted fine to very fine sands (0.21 to 0.07 mm or 2.3 to 3.8 ϕ). Sediments consist primarily of quartz sand, with a secondary component of rock-fragment and shell gravel (Meisburger and Judge, 1989). Five nonopaque heavy minerals (garnet, staurolite, epidote, amphiboles, and tourmaline) occur with regularity and with frequency of 2 % or higher (Meisburger and Judge, 1989). Mica, an easily eroded and transported mineral, and is often associated with sediments of finer grain size. Glauconite pellets are common in most sediment samples but are probably detrital grains and do not form in situ (Meisburger and Judge, 1989). The dominant foraminifera in all samples are *Elphidium excavatum* (Terquem).

Tides are semi-diurnal and have a mean range of approximately 1 m. Average annual significant wave height is 1.0 $\pm$ 0.6 m (1980-1991) with a mean peak spectral period of 8.3 $\pm$ 2.6 s (Leffler et al., 1993). Extratropical northeasters are the most common significant storms with increased incidence from October to March. Tropical storms and hurricanes can occur from July to October but are not as common.

Waves and Mean Currents

Along open ocean coasts, waves are nearly ubiquitous and contribute to shaping the morphology of the shallow seabed. Wind-generated ocean surface waves are the major driving force for nearshore circulation and sediment transport in the surf zone and inner continental shelf (Wright et al., 1991). As waves shoal in coastal waters, wave energy spectra evolve owing to refraction, nonlinear energy transfers to higher and lower frequencies (Elgar et al., 1990), and energy dissipation caused by wave breaking and bottom friction (Thornton and Guza, 1983). Less obvious, but equally important, are the effects of mean currents. Surf zone and inner shelf mean currents may be forced by a variety of mechanisms including waves, wind, tides, and regional pressure gradients, but the wave-driven surf zone component has been the most intensively studied (Hubertz, 1986; Thornton and Guza, 1986; Haines and Sallenger, 1994). Both longshore currents generated by oblique wave approach to the shoreline and strong near-bed offshore flows (undertow) are clearly wave-forced since current velocities drop to near zero outside the surf zone (Stive and Wind, 1986; Thornton and Guza, 1986; Haines and Sallenger, 1994). Of all the approaches explaining the generation of nearshore currents, those based on

radiation stress, the excess flux of momentum due to the presence of waves, have the strongest theoretical basis (Longuet-Higgins and Stewart, 1964). However, predictions of nearshore currents using only wave breaking and bottom conditions (topography and roughness) may be in error in magnitude and direction if other forces such as wind, tide, or regional pressure gradients are significant (Whitford and Thornton, 1993).

At intermediate depths over the shoreface, tidal- and wind-forced currents are frequently stronger in the near-bed region than wave orbital velocities (Wright et al., 1991). In the Middle Atlantic Bight, wind-driven, jet-like, southerly currents produced by northeaster storms have been observed on the inner shelf and can produce secondary, but strong, downwelling. These upwelling and downwelling flows related to wind stress are among the more powerful mesoscale motions which operate seaward of the wave-dominated surf zone (Wright et al., 1986).

Previous studies have recorded near-bottom and interior fluid flows during fair weather and storm conditions (Hubertz, 1986; Wright et al., 1986; Wright et al., 1991; Cacchione et al., 1994; Wright et al., 1994a; Wright et al., 1994b) and concluded that inner shelf processes are dominated by storm-generated flows. These storm-generated cross-shore mean flows have been proposed as dominant mechanisms in both onshore and offshore sediment movement (Roelvink and Stive, 1989; Trowbridge and Young, 1989; Wright et al., 1991). Wave and current bottom stresses also cause sediment mobilization on the surf zone and inner shelf and determine the amount of sediment available for transport (Lyne et al., 1990; Cacchione et al., 1994; Vincent and Downing, 1994; Maa et al., 1995). On the continental shelf, bed stresses due to waves will dominate

the resuspension of the bed materials, but the combined stresses due to the waves and currents are important for the net transport of sediment in either the longshore or cross-shore direction (Vincent and Downing, 1994).

In turbulent boundary layers, the bed shear stress, τ_o, is related to the shear velocity, u_*, by

$$u_* = (\tau_o/\rho)^{1/2} \quad (1)$$

where ρ is water density (Wiberg and Harris, 1994). Because the local shear stress remains constant with elevation within the logarithmic flow layer, the elevation dependent mean current velocity, $u_c(z)$, can be used to calculate u_{*c}, the shear velocity related to the mean current, and the hydraulic roughness length, z_o ,

$$u_c(z) = (u_{*c} \ln (z/z_o)) / K \quad (2)$$

where z_o is given by the vertical intercept (where $u_c(z) = 0$) in the extrapolated logarithmic velocity profile. K, von Karmon's constant, is 0.4, and z is distance above the seabed (Wright, 1995). A minimum of three velocity measurements within 1.5 m of the bed can be used to obtain a bed shear stress value, τ_o, (Drake and Cacchione, 1992).

On the inner continental shelf, interaction of waves and mean flows determine the magnitude of bed shear stress which suspends sediments, while the oscillatory and mean flows may transport the sediments independently. Wiberg and Smith (1983) indicate that

it is necessary to account for the presence of waves and wave-current interactions on the continental shelf when estimating bottom stresses, either from field data or theoretically. Waves and currents over sandy shorefaces experience an effective bottom roughness approximately consistent with existing semi-empirical representations of the roughness characteristics of wave formed sand ripples (Trowbridge and Agrawal, 1995), thus knowledge of all three, waves, currents and bedforms, are needed for accurate prediction of bed shear stresses and resulting sediment transport. Estimates of wave energy dissipation due to bottom friction are derived from empirical parameterizations typically without the benefit of field measurements of bottom roughness or sediment type. This lack of quantitative data obtained in either the laboratory or the field has left a major deficiency in our understanding of the dissipative processes.

In most inner shelf environments, waves coexist with wind-driven and tidal currents, causing the thin oscillatory boundary layer of waves to be nested at the base of the thicker current boundary layer. Bottom friction is enhanced in combined wave and current boundary layers, and the total bed stress is greater than a linear addition of the solitary wave and current contributions. A notable effect of the waves is to increase the apparent roughness height, z_o', estimated by extrapolation of the current log-layer profile (Wright, 1995).

The boundary layer structure of the overlying fluid and the roughness elements of the bed comprise a morphodynamic feedback loop (Sherman and Greenwood, 1984). Changes in the overlying water column directly impact the surface of the seabed that in turn will modify motions in the overlying fluids. The few local measurements of wave

bottom boundary layer (WBBL) dynamics have also been concentrated on coasts with relatively smooth, gently sloping sandy bottoms. On these shelves the vertical extent of the WBBL is typically small, on the order of a few centimeters, making it difficult to accurately measure small-scale velocity profiles given the resolving capabilities of existing technology (Foster et al., 1994). Subsequently, dissipation estimates have large uncertainty. Moreover, measurements in these regions are often complicated by the presence of nonstationary, migrating ripple fields of variable dimension, particularly when the bed elevation changes by more than the thickness of the WBBL. As a result, it has thus far been unrealistic to quantify the overall damping in a shoaling wave field over smooth, slowly varying topography from point measurements of dissipation rates. Sediment transport and bedform migration are two processes that are driven by this fluid-sediment interaction.

The transition from measurements of wave and current activity to predictions of sediment transport and bedform activity during storm conditions is difficult at best. Even with these challenges, examining wave and current induced sediment suspension over time scales of fractions of seconds to hours with simultaneous time series of flow velocities and sediment concentration is one method of investigating sediment transport which has met with increasing success (Madsen et al., 1993; Beach and Sternburg, 1996; Amos et al., 1999). Correlation of morphological changes with measured rates and directions of suspended sediments on the shoreface has been partly successful (Cacchione and Drake, 1982; Aagaard and Greenwood, 1994), and nearshore depth changes during autumn storms have been recorded where mean flows are the driving force behind

sediment transport (Hay and Bowen, 1993; Thornton et al., 1996). Though many studies have concentrated on the mechanisms of transport and the forces which can initiate and sustain sediment transport, the actual amplitudes and nature of bed responses on the shoreface have usually been inferred indirectly, not measured, until a series of deployments were begun on the shoreface of the Middle Atlantic Bight.

Research on the shoreface of Duck, NC has documented a variety of fluid motions and associated bed elevation changes in fair and foul weather conditions through numerous deployments of tripods to support electromagnetic current meters, arrays of optical backscatter sensors (OBS), acoustic altimeters, and pressure sensors. Wright et al. (1994b) deployed two tripods in 8 and 13 m depths during the "Halloween storm" of 1991 when wave heights exceeded 6 m and periods reached 22 s. The 8 m tripod was lost entirely and only the current and sediment concentration data were recovered from the 13 m site. Despite the loss of the instrumentation, data analysis of the recovered records showed suspended sediment fluxes were dominated by the contribution from mean flows, but infragravity oscillations and wave orbital velocities were also important (Wright et al., 1994b). Wind-driven mean longshore currents at 1.24 m above the bed reached 50 cm/s. Seaward directed cross-shore flows varied from 5-15 cm/s and intensified with groups of higher waves (Wright et al., 1994b). A previous series of four tripod deployments in 7-17 m depth measured cross-shore flows from near zero in fair-weather conditions to greater than 20 cm/s offshore during storms (Wright et al., 1991). From these deployments, they conclude mean flows dominate in storms and cause

offshore fluxes of sediment. Incident waves were the dominant source of bed shear stress and caused both shoreward and seaward transport.

Chapters

In Chapter 2, analyses of seabed elevation data from sonar altimeters at 3 depths (5.5, 8, and 13 m) are combined with co-located measures of wave characteristics to document the range of seabed elevation changes in response to the forcing of hurricanes and northeaster storms. Although it is well established that northeasters are the most common storms at Duck, NC, the maximum significant wave heights measured at Duck, NC since 1980 were recorded during hurricanes Gloria (1985) and Gordon (1994). The range of seabed elevations and patterns of net erosion and net accretion are different for hurricanes and northeaster storms at locations in the surf zone and on the continental shelf.

In Chapter 3, sonar altimeter measurements of seabed elevation changes throughout storms, rather than radiometric dating, are used to establish the chronology of sediments in post-storm cores. During the SandyDuck experiment in October 1997, diver-operated boxcores were collected near sonar altimeters at 5.5, 8, and 13 m water depths. Downcore depths to erosion surfaces in post-storm cores correspond remarkably well with erosion maxima measured by sonar altimeters during storm events. Although post-depositional processes, including the effects of bioturbation and subsequent storms, may remobilize these sediments, these cores provide well-constrained modern nearshore storm deposits.

In Chapter 4, sonar altimeter data are used to evaluate profile data that are traditionally used to define the seaward limit of *significant* net sediment transport, or the depth of closure (D_c) during storms. Due to physical limitations of survey equipment and personnel, beach profiles are surveyed pre-storm and during some stage of the post-storm beach recovery process when hydrodynamic and meteorological conditions permit. By comparing pre- and post-storm surveys, *integrated* effects of storms on beach profiles and D_c can be assessed. To incorporate seabed elevation changes throughout storms and extend observations to 13 m depth, continuous data from downward-looking sonar altimeters are used to evaluate the seabed elevation changes measured by less frequent beach profiles. An earlier version of this chapter will be published in a June 1999 volume for the Coastal Sediments conference (Beavers et al., 1999).

The method developed to collect boxcores in the active surf zone and deeper waters of the inner continental shelf is described in Appendix 1. The majority of this appendix was published in the 1997 volume for the annual American Academy of Underwater Sciences conference (Beavers et al., 1997a). The core processing procedure in Appendix 2 was initially based upon notes prepared by Judy Roughton and J. Bailey Smith of the US Army Corps of Engineers.

CHAPTER 2

SEABED ELEVATION RESPONSE TO STORM EVENTS

Introduction

Storm activity is often associated with erosion of the subaerial beachface (List and Farris, 1999) and inner surf zone. These same storms may also lead to erosion or accretion deeper on continental shelves due to exchange of sediments between onshore and offshore locations. Even with this sediment exchange, offshore decreases in profile variability (Nicholls et al., 1998) suggest that the inner continental shelf is responding to waves and currents at different temporal scales than the subaerial beachface and inner surf zone.

Many studies have concentrated on the forces which can initiate and sustain sediment transport on continental shelves, but the actual amplitudes and nature of seabed responses to storm events are not well constrained (Morton, 1988). In particular, processes controlling scour and creation of marine erosion surfaces are not well documented (Field et al., 1999).

With advances in technology, longer-term observations of seabed dynamics have the potential to increase our understanding of seabed elevation response to different types of storm events (Beavers et al., 1999). Field measurements of seabed elevation changes during northeaster storms (Wright et al., 1994a) and hurricanes (Beavers et al., 1999)

have been documented on the inner continental shelf, but rarely have both types of storm events been documented at the same location on the shelf.

By maintaining instrument packages at the same location for several years (1994-1997), temporal patterns in seabed response and the spatial variability of hydrodynamic forcing can be studied for a variety of storms. In order to obtain continuous seabed observations and document hydrodynamic conditions throughout storm events, instrument packages were deployed in 5.5, 8, and 13 m water depths beginning in 1994. Designed to span the transition from the inner continental shelf to the outer surf zone, these packages occupy a dynamic zone where both wind and wave forcing may be important (Fig. 2.1). The 2 major storm systems responsible for producing this wind and wave forcing at Duck, NC, are hurricanes and northeaster storms.

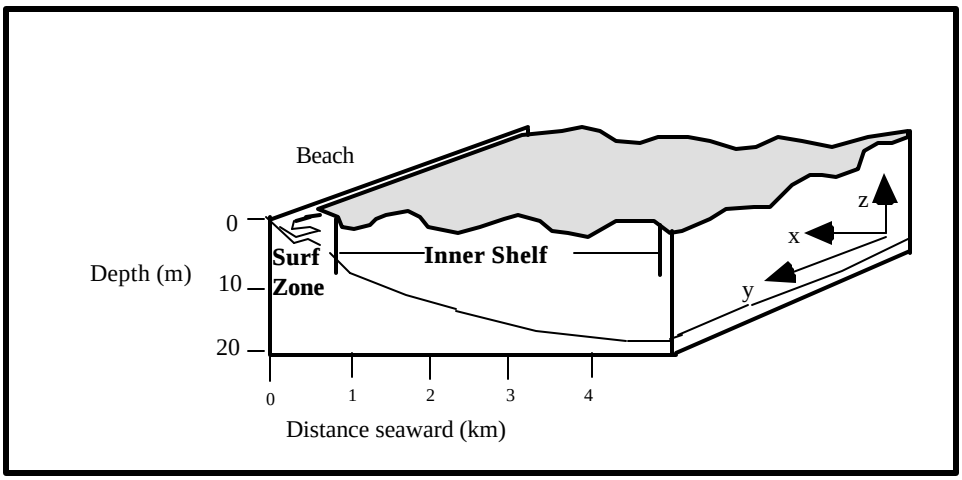

Figure 2.1. Definition sketch of the inner shelf and adjacent surf zone regions of the shoreface (adapted from Wright et al., 1991).

Storm Paths

Tropical cyclones or hurricanes form during June-November in the low latitudes of the Atlantic Ocean or Gulf of Mexico. When sunlight warms the upper ocean waters, evaporation and conduction transfer large amounts of heat and moisture to the atmosphere. As thunderstorms intensify in westward moving low-pressure troughs, known as tropical waves, a depression may develop (Barnes, 1998). Winds within this depression curve around the central low pressure, and the cyclone spins counterclockwise. As long as these cyclones remain over warm waters, they may intensify into tropical storms or, ultimately, hurricanes.

Strong counterclockwise winds also rotate around an area of low pressure in extratropical cyclones or northeaster storms. Warm waters of the Gulf Stream allow both storms to strengthen (Barnes, 1998). Even with these similarities, northeaster storms are distinct for several reasons. Northeasters lack a central warm air mass and well-defined eye. Northeasters typically occur in the winter months and form in 2 ways. A strong low-pressure system in the upper atmosphere may transfer energy to a developing low-pressure system off the mid-Atlantic coast. Other systems form near the Gulf of Mexico, cross into the south Atlantic, and drift into position off Cape Hatteras (Barnes, 1998). Sustained wind speeds in northeasters range from 10-25 m/s (20-50 mph), whereas hurricane force winds begin at 32 m/s (74 mph) (Dolan and Davis, 1992). Northeaster storms are more frequent, are usually geographically larger than hurricanes, and generally move slower (Dolan and Davis, 1992).

Since the early 1980's, the USACE Field Research Facility in Duck, NC (Fig. 2.2) has measured waves and tides on a routine basis. Tides are semi-diurnal and have a mean range of approximately 1 m. Average annual significant wave height is 1.0 $\pm$ 0.6 m (1980-1991) with a mean peak spectral period of 8.3 $\pm$ 2.6 s (Leffler et al., 1993). Although the greatest peak offshore wave heights were measured during hurricanes Gloria in 1985 (6.8 m) and Gordon in 1994 (6.5 m), over 20 of the 30 biggest peak wave events at Duck, NC were northeaster storms (FRF, 1999). Significant wave heights are comparable for both hurricanes and northeaster storms, but maximum wave conditions may last 2-3 times longer for northeaster storms in the western Atlantic than hurricanes.

The orientation of shorelines and shelves with respect to the paths of major storms controls storm dominance (Morton, 1988). The shoreline at Duck, NC (Fig. 2.2) faces the open North Atlantic Ocean, with shore-normal directed east-northeastward at approximately 70° true. Northeast incident waves from slow moving or nearly stationary northeaster storms often affect shelf processes and the underlying seabed for several days. The strongest storms at Duck, NC usually occur in October, November, December and March (Birkemeier et al., 1999) and are often northeaster storms.

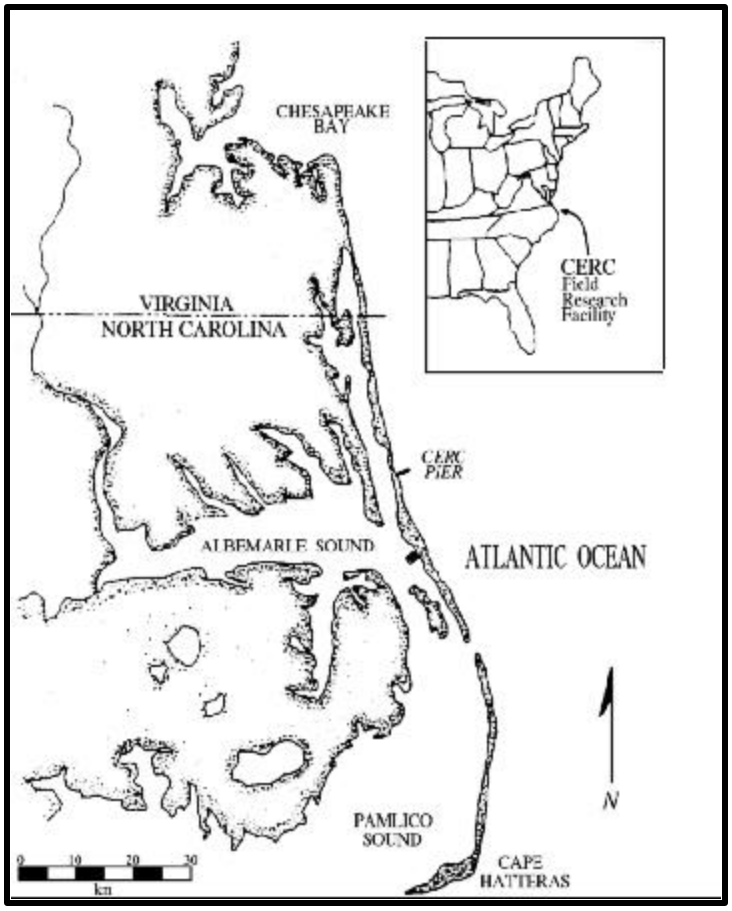

Figure 2.2. FRF location map.

Hurricanes approaching North Carolina from the south may follow many paths, but all hurricane landfalls in North Carolina have been south of Duck, NC. Some hurricanes skirt the eastern edge of the state, leaving the powerful, right-front quadrant of the storm at sea as the hurricane brushes the Outer Banks. Hurricanes Bertha and Fran made landfall at the southern end of the state near Wilmington, NC in 1996, whereas Hurricane Gordon stayed offshore and produced winds and high waves at Duck, NC from

November 17-19, 1994 before turning south and dissipating. Most hurricanes will cross the continental shelf in less than a day unless their path is parallel to the coast or looped. Even then, the influence of a hurricane on a given area is normally of limited duration because of the fast forward motion (Morton, 1988). August and September storms at Duck, NC are typically short duration, intense passing tropical storms and hurricanes (Birkemeier et al., 1999).

Bipod Instrumentation

Sedimentologic and hydrodynamic data were collected from 1994-1997 at the U.S. Army Corps of Engineers Field Research Facility (FRF) in Duck, North Carolina (Fig. 2.2). The FRF is located on the northern Outer Banks near the middle of Currituck Spit, a 100 km unbroken stretch of shoreline. This spit is a transgressive barrier island, approximately 800 m wide at the FRF, bordered by Currituck Sound on the west (Schwartz et al., 1997). The shoreface consists primarily of quartz sand, with a secondary component of rock-fragment and shell gravel (Meisburger and Judge, 1989). Sediments become finer offshore to 13 m depth (Schwartz et al., 1997) and are well-sorted fine to very fine sands (0.21 to 0.07 mm or 2.3 to 3.8 ϕ).

To study longer-term sediment dynamics on the inner continental shelf and outer surf zone, a multi-year monitoring program of near-bottom and interior flows and seabed elevation changes across the shoreface of the FRF was initiated in 1994 (Howd et al., 1994). Instrument packages to monitor waves, currents, and seabed elevation changes were deployed in 5.5 and 13 m water depths in September and October 1994 (Fig. 2.3). In May 1995, a third instrument package was deployed in 8 m water depth.

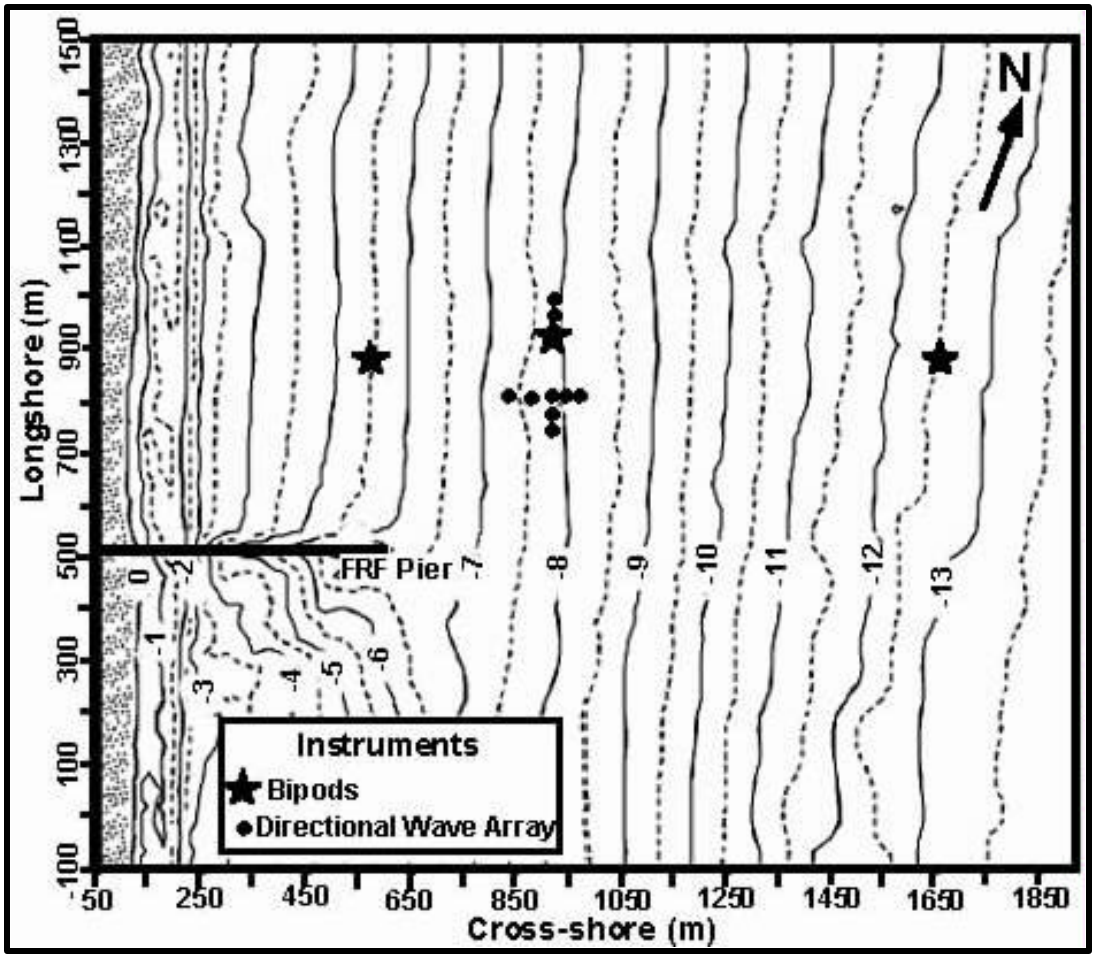

Figure 2.3. Location of bipod instrumentation (stars) at the FRF. Contours are in meters.

Instrument packages were secured on 'bipod' frames (Fig. 2.4) designed to sleeve over two 6.4 m long pipes jetted vertically 4 m into the seabed. Power and communications were provided from shore via armored multi-conductor cables. Except for sensor repairs or replacement, these instrument packages collected data during numerous storms from 1994-1997.

Current meters

Each bipod (Fig. 2.4) initially included 3 Marsh-McBirney electromagnetic current meters located on the offshore end of the frame. The biaxial electromagnetic current meters were replaced in fall 1997 with non-invasive triaxial acoustic current meters. This end of the frame was deployed to the southeast to minimize interference of current meters and vertical support with wave orbital velocities during northeast waves. Current meters were initially deployed at nominal elevations of 0.2, 0.55, and 1.5 m above the seabed to permit calculation of bed shear stresses associated with different flows by the velocity profile method (Drake and Cacchione, 1992). With a shoreline orientation of approximately N20W, longshore currents flow toward 340° (i.e. northward) or toward 160° (i.e. southward). Similarly, cross-shore currents are either onshore at 250° (westward) or offshore at 70° (eastward).

Pressure sensor

A pressure sensor (Fig. 2.4, P), sonar altimeter (S), and electronics housings (A, B, and C) were secured to the frame crossbeams. Current meters and Sensometric strain

gauges were sampled at 2 Hz. Pressure fluctuations were measured to allow calculation of the wave spectrum and water elevation (tides). Initially, an analog Sensometric strain gauge (Fig. 2.4, P) was deployed with each instrument package. These sensors were relatively inexpensive and reliable, but often exhibit mean pressure drifts over long time periods, such as 10-20 cm in a month. In September 1997, digital Paroscientific gauges replaced the strain gauges for more precise and stable pressure measurements. These gauges output voltage signal with a frequency proportional to the pressure and operate at a nominal 38 kHz. The Tattletale Model 8 operated in a frequency-count mode to measure the Paroscientific signal over a 50 ms averaging interval, at a 2 Hz rate. This sample interval was determined to be short enough to have negligible filtering effect for wave measurements (2+ s), and long enough for an accurate pressure (frequency) measurement of better than 1 mm.

Wave height, H_{mo}, was computed as an energy-based statistic equal to four times the standard deviation of the sea surface elevations. Wave height reported from the pressure gauge has been compensated for hydrodynamic attenuation using linear wave theory. Wave variance is computed from energy spectra and band limited to frequencies > 0.05 Hz (period <20 s) with a high frequency cutoff based on wave attenuation where linear theory amplitude correction is 10. Wave period is identified from the computation of a variance (energy) spectrum with 60 degrees of freedom calculated from a 34 minute record. Peak wave period, T_p, is defined as the period associated with the maximum energy in the spectrum.

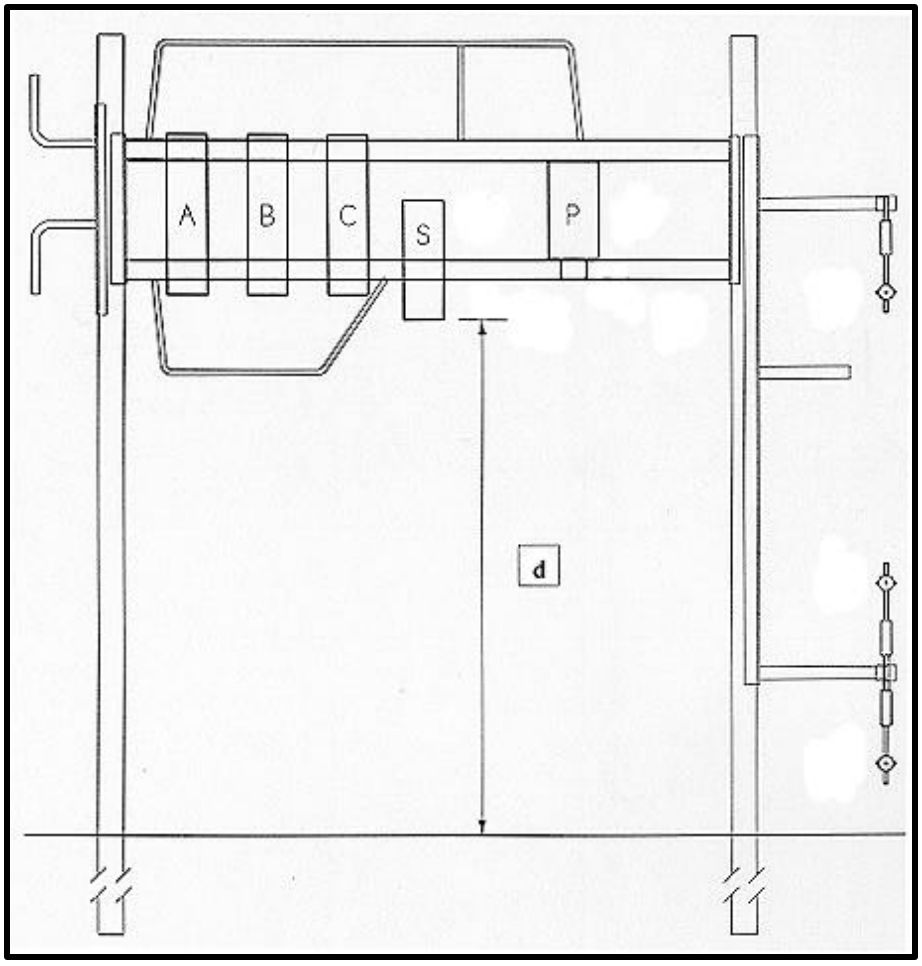

Figure 2.4. Bipod instrumentation.

Sonar altimeter

The Datasonics altimeter (Fig. 2.4, S) transmits a 210 kHz acoustic pulse once per second (1 Hz) with 'bottom' return echoes detected after each pulse. Returns are range-binned for 34 minutes. The bin with the maximum number of returns is recorded as the seabed elevation during that 34-minute period. In laboratory tests, the mean distance to

the bottom (Fig. 2.4, d) measured with the altimeter was accurate to ± 1 cm of an independent distance measurement. The altimeter transducer beamwidth is approximately 10° and results in an approximately 20 cm diameter footprint at 1 m range. The footprint of the sonar altimeter is too large to resolve short wavelength (1-5 cm) ripples (Gallagher et al., 1996); instead, larger scale patterns of erosion and deposition are resolved.

Boxcores

During 1994-1997, the bipod instrument locations served as the site of over 150 diver-collected boxcores which provide a 15 cm wide x 30 cm deep section of the near surface sediments (Appendix 1). Cores were collected during the calm summer months to serve as a fair weather baseline for cores collected directly after northeaster storms and hurricanes. This sediment coring program tested the correlation between seabed elevation changes recorded by the altimeters and the thickness of depositional units observed in the cores and investigated the spatial variability of sediments and preserved sedimentary structures in the vicinity of the bipods. The altimeter data agree with depth to erosion contacts in the post-storm boxcores (Chapter 3). This independent test of seabed altimeter data verifies the fluctuations in seabed elevation measured by a sonar altimeter (Fig. 2.5) during storm events are indeed real.

Results

Continuous records of wave heights and seabed elevations throughout hurricanes and northeaster storms were used to evaluate the range in seabed elevations and net

seabed elevation changes at 3 cross-shore locations in 5.5 m, 8 m, and 13 m water depths (Fig. 2.3). During storm conditions, incident waves break and propagate into the surf zone, an area dynamically defined by the presence of active wave breaking. In the inner surf zone, wave energy becomes saturated and root-mean-square wave height (H_{rms}) is a function of local water depth (h),

$$H_{rms} = \gamma h \qquad (1)$$

where γ varies with bottom slope and wave steepness. Field studies in Duck, NC have shown γ has a range of 0.29-0.55 (Sallenger and Holman, 1985). Using a value of 0.4 for γ in Eqn. 1 (Thornton and Guza, 1983), the depth at the edge of the surf zone (h_b), the point at which most waves are breaking, was calculated for each storm based on wave heights recorded at a waverider buoy 4 km offshore (Tables 2.1 and 2.2).

To compare seabed elevation changes at all locations, the depth (h) at each location (5.5 m, 8 m, or 13 m) was converted to a dimensionless 'depth' (h_r) relative to the depth at the edge of the surf zone (h_b) for each storm

$$(h - h_b)/ h_b = h_r \qquad (2)$$

For example, during a February 1996 northeaster (H_{rms} = 2.3 m), the edge of the surf zone was in 5.7 m depth (Table 2.2), and the relative depth (h_r) at the 13 m bipod was 1.3. Also during this northeaster, the 5.5 m bipod was at the edge of the surf zone (h_r = -0.03), whereas the 8 m bipod was outside of the surf zone on the inner continental shelf (h_r = 0.4).

The range in seabed elevation at each site was defined by the maximum and minimum seabed elevation recorded during a maximum of 11 times for each storm (Fig. 2.5). The first 5 thresholds were established during increasing wave heights. When thresholds of 1.0 m, 1.5 m, 2.0 m, 2.5 m, and 3.0 m in wave heights (H_{mo}) were exceeded at the 13 m bipod (Fig. 2.5a), corresponding seabed elevations at the 5.5, 8, and 13 m were evaluated. The next 6 times correspond with maximum wave height, and the final time wave heights remain above thresholds from 3.0 m to 1.0 m in 0.5 m intervals. This method was chosen to evaluate the seabed response to changes in wave height but may underestimate the range in seabed elevations. When the maximum or 0.5 m increments of wave height do not correspond with the seabed erosion maxima (e.g.- Fig 2.3d), the lowest elevation measured by the sonar altimeter may not be included in calculating the range of seabed elevations at that location during the storm.

Net seabed elevation change for each storm was calculated as the difference between seabed elevation measurements at each location when wave heights at the 13 m site first and last exceeded the 1.0 m thresholds (Fig. 2.2, solid vertical lines). Net seabed elevation change calculated by this method does not evaluate post-storm seabed adjustments. Values of net change and range of seabed elevations may be in error if small-scale bedforms with wavelengths less than the approximately 20 cm diameter sonar altimeter footprint are present (Gallagher et al., 1996).

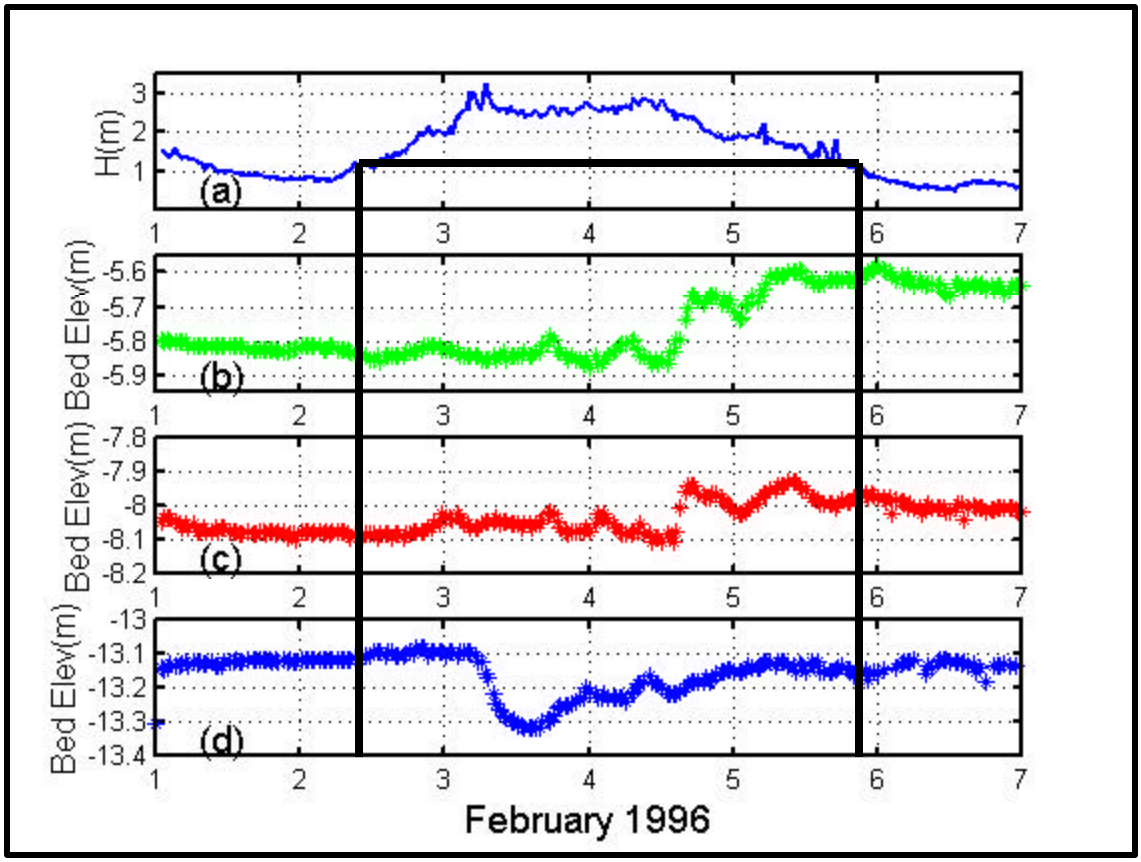

Figure 2.5. Wave heights (a) and seabed elevation changes measured at 5.5 m (b), 8 m (c), and 13 m (d) sites during February 1996 northeaster storm. Net seabed elevation change is calculated as the difference in seabed elevations when wave heights (a) first exceed 1.0 m (solid vertical line, left) and last exceed 1.0 m (solid vertical line, right).

Five hurricanes (Table 2.1) were included in these analyses. Seabed elevation changes were measured at all 3 locations during each storm with the following exceptions: Gordon - no 8 m data, Bertha - no 5.5 m or 13 m data, and Fran- no 5.5 m

data. A total of 11 realizations of seabed elevation changes during hurricanes were analyzed.

Table 2.1. Wave heights (H_{rms}) and water depth at the surf zone edge (h_b) for 1994-1997 hurricanes.

Year	**Dates**	**Name**	**H_{rms} (m)**	**h_b (m)**
1994	November 16-22	Gordon	4.6	11.5
1995	August 13-21	Felix	3.3	8.2
1996	July 10-13	Bertha	2.1	5.3
1996	August 29-September 3	Edouard	2.4	6.0
1996	September 4-7	Fran	2.4	6.0

Six northeaster storms (Table 2.2) were included in these analyses. These storms include the Duck 94 (October 1994) and SandyDuck (October 1997) experiment storms. October 1995 and 1996 northeaster storms and northeaster storms in January and February 1996 were also included. Seabed elevation changes were measured at all 3 locations during each storm with the following exceptions: October 1994 - no 8 m data and October 1996- no 5.5 m data. A total of 16 realizations of seabed elevation changes during northeaster storms were analyzed.

Table 2.2. Wave heights (H_{rms}) and water depths at the surf zone edge (h_b) for selected 1994-1997 northeaster storms.

Year	**Dates**	**H_{rms} (m)**	**h_b (m)**
1994	October 10-20	3.2	8.0
1995	October 20-21	1.5	3.7
1996	January 6-8	2.4	6.0
1996	February 2-5	2.3	5.7
1996	October 3-9	2.1	5.1
1997	October 15-23	2.8	6.9

Net Seabed Elevation Changes

In Figure 2.6, net seabed elevation changes for hurricanes (stars) and northeaster storms (circles) are compared. By converting the depth (h) at each location (5.5 m, 8 m, or 13 m) to a dimensionless 'depth' (h_r- Eqn. 2) relative to the depth at the edge of the surf zone (Fig. 2.6, solid vertical line at 0), data from all storms and locations can be compared. Locations inside the surf zone during maximum wave heights will plot as negative 'depths', and locations beyond the surf zone edge (at 0) will plot at increasingly positive 'depths' with increasing distance from the surf zone. Both northeaster storms and hurricanes have seabed elevation measurements from 4 locations in the surf zone, but

northeaster storms have measurements from a greater number of locations (11 vs. 7) offshore of the surf zone.

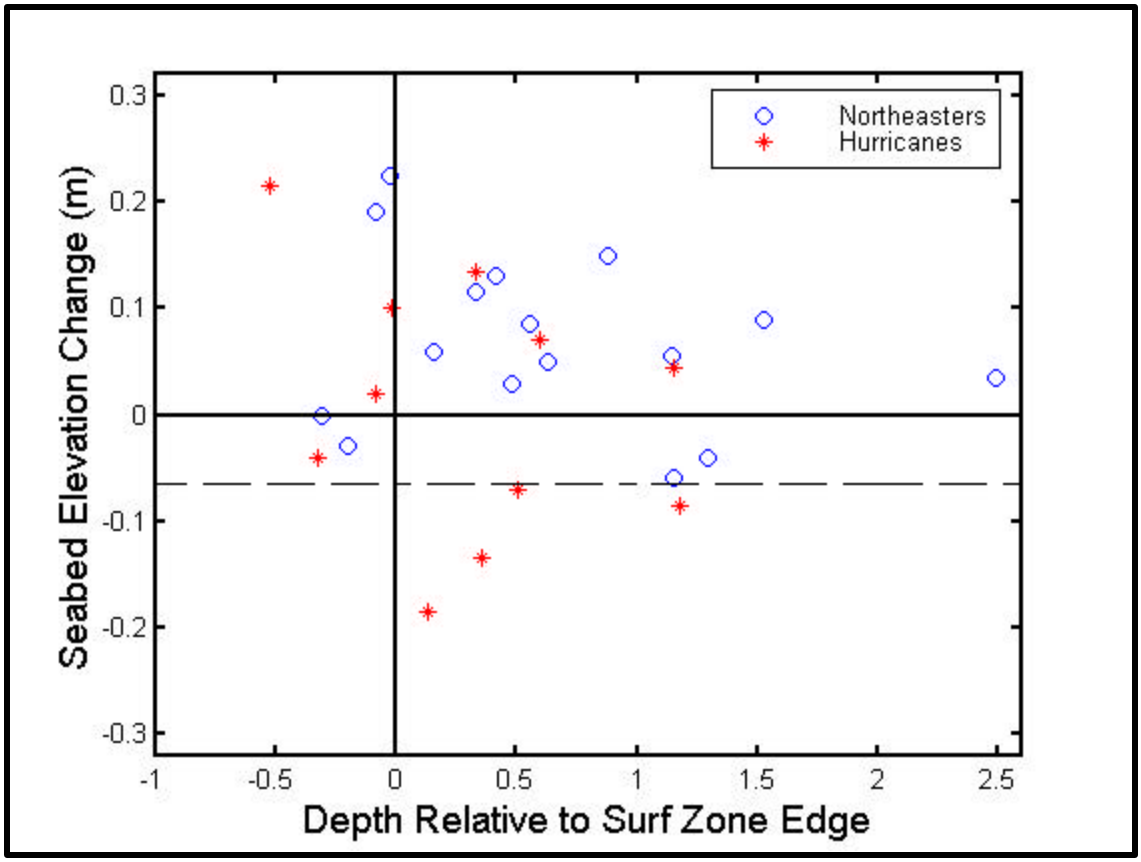

Figure 2.6. Net seabed elevation changes for hurricanes (star) and northeaster storms (circle) during 1994-1997. No locations exceeded 6 cm of net erosion (dashed line) during northeaster storms.

Both hurricanes and northeaster storms cause net erosion (negative seabed elevation change) and net accretion (positive seabed elevation change) at locations within and offshore of the surf zone. The range of net seabed elevation changes during northeaster storms is approximately 30 cm (-6 cm to 23 cm) and is less than the

approximately 40 cm range measured during hurricanes (-19 cm to 22 cm). Although both hurricanes and northeasters result in over 20 cm of net accretion at some surf zone locations, these northeasters storms never resulted in over 6 cm of net erosion at any location in the surf zone or on the inner shelf (Fig. 2.6, dashed line). Hurricanes resulted in greater magnitudes of net erosion at most locations, exceeding 20 cm of net erosion at the 13 m bipod during hurricane Gordon.

Northeaster storms and hurricanes result in maximum values of net seabed accretion in the surf zone (Fig. 2.6), but maximum values of seabed erosion occurred outside the surf zone during hurricanes. During these storms, wind-generated ocean surface waves are the major driving force for nearshore circulation and sediment transport in the surf zone and inner continental shelf (Wright et al., 1991). With increased dissipation of wave energy in the surf zone during wave breaking and associated bottom friction (Thornton and Guza, 1983), it is not surprising to see a wider range of seabed elevations within and near this dynamic zone. As expected, net seabed erosion and accretion diminished with distance offshore of the edge of the surf zone.

Hurricanes

Even though the net seabed accretion (Fig. 2.7, stars) is greatest within the surf zone, it is surprising that net seabed erosion and the range of seabed elevations (Fig. 2.7, bars) observed during hurricanes is not always greatest inside the surf zone. Several locations experienced a range in seabed elevations of approximately 30 cm. This

approximately 30 cm range was measured when the 5.5 m location was within the surf zone during hurricane Gordon, but the 13 m location measured corresponding approximately 30 cm ranges in seabed elevations when this location was offshore of the surf zone during hurricanes Gordon and Felix.

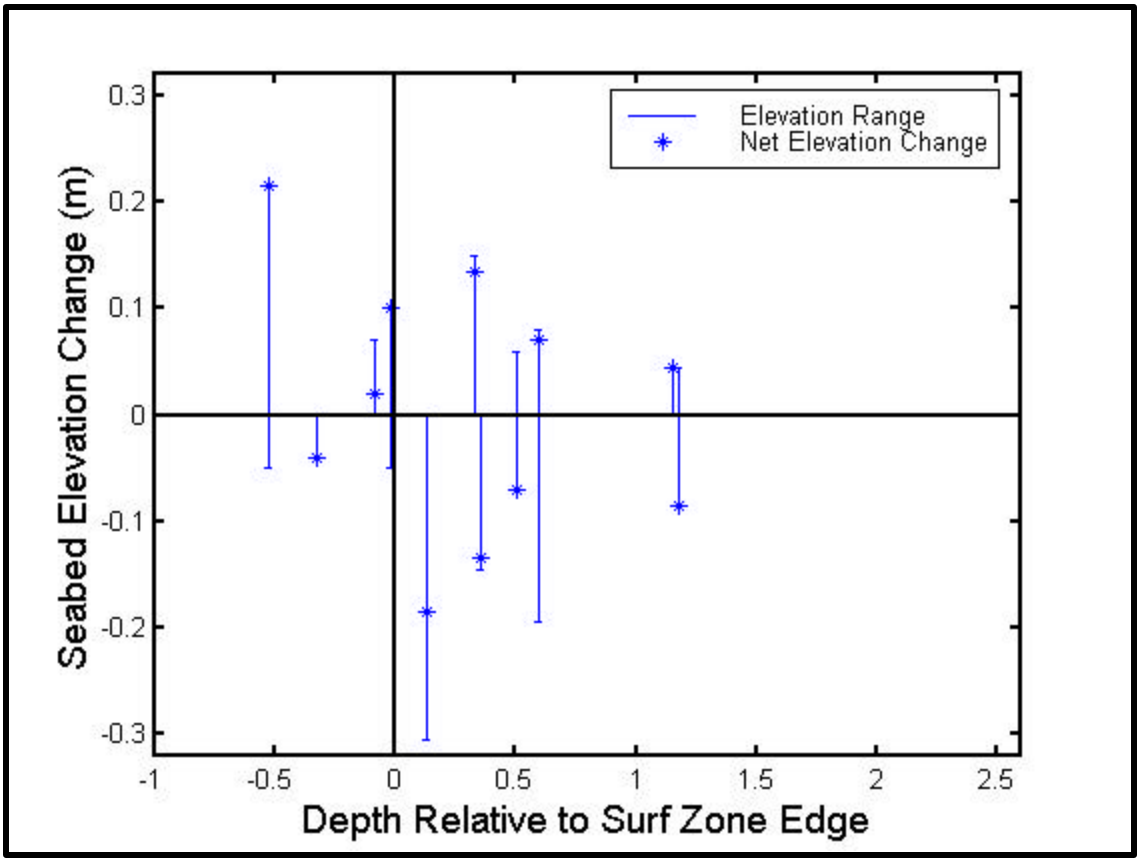

Figure 2.7. Net (star) and range (bar) of seabed elevations for 5 hurricanes during 1994-1997.

Even more surprising, the 8 m location always experienced an approximately 15 cm range in seabed elevations whether it was encompassed by the surf zone edge or remained offshore of the edge of the surf zone. The 5 m location was always in the surf zone during hurricanes, but only had a range of approximately 5 cm during hurricanes

Edouard and Felix. During hurricanes Edouard and Fran, the 13 m location had respective ranges of seabed elevation changes of approximately 5 and 15 cm. Hurricanes are almost as likely to cause net erosion (5 occurrences) as net deposition (6 occurrences) at these surf zone and inner shelf locations.

Northeaster storms

Like hurricanes, net seabed accretion (Fig. 2.8, circles) during northeaster storms is greatest within the surf zone, but the range of seabed elevations (Fig. 2.8, bars) during northeaster storms is not always greatest inside the surf zone. Unlike hurricanes, northeaster storms are more likely to cause net accretion (12 occurrences) than no net change in seabed elevation or net deposition (4 occurrences) at these surf zone and inner shelf locations.

Wave heights for the northeaster storm in October 1995 (Table 2.2) were lower than wave heights for the smallest hurricane (Bertha) (Table 2.1). During the October 1995 northeaster storm, the 5.5 m location was offshore of the surf zone, and the 13 m site was in 2.5 times greater depth than the edge of the surf zone. With this distance from the edge of the surf zone, it is not unexpected that the range in seabed elevations (8 cm) was small.

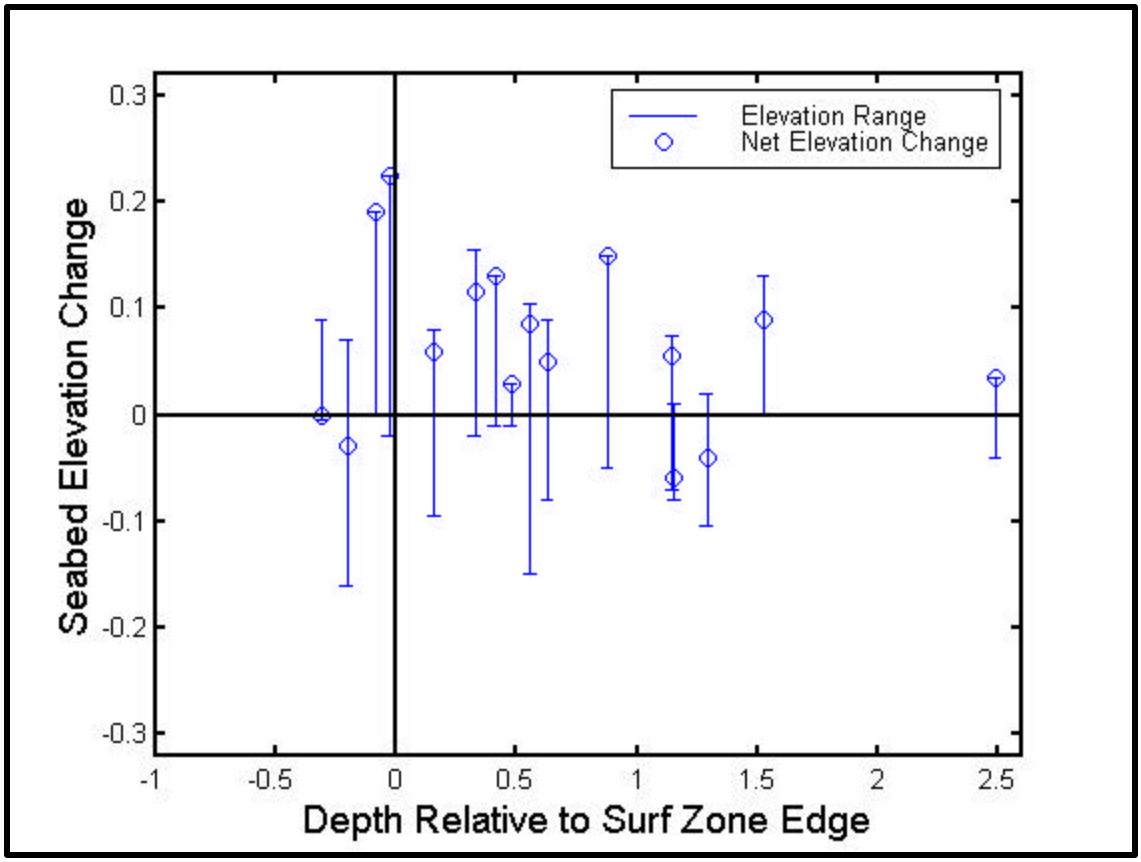

Figure 2.8. Net (circle) and range (bar) of seabed elevations for 6 northeaster storms during 1994-1997.

An approximately 25 cm range in seabed elevations was measured when the 5.5 m location was within the surf zone during the February 1996 and October 1997 northeasters. The 8 m location measured a corresponding approximately 25 cm range when this location was offshore of the surf zone during October 1996. All other locations experienced ranges in seabed elevation (from 9-20 cm), whether or not they were within the outer surf zone at the peak of the storm or always offshore of the surf zone.

Discussion

By comparing seabed elevation changes during 1994-1997 for 5 hurricanes and 6 northeasters storms, some intriguing trends have emerged. Both northeaster storms and hurricanes resulted in maximum values of net seabed accretion inside the surf zone. As expected, net seabed erosion and accretion diminished with distance offshore of the edge of the surf zone. This inverse relationship between net seabed elevation change and distance offshore of the surf zone indicates linking sedimentation processes across time scales and surf zone and inner shelf environments must incorporate analyses of the transition in fluid motions from the inner shelf to the surf zone.

Even though net seabed accretion is usually greatest when the 5.5 or 8 m locations are within the outer surf zone, net seabed erosion and the range of seabed elevations are not always greatest inside the surf zone. The maximum range in seabed elevations for locations in the surf zone and on the inner continental shelf was approximately 25 cm during northeaster storms and approximately 30 cm during hurricanes. During hurricanes, the range in seabed elevations was approximately 15 cm at the 8 m location and approximately 5 cm at the 5.5 m location. During northeaster storms, all locations experienced a various range of seabed elevation changes (8-25 cm) and did not cluster around any particular range like seabed elevation ranges during hurricanes.

Given the constraints that these analyses are based on a small number of storms with variable duration, maximum wave heights, wave periods, and currents, these data indicate hurricanes and northeaster storms have different impacts on the seabed at these surf zone and inner shelf locations. Northeaster storms are more likely to cause net

accretion than no net change in seabed elevation or net deposition, whereas hurricanes are almost as likely to cause net erosion as net deposition. With overlapping paths and greater significant wave heights, hurricanes may transport and rework sediment in deeper water than northeasters (Morton, 1988). Additional research on the effects of wave period, currents, and storm duration may help elucidate the reasons for these differences in seabed response for northeaster storms and hurricanes.

Conclusions

1. Northeaster storms and hurricanes result in maximum values of net seabed accretion at locations in the outer surf zone. Net seabed erosion and accretion diminished with increasing distance offshore of the edge of the surf zone.
2. The maximum range in seabed elevations was approximately 25 cm during northeaster storms and approximately 30 cm during hurricanes.
3. At these outer surf zone and inner continental shelf locations, northeaster storms are more likely to cause net accretion than no net change in seabed elevation or net deposition, but hurricanes are almost as likely to cause net erosion as net deposition.

CHAPTER 3

STRATIGRAPHIC SIGNATURE OF A NORTHEASTER STORM EVENT ON THE SURF ZONE AND INNER CONTINENTAL SHELF

Introduction

Translating observations of modern depositional environments to ancient analogs in the stratigraphic record is one of the most fundamental tasks of sedimentary geologists; it is also one of the most difficult (Davis, 1992). Due to the difficulty of monitoring the evolution of nearshore morphology during storms, laboratory flumes have previously been the only setting where it was feasible to continuously monitor 'sea'bed configuration and sample shallow stratigraphy created during simulated high-energy events (Arnott and Southard, 1990).

High wave orbital velocities and mean currents in the nearshore restrict seabed observations by SCUBA divers to calm conditions (Davis, 1965; Clifton et al., 1971; Davidson-Arnott and Greenwood, 1976; Greenwood and Mittler, 1979; Hunter et al., 1979). During storms, increased concentrations of suspended sediments (Vincent et al., 1991; Beach and Sternburg, 1996; Osborne and Vincent, 1996; Battisto et al., 1999) can obscure the view of the seabed and limit observation of the bottom using underwater stereo cameras or video cameras (Amos et al., 1999). This intense hydrodynamic regime also imposes constraints on nearshore instrumentation and data transmission.

Acoustic instrumentation deployed in arrays on frames (Hay and Bowen, 1993; Gallagher et al., 1996; Jette and Hanes, 1997) and towed side-scan sonar surveys (Thornton et al., 1998) have increased the variety of nearshore environments and conditions under which seabed observations have been made. The first near-continuous 2-dimensional images of nearshore seabed configuration during storms were provided by rotary fan-beam sonars (Hay and Wilson, 1994) over an area exceeding 10 m^2. The transitions in bed configuration associated with variations in wave state at a fixed site (Hay and Wilson, 1994) are similar, but not identical, to the spatial distributions of bedforms across the nearshore observed by Clifton (1971). The order of bed state progression observed with sonars during increasing wave orbital velocities at Duck, NC is (1) irregular 3-D, short crested ripples, (2) oblique cross-ripples, combined with patchy, shore parallel ripples and occasional megaripples, (3) long-crested shore-parallel ripples, with occasional megaripples, and (4) 'flat' bed conditions (Hay and Wilson, 1994).

Until this study, linking seabed observations to the stratigraphic record has been limited since seabed changes during storm and non-storm conditions have not been observed where cores were collected. Even though internal sedimentary structures in nearshore cores have been interpreted as storm deposits (Clifton et al., 1971; Davidson-Arnott and Greenwood, 1976; Greenwood and Mittler, 1979; Morton, 1988), this link was not directly established.

Recent advances in acoustic imaging technology provide the opportunity to directly link seabed changes during storms to preserved stratigraphy. The chronology of

storm events that erode and deposit sediments may be quantified by remote observation of both the seabed with sonar altimeters (Jette and Hanes, 1997; Gallagher et al., 1998) and hydrodynamic forcing with co-located pressure sensors and current meters. With the chronology of storm sedimentation provided by remote observation, diver-operated cores collected post-storm can be interpreted to reveal the stratigraphic signature of storm deposits.

SandyDuck97 Experiment

Sedimentologic and hydrodynamic data were collected during the SandyDuck97 nearshore experiment (Burns, 1998) held at the U.S. Army Corps of Engineers Field Research Facility (FRF) in Duck, North Carolina. The FRF is located on the northern Outer Banks near the middle of Currituck Spit, a 100 km unbroken stretch of shoreline. This spit is a transgressive barrier island, approximately 800 m wide at the FRF, bordered by Currituck Sound on the west (Schwartz et al., 1997). The shoreline at the FRF faces the open North Atlantic Ocean, with shore-normal directed east-northeastward at approximately 70° true. The shoreface consists primarily of quartz sand, with a secondary component of rock-fragment and shell gravel (Meisburger and Judge, 1989). Sediments become increasingly finer offshore to 13 m depth (Schwartz et al., 1997) and are well-sorted fine to very fine sands (0.21 to 0.07 mm or 2.3 to 3.8ϕ).

Timing of the six-week SandyDuck experiment from mid-September – October 1997 was based on previous studies of sandbar behavior at Duck and expectations that a wide range of conditions would occur. Incident significant wave heights varied from

calm (<0.5 m) to a short-lived peak of just over 3.5 m during the "SandyDuck storm" that occurred between October 18 and 22, 1997. The SandyDuck storm was an extratropical northeaster, the most common significant storm that occurs at the FRF.

Bipod Instrumentation

By October 1, 1997, instrument frames were deployed at 3 locations in 5.5, 8, and 13 m water depths along a cross-shore transect (Beavers et al., 1999). Instrument packages were secured on 'bipod' frames designed to sleeve over two 6.4 m long pipes jetted vertically 4 m into the seabed. Power and communications were provided from shore via armored multi-conductor cables.

Each bipod included 3 SonTek Acoustic Doppler Velocimeters (ADV) located on the offshore end of the frame. This end of the frame was deployed to the southeast to minimize interference of instruments and vertical support with measured wave orbital velocities during northeast waves. With a shoreline orientation of approximately N20W, longshore currents flow toward 340° (i.e. northward) or toward 160° (i.e. southward). Similarly, cross-shore currents are either onshore at 250° (westward) or offshore at 70° (eastward). Located 18 cm from the current meter transducer, ADV sampling volumes were approximately 30 cm (bottom), 85 cm (middle), and 160 cm (top) above the seabed when frames were deployed.

A sonar altimeter, pressure sensor, and electronics housings were secured to the frame crossbeams. Paroscientific pressure gauges measured pressure fluctuations to allow

calculation of wave height, wave period, and water elevations. Current meters and pressure gauges were sampled at 2 Hz.

The Datasonics altimeter transmits a 210 kHz acoustic pulse once per second (1 Hz) with 'bottom' return echoes detected after each pulse. Returns are range-binned for 34 minutes. The bin with the maximum number of returns (from a total of 2048 returns) is recorded as the seabed elevation during that 34-minute period. In laboratory tests, the mean distance to the bottom measured with the altimeter was accurate to $\pm$ 1 cm of an independent distance measurement. The altimeter transducer beamwidth is approximately 10° and results in an approximately 20 cm diameter footprint at 1 m range. The footprint of the sonar altimeter is too large to resolve short wavelength (1-5 cm) ripples (Gallagher et al., 1996); instead, larger scale patterns of erosion and deposition are detected.

The lowermost ADV was used as a second of seabed altimeter. The ADV transmits a 4 MHz acoustic pulse and detects 'bottom' return echoes after each pulse. During 9 minutes of each 3 hour interval, the bottom ADV was sampled for 3 minutes to collect 50 'bottom' returns. Ignoring outlier values based on a known acceptable range of valid data, a median distance to the 'bottom' was determined, and a distance to the seabed was computed by averaging values within 5 cm of the median. This results in one value of the seabed location every 3 hours and provides a verification of sonar altimeter data.

With a transducer beamwidth of less than 1°, an approximately 2 cm diameter footprint is formed when the ADV acoustic pulse is transmitted from 50 cm above the seabed. Even though the ADV is collecting data from a smaller area of seafloor than the

sonar altimeter (approximately 2 cm vs. approximately 20 cm), the ADV operates at a higher frequency (4 MHz vs. 210 kHz) and is more likely to record false bottom returns during storm events with high levels of suspended sediments. Given the limitations that the ADV is only sampled once every 3 hours and is subject to greater variability during storms, sonar altimeter measurements will be used as the primary record of seabed altimetry.

Boxcores

Diver-operated boxcores (15 cm wide x 10 cm deep x 30 cm long) were collected on October 14 and 24 at all 3 instrumented locations. By comparing pre- and post-storm cores, sediment structures formed by physical processes during the SandyDuck storm can be identified in core stratigraphy. These primary structures form during or slightly after sediment accumulation and exclude secondary biogenic structures (Reineck and Singh, 1980).

The core process is briefly described. For more detailed information on boxcore collection and processing, please consult the Appendix. The cores were opened in the laboratory and planed to a 2 cm thick slab. The central 13 cm of sediment was placed in a plexiglass tray with 1 cm molded sides. Using only the central portion of the core reduced the structural distortion that occurred at the sides of the corer, but downwarping is still visible on the edges of many cores. Warping of sediment along the back side of the corer displaced the core sediments as an entity and did not affect the relationships between bedding planes.

Information on internal structure of the cores was obtained using 2 methods. First the processed 1 cm thick section of core was exposed to xrays using a portable veterinary xray unit. Next, cheesecloth was placed on the sediment surface, and a mixture of epoxy resin and hardener was painted over the cheesecloth to create a relief peel. Final structural interpretation of the cores was based on both surface relief features and xrays.

During core extraction, boxcore sediments were subsampled at the sediment-water interface (core top), 3-5 cm downcore, and 13-15 cm downcore for grain size analyses. Sediment samples were wet sieved with a 63 μm (4 ϕ) mesh screen, dried, and weighed. Approximately 20 g of the > 63 μm (4 ϕ) fraction was dry sieved in a 0.5 ϕ interval sieve stack on a sieve shaker for 10 minutes.

Since the location of each core relative to the instrumentation on the frame is known, seabed elevation data measured by a sonar altimeter can be used to establish the chronology and associated thickness of strata preserved in the cores. The stratigraphic signatures of a northeaster storm in 5.5, 8, and 13 m water depths are evaluated in light of synoptic hydrodynamic conditions that caused bed shear stresses associated with the deposition, erosion, and transport of seabed sediments.

Results

By the morning of October 19, 1997, a stationary front had developed into a low pressure system about 100 km offshore of Cape Hatteras, North Carolina. During this SandyDuck northeaster storm, maximum onshore winds reached 18 m/s at 1408 EST on October 19. The maximum significant wave height measured by an offshore Waverider

buoy reached 3.87 m at 1600 EST on October 19. The peak spectral period (T_p) of these waves was 9.1 s. Further inshore at 13 m water depth, maximum wave heights (H_{mo}) of 3.49 m (T_p=9.5 s) were measured at 1708 EST on October 19 (Fig. 3.1).

During storm conditions, incident waves break and propagate into the surf zone, an area dynamically defined by the presence of active wave breaking. In the inner surf zone, wave energy becomes saturated and root-mean-square wave height (H_{rms}) is a function of local water depth (h),

$$H_{rms} = \gamma h \quad (1)$$

where γ varies with bottom slope and wave steepness. Field studies in Duck, NC have shown γ has a range of 0.29-0.55 (Sallenger and Holman, 1985). Using a value of 0.4 for γ in Eqn. 1 (Thornton and Guza, 1983), the depth at the edge of the surf zone (h_b = 6.9 m) almost extended to 7 m water depth when root-mean-square wave heights reached 2.8 m. During this northeaster, the 5.5 m location was well within the surf zone, and the 8 m location was on the offshore edge of the surf zone at the height of the storm. The inner continental shelf 13 m location was always offshore of the surf zone.

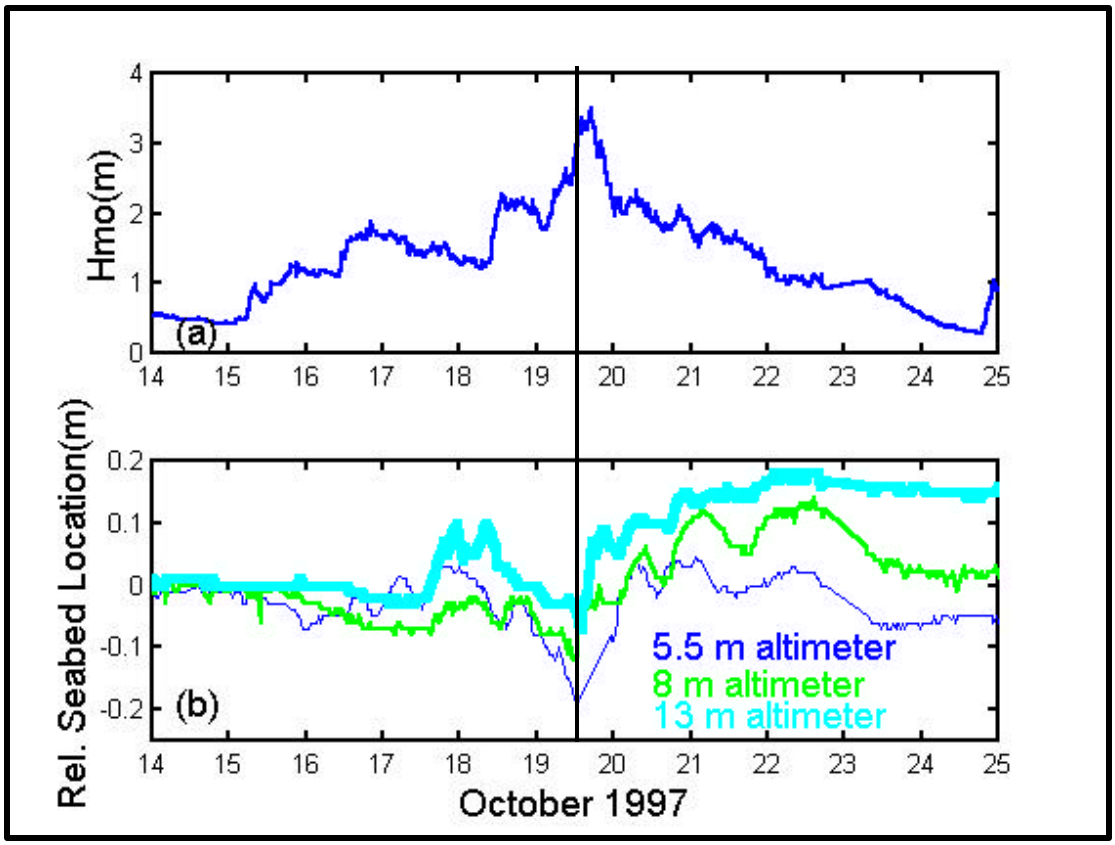

Figure 3.1. October 1997 (a) wave heights and (b) relative seabed locations.

Figure 3.2 presents the mean longshore and cross-shore current velocities recorded approximately 30 cm above the seabed by the bottom current meters. Longshore currents were usually directed to the south and exceeded 50 cm/s at all locations by 1500 EST on October 19. Cross-shore currents were predominately directed offshore and reached the greatest velocities at 13 m. Offshore flows were always less than 10 cm/s at 5.5 m but reached 29 cm/s at 1334 EST on October 19 at 13 m.

Seabed elevation changes measured at the 5.5, 8, and 13 m bipods are presented relative to the pre-storm seabed elevation on at each location on October 14 (Fig. 3.1).

Several similarities exist for seabed behavior during the northeaster storm. At all locations, the seabed experienced net erosion during storm spin-up on October 18-19 when wave heights and current velocities were increasing. On October 19, seabed erosion maxima (Fig. 3.1, solid vertical line) preceded maximum wave heights by $\leq$5 hours but coincided with maximum cross-shore current velocities at 13 m (Fig. 3.2, solid vertical line). Bed shear stresses (for calculations see Chapter 1) were greatest for current profiles measured during the seabed erosion maxima on October 19.

As wave heights peaked, currents decreased, and sediment accreted at all locations (Fig. 3.1, right of solid vertical line) and formed storm deposits. Differences in seabed behavior during and after the storm have a significant effect upon the structure and thickness of sediment preserved from this event. Resulting storm deposits are next presented for a 13 m inner continental shelf location, an 8 m location near the offshore edge of the surf zone, and a 5.5 m location well within the surf zone.

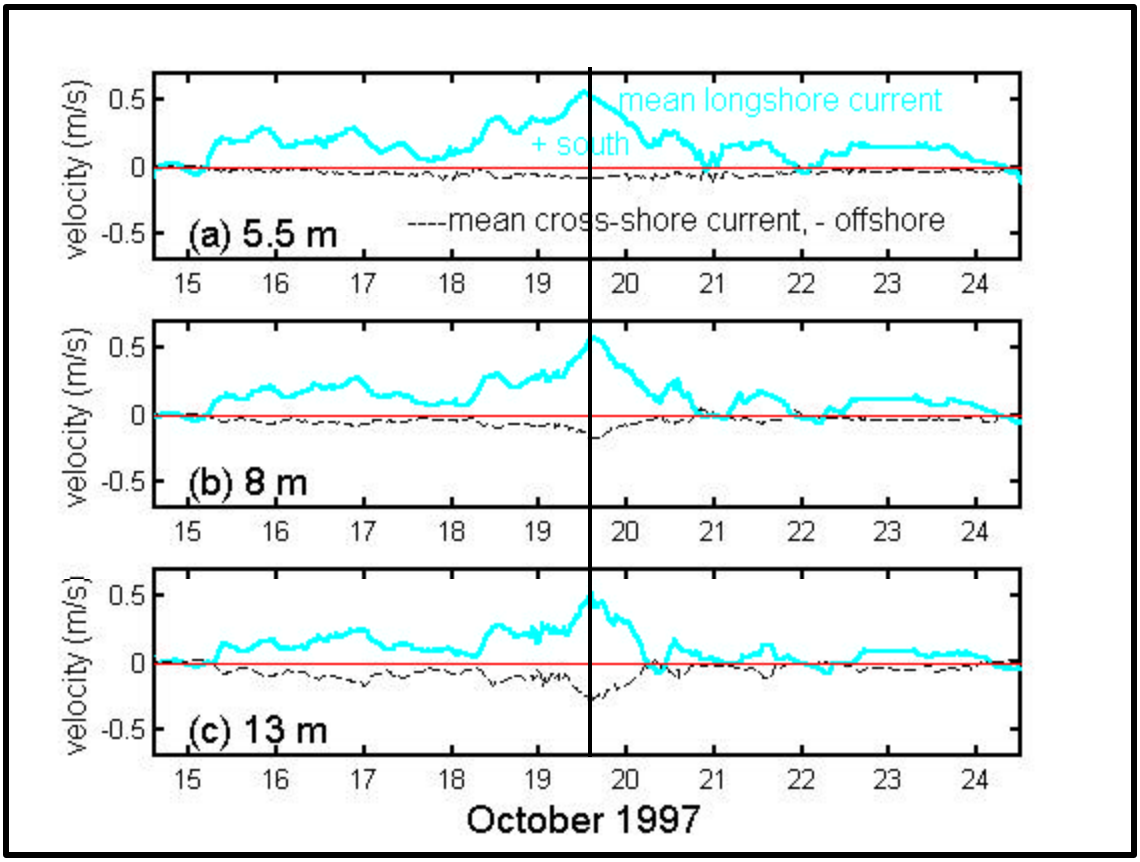

Figure 3.2. October 1997 longshore and cross-shore currents at (a) 5.5, (b) 8, and (c) 13 m water depths.

Inner Shelf Stratigraphic Signatures: 13 m site

Although many studies have documented hydrodynamic processes during storm events, the amplitudes and nature of seabed responses on the inner continental shelf have rarely been measured (Wright et al., 1994a). Figure 3.3a presents the seabed elevation changes measured in 13 m during October 1997. Seabed elevation measurements from a

210 kHz sonar altimeter (Fig. 3.3a, solid line) are compared with boundary detection of the seabed by a 4 MHz ADV (Fig. 3.3a, +), located 1.5 m away. Both instruments record the same trends in seabed elevation but are limited by the conditions in which they can precisely measure seabed elevations.

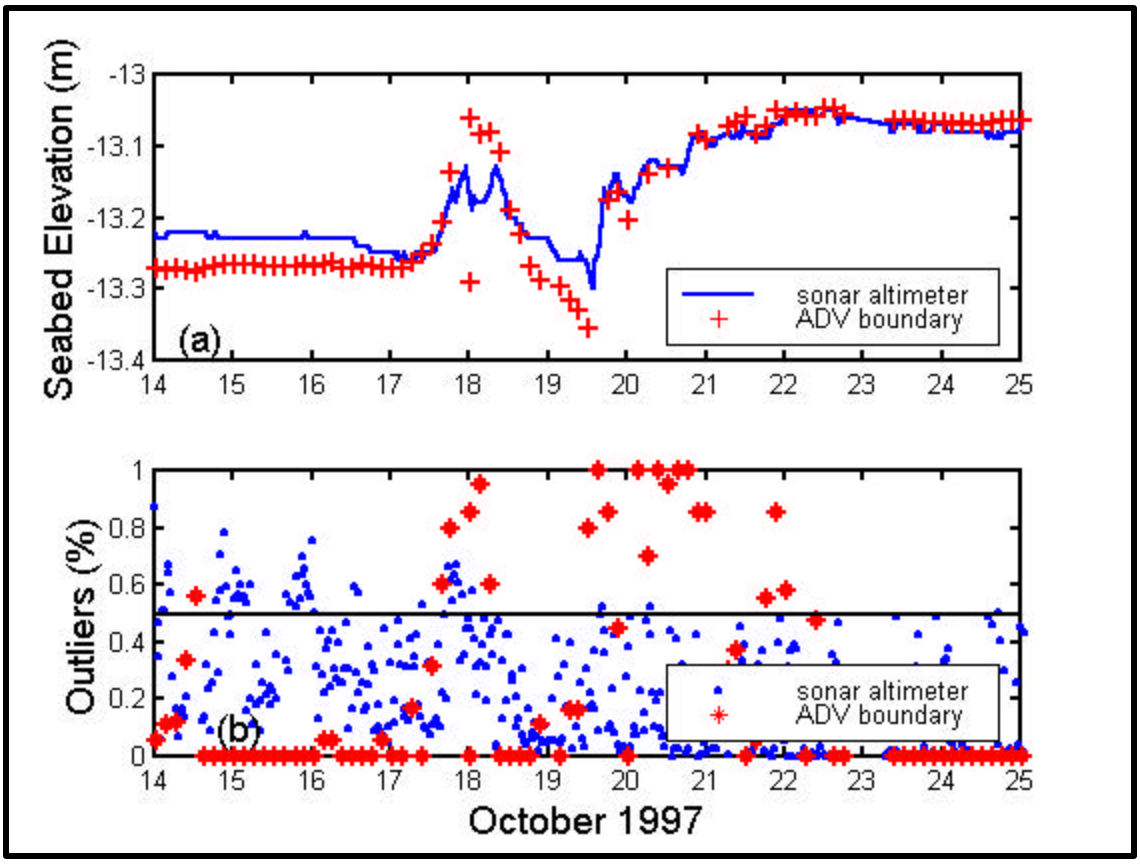

Figure 3.3. (a) Seabed elevation changes and (b) data outliers measured in 13 m water depth during October 1997.

Offsets in pre-storm seabed elevations on October 14 are < 6 cm (Fig. 3.3a) and may partially be attributed to the rippled seabed observed by SCUBA divers on October

14. ADV measurements of seabed elevation in an approximately 2 cm diameter footprint are robust with few outliers (Fig. 3.3b, stars), but sonar altimeter returns from a larger, approximately 20 cm diameter footprint cannot resolve bedforms with characteristic length scales < 20 cm. Although outliers, defined as all measurements outside the mode, are not uncommon in sonar altimeter measurements (Fig. 3.3b, dots), >50 % of the seabed measurements during several sampling intervals on October 14-16 were outliers. Higher variability in sonar altimeter measurements may be caused by (1) returns from the vertical extent of the footprint over a rippled seabed, (2) a change in the scattering properties of the seabed due to sediment dilation during ripple formation (Gallagher et al., 1996), or (3) bedform migration during longer sampling intervals.

ADV measurements of seabed elevation can be used to detect small scale ($\pm$1 cm) seabed elevation changes during non-storm conditions, but sonar altimeters are better instruments for documenting storm-induced seabed elevation changes on the inner shelf. With >50 cm/s currents measured on October 19, small ripples were likely replaced by a highly mobile plane bed in 13 m depth. With an approximately 20 cm diameter footprint, the sonar altimeter can measure the vertical excursion of a planar seabed more precisely than a rippled seabed (Fig. 3.3b, dots). Additionally, the higher frequency 4 MHz ADV measurements (Fig. 3.3b, stars) are not as robust as the lower frequency 210 kHz sonar altimeter measurements during the storm on October 18-22. The higher frequency measurements are more sensitive to suspended sediments. Concentrations of suspended fine sediments (<60 μm) were high during the storm, and samples exceeding 0.2 g/L

were collected near the seabed at the end of the FRF pier in 6 m water depth on October 20 (Battisto et al., 1999).

Figure 3.4 presents the xrays of cores collected on October 14 and 24. Both cores have been positioned along the sonar altimeter record according to the seabed elevation when they were collected. When depths, equal to negative elevations, are used to reference core features, either the entire range of a feature (e.g.- 13.25-13.30 m) or the depth downcore to the base of the feature and the side of the core (e.g.- 13.25 m (left)) may be given. Sediment peels provide additional information on the core structure; however, those images are not presented.

A pre-storm core was collected on October 14 when the seabed was at 13.22 m depth (Fig. 3.4, left). Preserved primary structures include sub-parallel laminations with 1-2 mm scale spacing in the lower portion of the core. Laminae are visible as alternating black and dark grey horizontal bands from 13.30-13.43 m. Core sediments are very fine sands: 3.7 ϕ at 13.25-13.27 m and 13.35-13.37 m and contain 4 % silt sized or smaller (<63 μm) sediment by weight (Fig. 3.5c).

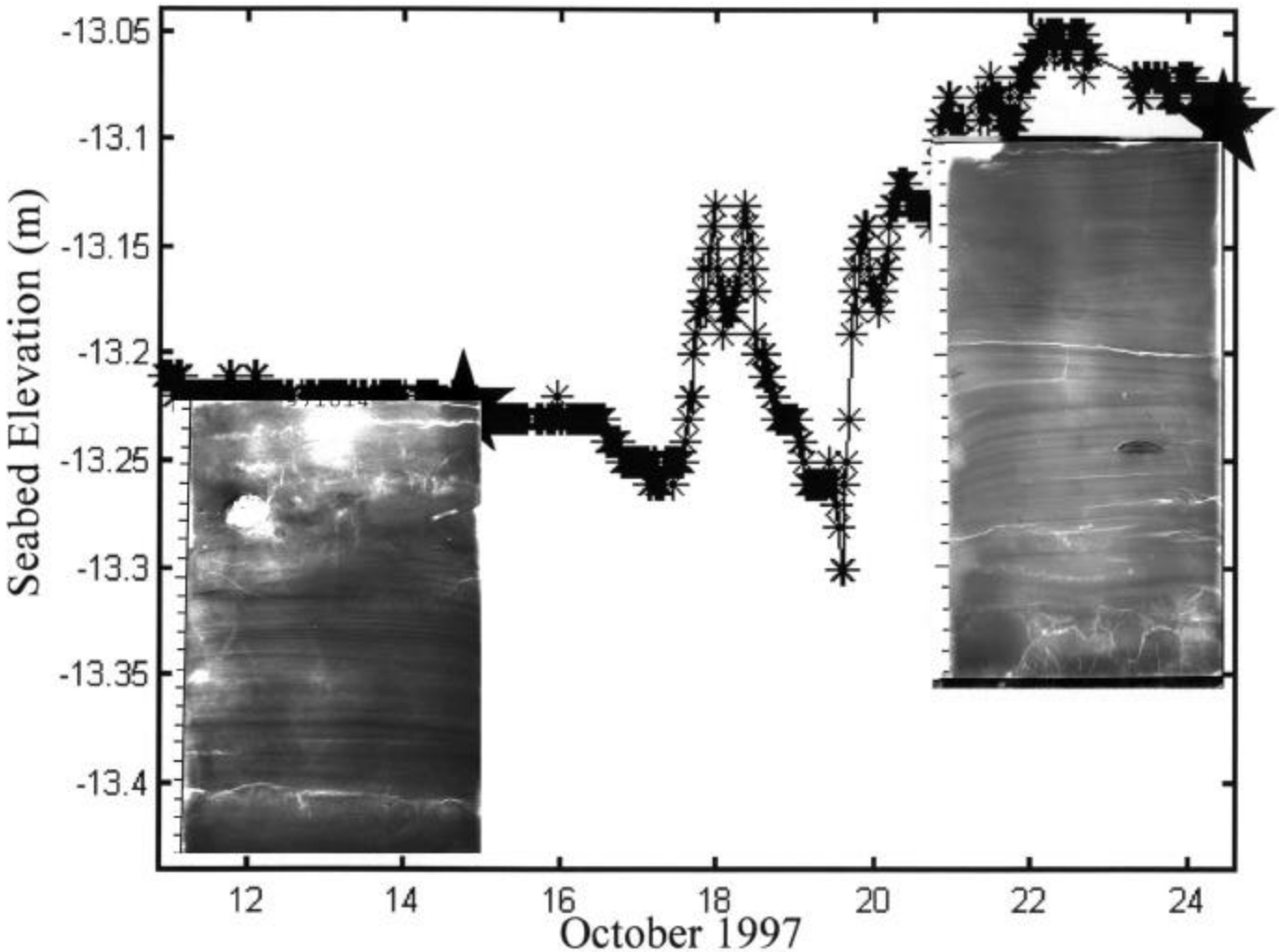

Figure 3.4. Xrays of pre-storm core collected on October 14 (left) and post-storm core collected on October 24 (right) on time-varying seabed in 13 m water depth. Offshore is to the right in xrays.

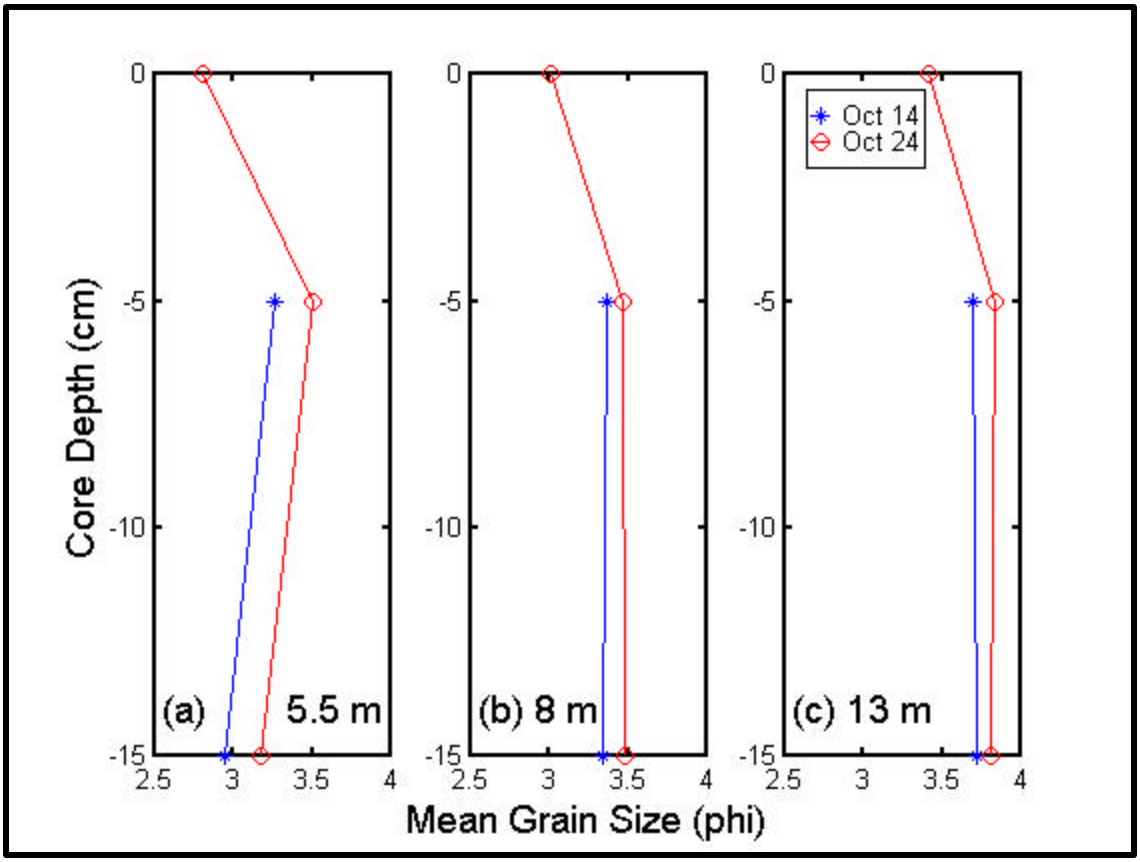

Figure 3.5. Mean grain size changes by depth downcore for boxcores collected on October 14 (stars) and 24 (circles) in 5.5 m (a), 8 m (b), and 13 m (c) water depths.

Secondary or biogenic core features include a bioturbated upper 9 cm (Fig. 3.4, left). Ripples and worm tubes were observed on the seabed when this core was collected, but bioturbation has removed any trace of ripple cross-laminations that might have been associated with the formation and migration of ripples. A gastropod shell fragment is visible as a light circle (left) at 13.29 m. Numerous polychaete worms have reworked the primary sediment structures and created less dense (lighter) areas of the core between

13.25-13.30 m and along the left side of the core to 13.37 m. Worm tubes are preserved at 13.29 m (right), 13.33 m (left), and 13.37 m (left). Cracks, visible as lighter areas near the core surface at 13.24 m (right), are an artifact of core processing and are not uncommon at the core surface, along bedding planes, or in the thinner region at the base of a core.

During the storm, the seabed eroded to 13.30 m depth at 1334 EST on October 19 (Fig. 3.6). Also at this time, mean cross-shore currents of 29 cm/s were directed offshore. Shortly thereafter at 1422 EST, maximum longshore currents of 52 cm/s to the south were measured (Fig. 3.2). Just over 2.5 hours after the seabed erosion maxima, wave heights reached a maximum of 3.49 m at 1708 EST (Fig. 3.6).

After 1334 EST on October 19, sediments began to accumulate. Since neither erosion nor deposition occur in a continuous manner in most environments, it is not surprising that cycles of deposition (Fig. 3.8, a-c) were followed by limited intervals of erosion during the net deposition of this storm deposit. Local maxima in seabed accretion appear to correspond with local maxima in wave height, whereas local maxima in erosion appear to correspond with local minima in wave height (Fig. 3.6).

Bed shear stress, τ_o, (Fig. 3.7) was calculated from measured mean currents according to the method in Chapter 1 (Eqns. 1 and 2). Maximum values of bed shear stress coincide with the seabed erosion maxima. As values of bed shear stress decreased, sediments were deposited.

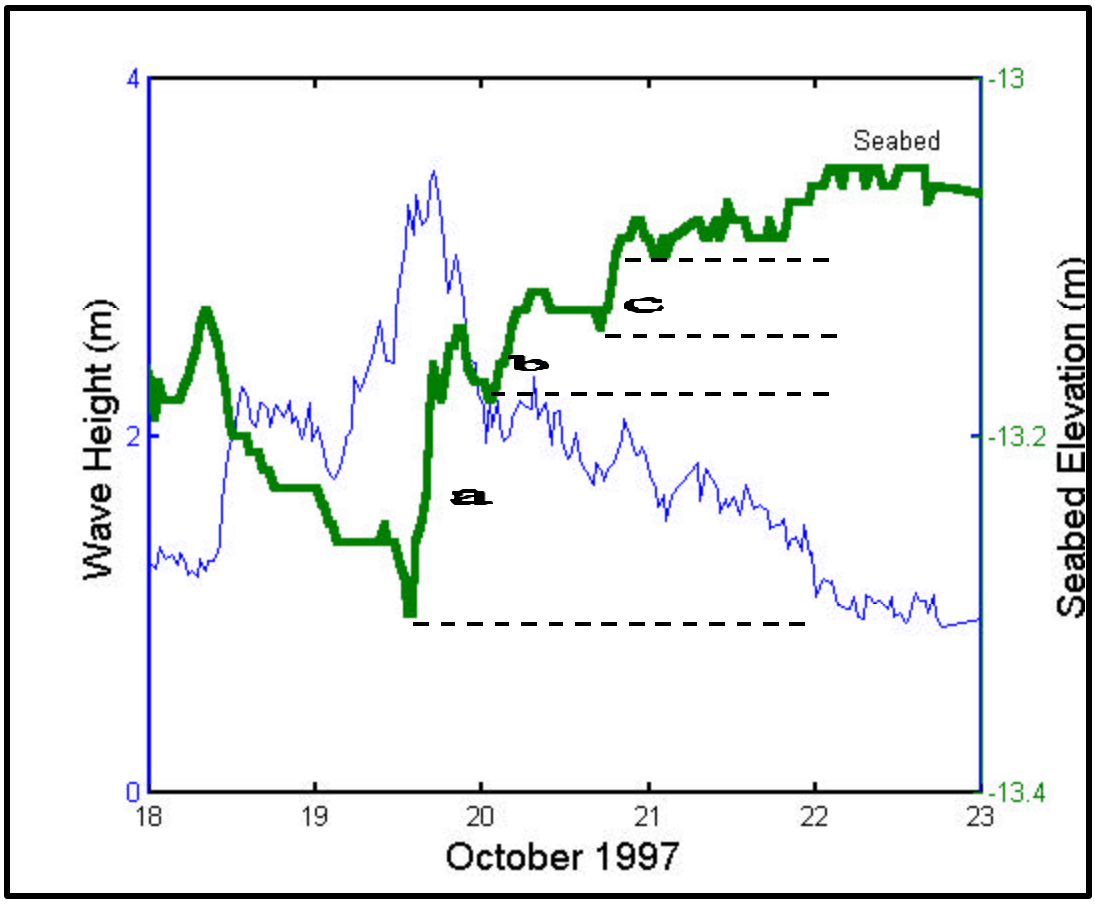

Figure 3.6. Wave height and seabed elevation changes associated with deposition of units a, b, and c in SandyDuck storm deposit at 13 m location.

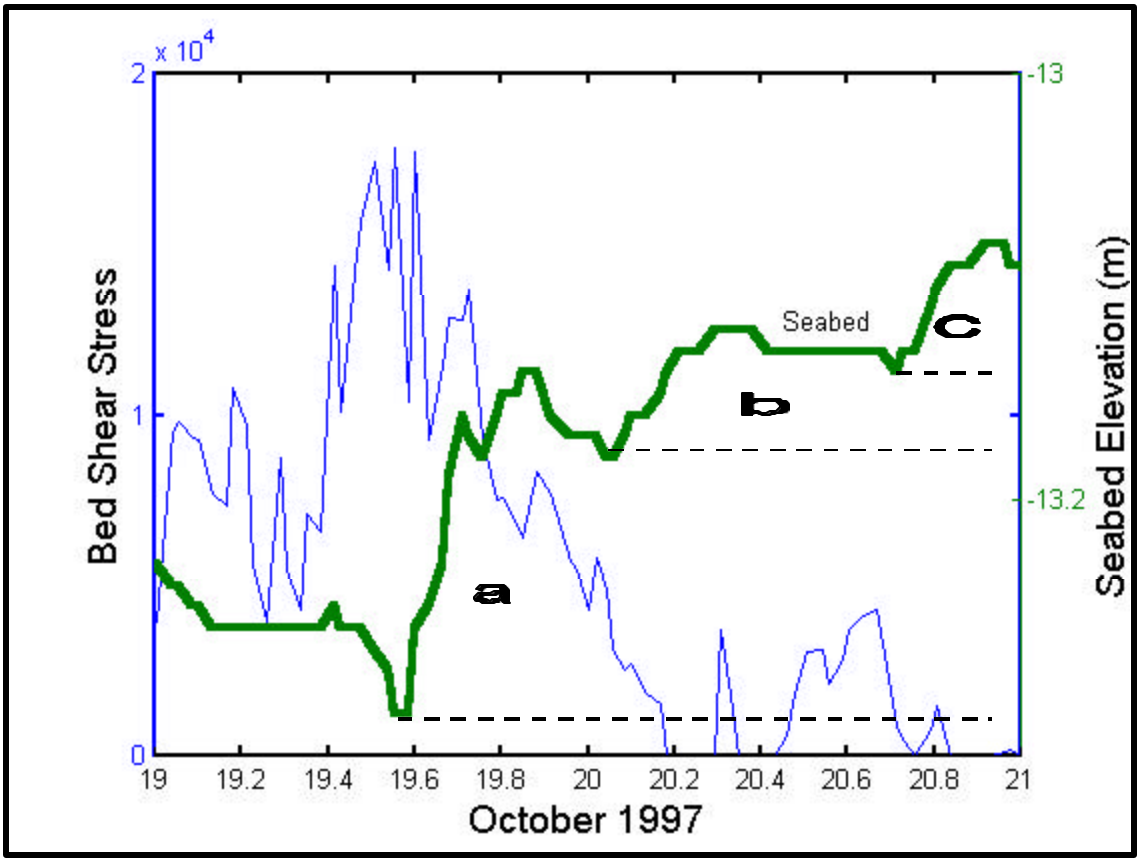

Figure 3.7. Bed shear stress and seabed elevation changes associated with deposition of units a, b, and c in SandyDuck storm deposit at 13 m location.

By October 24, the seabed was at 13.08 m depth when the post-storm core was collected (Fig. 3.8). Net deposition of 22 cm occurred since the storm erosion depth of 13.30 m at 1334 EST on October 19. The upper 2 cm of core sediments were likely reworked by post-storm seabed activity, so deposition of only the initial 20 cm of sediment during the SandyDuck storm is indicative of storm processes.

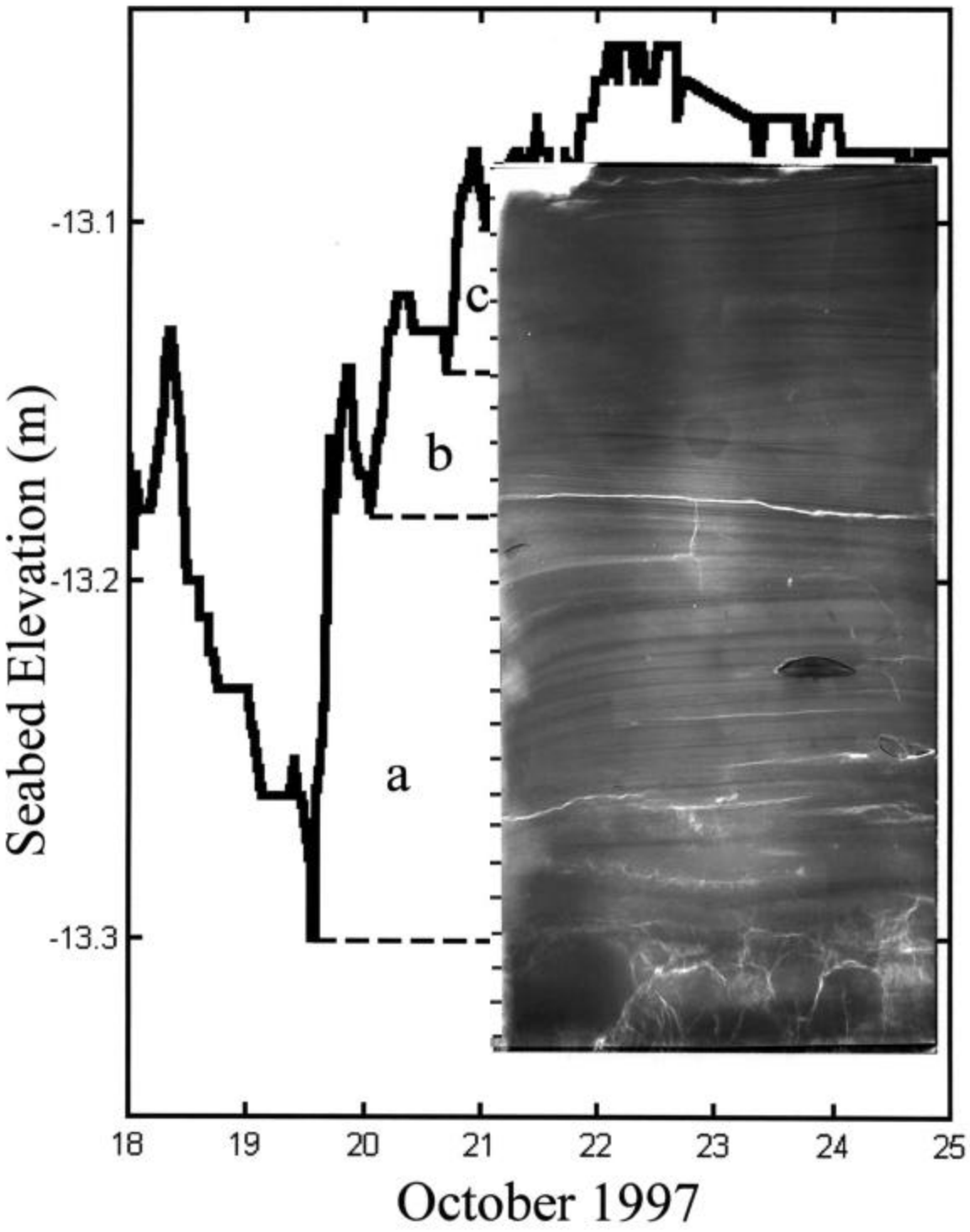

Figure 3.8. Xray of SandyDuck storm deposit. Core was collected on October 24, 1997 when seabed elevation (solid line) was -13.08 m.

According to the sonar altimeter record (Figs. 3.6-3.8, dark solid line), the initial 12 cm of storm strata in interval a (13.18-13.30 m) were deposited in the 3 hours following the storm erosion maxima. From 13.25-13.30 m depth, cross-bedded strata include numerous intact and fragmented small surf clams (*Mulinia lateralis*). At 13.23 m (right), a surf clam shell is convex up, whereas another surf clam fragment at 13.25 m (right) is concave up. Cracks (lighter areas) in the core above 13.30 m correspond with bedding surfaces. Above 13.25 m, cross-bedded sediments are replaced by alternating dark and light horizontal bands of parallel to sub-parallel laminated sediments with 1-4 mm thick laminae. The thinnest laminae are usually composed of fine sediments (usually dark bands), and the thickest laminae are coarser. Larger sand sized sediments are dominated by quartz, which is less dense than the finer, common heavy minerals, and will appear lighter in xrays. Sediments from 13.21-13.23 m are very fine sands (3.8 ϕ) and consist of 24% silt-sized or smaller sediments by weight (Fig. 3.5c). Above 13.21 m, laminae become increasingly thinner (1-2 mm thick).

The next 4 cm of storm strata (13.14-13.18 m) were deposited in the 3 hours following a local erosion maxima (Fig. 3.8, b). A crack across the core just above 13.18 m parallels the bedding. Sub-parallel laminations from 13.16-13.18 m are overlain by small scale onshore dipping cross-beds at 13.16 m and probably formed by ripple migration. From 13.14-13.16 m, larger scale cross-beds with an erosional base and topset, foreset, and toeset laminae may be classified as hummocky cross-stratification (Duke et al., 1991).

The next 4 cm of storm strata (13.10-13.14 m) were deposited in the 2.5 hours following another local erosion maxima (Fig. 3.8, c). Parallel to sub-parallel laminations with 1-2 mm thick laminae are dominant. Sediments are very fine sands (3.8 ϕ) and consist of 26 % silt-sized or smaller sediments by weight (Fig. 3.5c).

The variability in primary sediment structures in this storm deposit can be linked to fluctuations in hydrodynamic forcing. Although wave heights (Fig. 3.6) and associated orbital velocities increased to the peak of the storm, mean longshore and cross-shore currents and associated bed shear stresses (Fig. 3.7) were decreasing when cross-bedded strata were deposited at the base of the storm deposit (13.25-13.30 m). At maximum orbital velocities, parallel to sub parallel laminated sediments were deposited (13.18-13.25 m), potentially associated with plane bed conditions. As wave heights and currents continued to decrease, additional sub-parallel laminated sediments were deposited (13.16-13.18 m). As wave heights increased to another local maxima and cross-shore flows decreased, bedforms, presumably small ripples, migrated onshore and deposited onshore dipping foreset laminae (13.16 m). As longshore and cross-shore flows continued to decrease before reversing a few hours later, a hummocky cross-stratified unit was deposited (13.14-13.16 m). The upper 4 cm of sub-parallel laminated sediments (13.10-13.14 m) were deposited when currents were yet again decreasing after a local current velocity maxima on October 20.

Sediments deposited in 13 m may have originated from areas to the north since southerly longshore flows were common throughout this event. Even though cross-shore flows were dominantly directed offshore, reversals in flow direction were documented for

both longshore and cross-shore flows (Fig. 3.2) (P. Howd, pers. comm.). The increased percentage of silt in the cores may indicate an offshore source of sediments during periods of onshore flow, since inshore sediments are generally coarser (Fig 3.5c). A longer core on October 24 would have encountered another laminated zone below 13.33 m, comparable to the sediments collected below this depth on October 14, since these strata remained below the storm seabed erosion maxima of 13.30 m (Fig. 3.4).

Surf Zone Edge Stratigraphic Signatures: 8 m site

On October 14, the seabed was at 7.85 m depth when a pre-storm core was collected (Fig. 3.9, left) at the 8 m site. Primary sediment structures include sub-parallel laminations at the core surface from 7.85 - 7.87 m. From 7.87 - 7.89 m, increased abundance of denser heavy minerals create a darker zone on the xray. The absence of distinct laminations below 7.89 m is attributed to bioturbation. A 3 cm length of a polychaete worm tube is preserved in the sediment peels at 7.95 m. An articulated bivalve is present at 7.94 m (center), and a gastropod is located at 8.01 m (left). Little surf clams (*Mulinia lateralis*) occur throughout the core and are concentrated at 7.89 m (left) with small gravel. Core sediments are fine sand: 3.4 ϕ at 7.88-7.90 m and 3.3 ϕ at 7.98-8.0 m (Fig 3.5b).

During the northeaster storm on October 19, wave heights reached 3.44 m at 1600 EST, and the edge the surf zone moved offshore, almost to 7 m depth. A seabed erosion

maxima of 7.97 m occurred at 1216 EST. Maximum mean currents were recorded at 1516 EST and were directed offshore at 18 cm/s and south at 58 cm/s.

On October 24, a post-storm core was collected in 7.84 m depth and documented net deposition of 13 cm. The initial 8 cm of storm strata (7.89-7.97 m) were deposited in the 1.5 hours following the storm erosion maxima (Fig. 3.10, a) when wave heights and currents were all increasing. Primary core features include a lag or accumulation of shell and gravel from 7.89-7.92 m, dominated by numerous intact and fragmented small surf clams in both concave and convex up positions. The lack of a basal erosion contact in the core at 7.97 m is somewhat surprising.

Above 7.89 m, the shell and gravel lag deposit is overlain by cross-stratified sediments with cracks visible along bedding planes from 7.84-7.86 m (Fig. 3.10). The 4 cm of sediment from 7.85-7.89 m (Fig. 3.10, b) were deposited during decreasing longshore and cross-shore currents and a local maxima in wave height. A high concentration of heavy mineral sediments form a dark layer in the xray at 7.87-7.88 m.

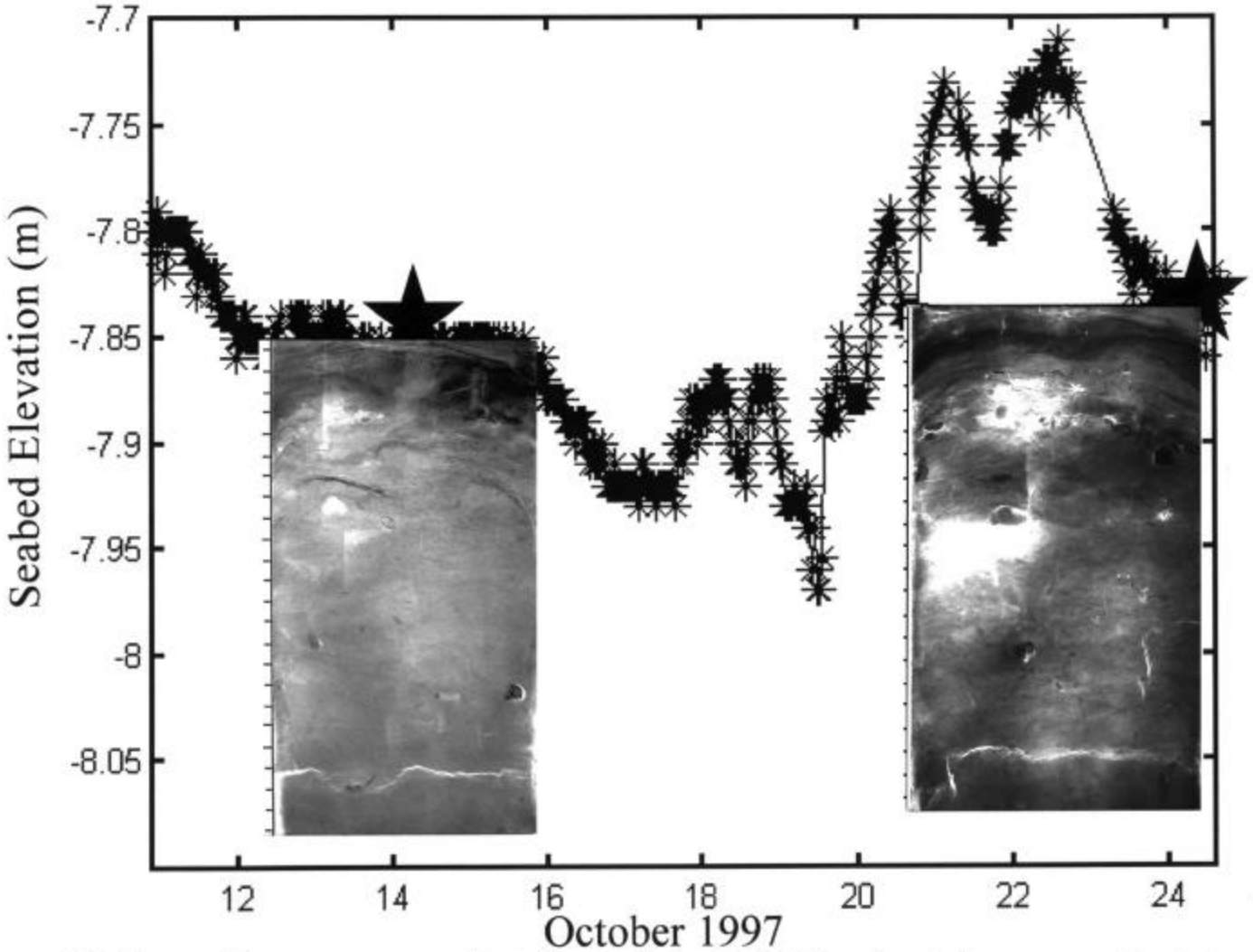

Figure 3.9. Xrays of pre-storm core collected on October 14 (left) and post-storm core collected on October 24 (right) on time-varying seabed in 8 m water depth. Offshore is to the right in xrays.

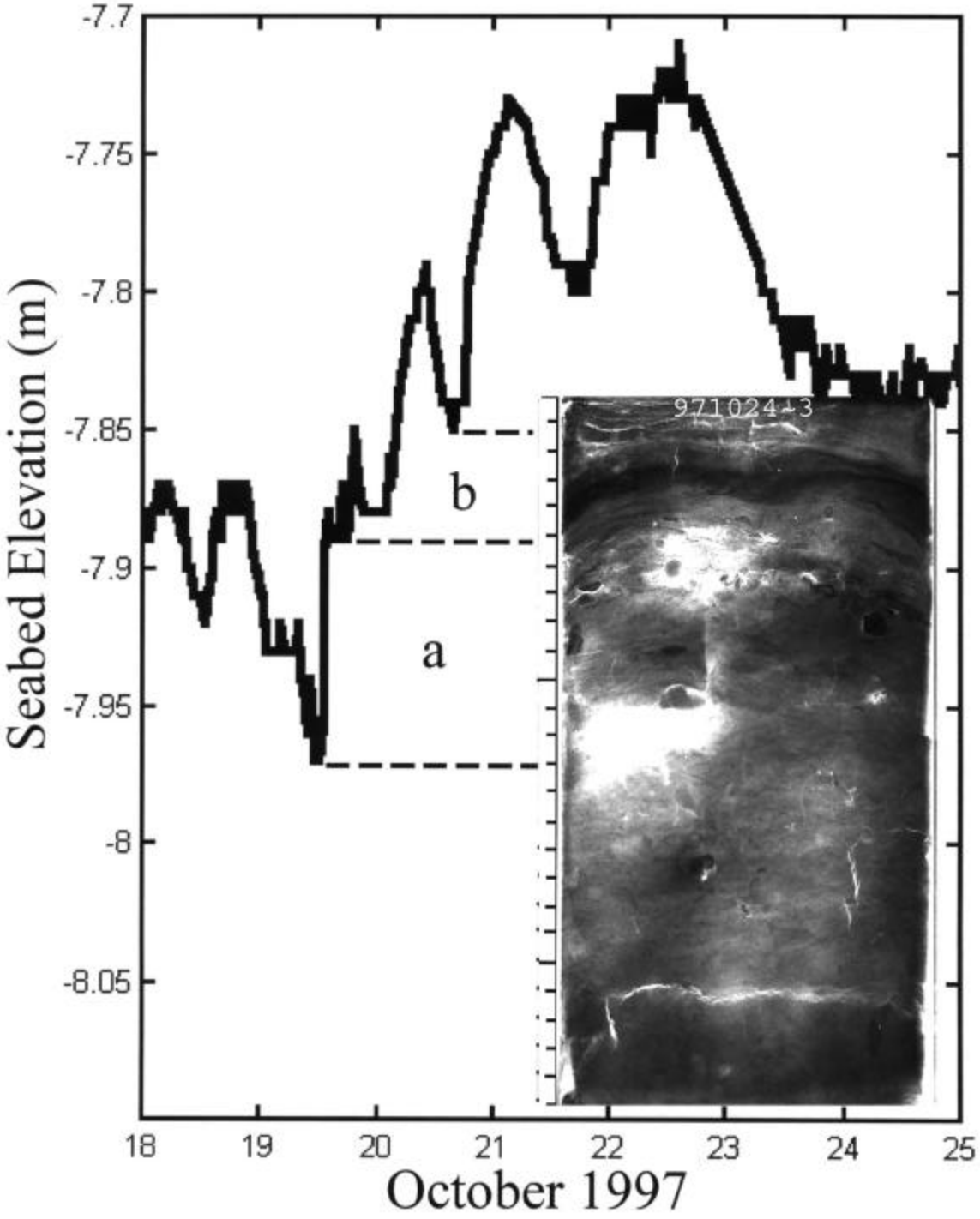

Figure 3.10. Xray of SandyDuck storm deposit. Core was collected on October 24, 1997 when seabed elevation (solid line) was -7.85 m.

Sediments from 7.88-7.90 m are fine sands (3.5 ϕ) with 4 % silt-sized or smaller sediments by weight (Fig 3.5b).

Physical processes which correspond with post-storm core features include increasing currents and wave heights during deposition of a surf clam and gravel lag at 7.89-7.92 m. Cross-bedded sediments dominated by heavy minerals were deposited from 7.85-7.89 m during decreasing currents and a local maxima in wave height. As expected, sediments below 7.97 m are indeed similar to sediments below 7.97 m in the pre-storm core collected on October 14; however, absence of a distinct basal erosion contact in the post-storm core was not expected.

Surf Zone Stratigraphic Signatures: 5.5 m site

On October 14, the seabed was at 5.76 m depth when a pre-storm core was collected at the 5.5 m site (Fig. 3.11, left). Cross-bedding from 5.81-5.83 m and parallel to sub-parallel laminations from 5.83-5.85 m are the dominant primary structures in this core. Below 5.80 m, polychaete worm tubes (light, irregular 2-3 mm diameter tubes) are common but are not as prevalent in the upper 5 cm. The upper 5 cm from 5.76-5.81 m and all sediments downcore from 5.85 m are bioturbated. A surf clam shell is convex up at 5.93 m (right). Grain size analyses indicate core sediments from 5.79-5.81 m are fine sands (3.3 ϕ) with only 2 % silt sized or smaller sediments by weight (Fig. 3.5a).

During the SandyDuck northeaster storm, wave heights reached 2.69 m and maximum currents of 57 cm/s to the south were recorded by 1216 EST on October 19. Unfortunately, a data gap exists for several hours beginning 1216 EST on October 19

when the seabed had eroded to 5.95 m. This instrumentation was not working from 1216-2200 EST. Wave heights, currents, and seabed elevation changes may have exceeded the values recorded at 1216 EST, so these storm parameters will be used cautiously.

On October 24, the seabed was at 5.81 m depth when a post-storm core was collected (Fig. 3.12) to document net deposition of 15-18 cm that occurred since the height of the storm. Post-storm core features include parallel to sub-parallel laminations above 5.99 m and numerous small surf clam shells at 5.95-5.96 m. Below 5.99 m the sediments lack primary structures like the sediments below 5.99 m in the core collected on October 14 (Fig. 3.11). Although the maximum depth recorded by the altimeter was 5.95 m, the continuous nature of boxcore deposition above a distinct basal erosion contact (Fig. 3.12, a) indicates an erosion depth of 5.99 m was likely on October 19.

Assuming a maximum depth of erosion of 5.99 m, 4 cm of parallel to sub-parallel laminated sediments (5.95-5.99 m) with 1-4 mm thick laminae were deposited following the storm erosion maxima (Fig. 3.12, a). Primary core features also include a lag of shell and gravel from 5.95-5.96 m, dominated by numerous intact and fragmented small surf clams (*Mulinia lateralis*) in both concave and convex up positions. This shell and gravel lag corresponds to a horizontal crack (light band) across the core. Grain size analyses indicate core sediments near this lag deposit (5.94-5.96 m) are fine sands (3.2 ϕ) with only 1 % silt sized or smaller sediments by weight (Fig. 3.5a).

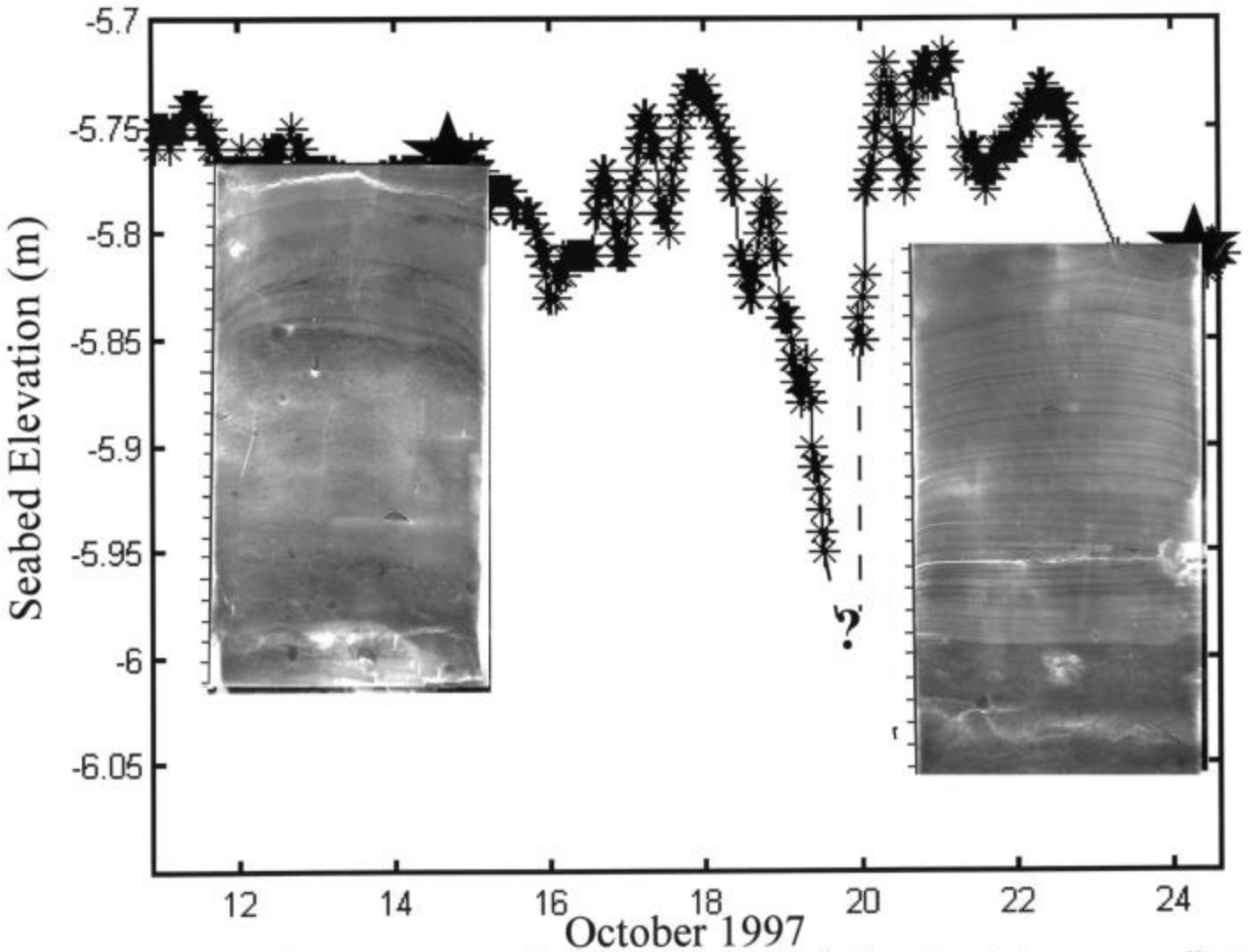

Figure 3.11. Xrays of pre-storm core collected on October 14 (left) and post-storm core collected on October 24 (right) on time-varying seabed in 5.5 m water depth. Offshore is to the right in xrays.

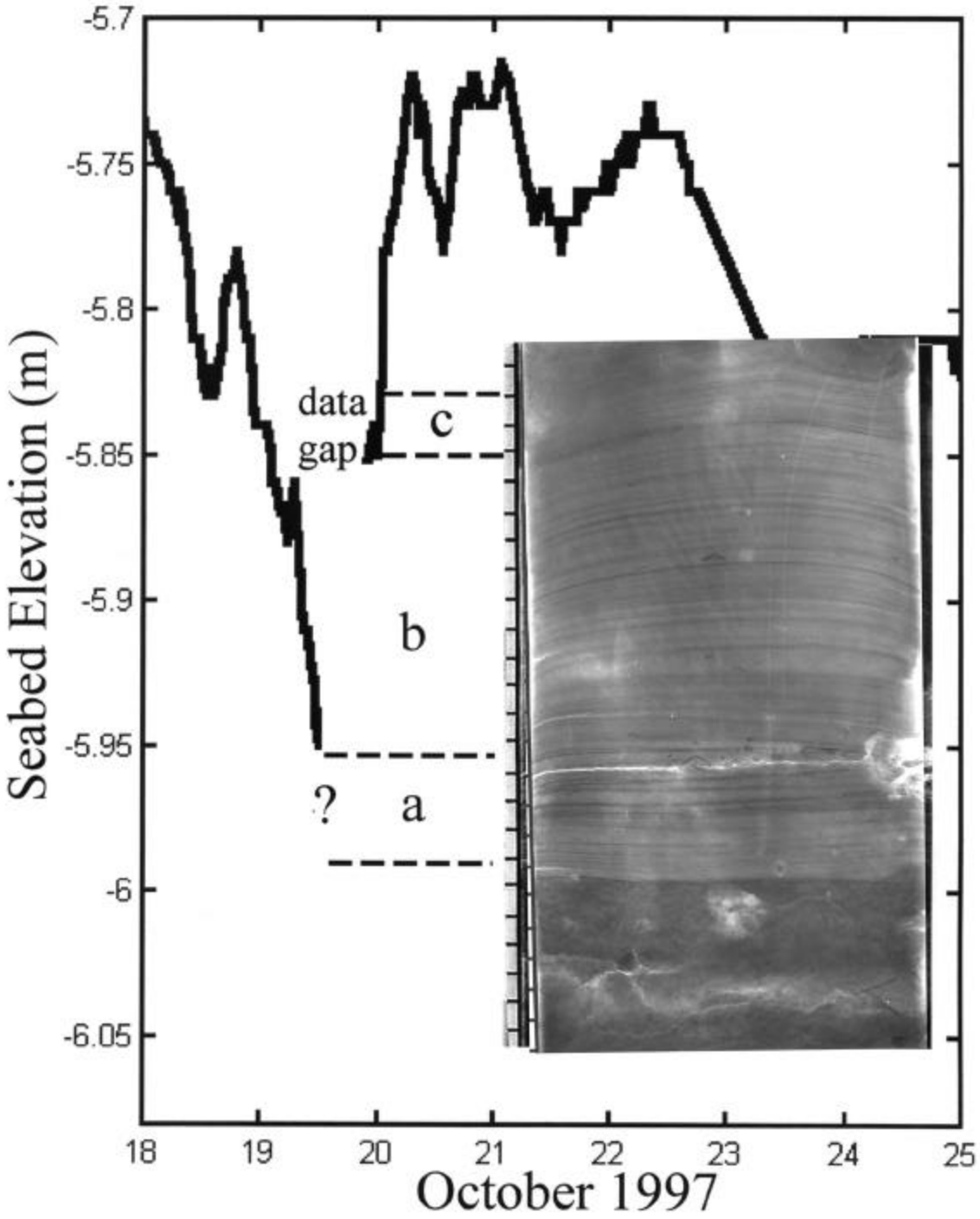

Figure 3.12. Xray of SandyDuck storm deposit. Core was collected on October 24, 1997 when seabed elevation (solid line) was -5.81 m.

The shell lag deposit is overlain by more alternating dark and light bands of parallel to sub-parallel laminated sediments. The 10 cm of sediment from 5.85-5.95 m (Fig. 3.12, b) may have been deposited during decreasing longshore and cross-shore currents and decreasing wave height. Sediments from 5.84-5.86 m are fine sands (3.5 ϕ) with 4 % silt sized or smaller sediments by weight (Fig. 3.5a).

By late October 19, the instruments were again recording data. The 3 cm of sediment from 5.82-5.85 m (Fig. 3.12, c) were deposited during increasing longshore and cross-shore currents and decreasing wave height. Sub-parallel laminations (2-3 mm thick) are overlain by ripple cross-stratified sediments beginning at 5.83 m.

Observations of physical processes that correspond with post-storm core features were limited by a data gap for 10 hours during the storm. The upper 3 cm of the storm deposit (5.82-5.85 m) were created during increasing currents and decreasing wave height. The presence of a distinct basal erosion contact in the post-storm core indicates a total of 18 cm of sediment can be attributed to surf zone processes during this northeaster storm. Sediments below the erosion maxima of 5.99 m on October 24 lack primary sediment structures, have probably been reworked by bioturbation, and appear similar to sediments below 5.99 m on October 14.

Discussion

Remote acoustic observation of the seabed and diver-collected cores were combined to document seabed fluctuations of approximately 25 cm in 5.5, 8, and 13 m water depths during a 10 day interval in October 1997 that included a northeaster storm

(Fig. 3.1). Although a previous deployment in 14 m depth offshore of the FRF during 1992 measured seabed fluctuations up to 18 cm (Wright et al., 1994a), nearshore scientists are just beginning to attribute sonar altimeter measurements of seabed elevation changes in excess of 10 cm to factors other than scour around instrument frames (Gallagher et al., 1998). Although some scour probably occurred around instrument pipes, the corroborating locations of (1) basal erosion contacts in cores collected at least 1 meter away from the frames and (2) sonar altimeter measurements of erosion maxima below the frames (Figs. 3.6-12) indicates scour around pipes was minimal.

Sediment Mobility

As post-storm cores illustrate, sediments deposited during storms record surf zone and inner continental shelf processes and can be collected after these processes have diminished. According to seabed elevation data, storm deposits reached maximum thickness of 25 cm at all locations, but sampled storm deposits are only 18 cm thick at 5.5 m, 13 cm thick at 8 m, and 22 cm thick at 13 m due to erosion during subsequent seabed activity. Sediments transported to 5.5 m and 8 m water depth and deposited in the surf zone during the storm did not remain above the pre-storm seabed level by October 24 (Fig. 3.1). In contrast, 15 cm of sediment transported to an inner shelf location in 13 m water depth remained above the 'pre-storm' seabed level through November 1997 (Fig. 3.7), resulting in net post-storm accretion only on the inner shelf.

Steve Elgar (pers. comm.) collected sonar altimeter measurements of seabed elevation changes inshore of 5.5 m water depth during this storm. In the inner surf zone, the seabed eroded on October 17-18, remained in an eroded state until October 20, and then began to accrete. By October 22, the seabed between 260 m and 390 m offshore had returned to the pre-storm elevation measured on October 17 (pers. comm. Steve Elgar). Foreshore surveys conducted by List and Farris (1999) also document erosion from October 13-20, and the accretional pattern along the beach from October 20-25 was nearly a mirror image of the previous erosional pattern. Since altimeters and beach surveys inshore of 13 m did not record net erosion or accretion, the sediments deposited at 13 m during this northeaster storm may have originated from a source outside of the SandyDuck instrument array-either further offshore or alongshore.

Since sediment is suspended during storms, it is unlikely that all sediment is deposited where it was initially eroded. Maintaining the equivalent of 10+ cm of 'eroded' sediment in suspension is inconsistent with measured sediment concentrations. Even though respective concentrations of suspended sands and fines approached 1 g/L and 0.1 g/L at 2003 EST in 6 m depth on October 19 (Battisto et al., 1998), these concentrations are much less than would be created by mixing 10 cm of sediment throughout the water column of a 1 km wide surf zone. With wave orbital velocities suspending sediments, mean currents with velocities exceeding 50 cm/s would advect sediments. Further evidence of sediment transport includes consistently finer mean grain sizes at all locations (Fig. 3.5) in all depths downcore. Since mean grain size decreased by 0.1-0.2 ϕ

at all locations, the source of sediment is further indicated to be finer sediments from offshore or longshore.

Even if longshore or offshore sources of sediment could be identified, the effects of seabed microstratigraphy of the upper 30 cm sediment column must be considered. As these cores have shown, grain diameters are not homogeneously distributed below the seabed surface but vary appreciably over short depth intervals (cm scale). As successive layers are exhumed during an erosion event, the mean grain size of sediments at the sediment water interface may change and thus sizes of grain-size dependent bedforms may change.

Primary sediment structures

With coincident measurements of hydrodynamic forcing, the primary structures in storm signatures can be characterized as follows:

Parallel to sub parallel laminations: are deposited in inner continental shelf and surf zone environments. Units are 10+ cm thick and may include shell lags. Individual laminae are 1-4 mm thick. Laminae were deposited during increasing wave heights and decreasing (at 13 m) or increasing (at 5 m) mean currents.

Cross-stratified units: are deposited in inner continental shelf and surf zone environments. Units are 2-6 cm thick and are deposited above shell lags (at 8 m) and basal erosion contacts (at 13 m). Individual laminae are 1-3 mm thick. Cross-stratified sediments include ripple cross-stratification and an occurrence of hummocky cross-

stratification. These units were deposited during gradients in physical processes including increasing and decreasing wave heights and decreasing (at 8 m and 13 m) or increasing (at 5 m) mean currents.

Shell and gravel lag deposits: are deposited in inner continental shelf and surf zone environments. Units are 1-4 cm thick and are deposited above bioturbated sediments (at 8 m) and parallel to sub-parallel laminations (at 13 m). Lags are deposited during increasing wave heights and increasing (at 8 m) mean currents.

Basal erosion contacts: were very distinct in surf zone sediments from 5 m and are slightly obscured by the thin sediments at the core base in 13 m. However, an anticipated basal erosion contact at 7.97 m was not present in the core collected on October 24.

Recent observations of seabed accretion events by Hanes et al. (1998) along a 1.5 m cross-shore array have documented similar magnitudes of seabed erosion followed by mm scale seabed accretion in 4 m water depth during this SandyDuck northeaster storm. The post-storm core collected 200 m offshore at 5.5 m depth (Fig. 3.12) documents mm scale parallel to sub parallel laminations during the same storm when these mm scale accretion events were observed in 4 m depth. Laboratory observations of migrating low-relief bed waves over aggrading plane beds result in deposition of planar laminae (Bridge and Best, 1997); a similar mechanism may be responsible for the creation of these laminated storm sediments.

Preferentially oriented shells, hummocky cross-stratification (Fig. 3.7, 13.14-13.16 m), and ripple cross-stratification were documented in these storm deposits. Although these sedimentologic features have been described (Morton, 1988) and modelled (Clifton, 1976; Myrow and Southard, 1991) as diagnostic features of marine storm deposits, these cores validate previous studies and provide opportunities to test models of storm deposition in future studies.

Deposition rates

Only 4-20 hours of deposition are recorded in storm deposits from the surf zone and inner continental shelf. According to sonar altimeter data, these sediments accreted in 2 or more phases. Deposition rates may have been fast as 5 cm/hr at the base of these deposits, but all deposition rates exceed 1 cm/hr.

Storm deposits are associated with rapid erosive and depositional events in seabed elevation records(Smith et al., 1995). However, not every rapid erosion and deposition event observed in the nearshore can be attributed to a storm deposit, since migrating bedforms can cause large excursions of the seabed (Gallagher et al., 1998). Although 'event' deposits form a majority of modern and ancient nearshore sedimentary strata, these units form during a minor percentage of the time (Dott, 1996).

Conclusions

Combining deployed instrumentation and diver-operated cores in the nearshore is critical to better understanding sediment fabric. This combination has proved successful

in documenting the sedimentary strata created by a northeaster storm. Storm deposits from the surf zone and inner continental shelf reached a maximum thickness of 25 cm at all locations, but sampled storm deposits are only 18 cm thick at 5.5 m, 13 cm thick at 8 m, and 22 cm thick at 13 m due to post-deposition erosion by subsequent seabed activity. Storm sediments accreted in 2 or more phases that totaled 4-20 hours. Deposition rates may have been fast as 5 cm/hr at the base of these deposits, but all deposition rates exceed 1 cm/hr. Since mean grain size decreased by 0.1-0.2 ϕ at all locations, the source of sediment which resulted in 15 cm of net deposition on the inner shelf was probably further offshore or to the north.

Primary sediment structures created by a northeaster storm include parallel to sub parallel laminations, cross-stratification, shell and gravel lags, and basal erosion contacts. Laminae were 1-4 mm thick and were deposited during increasing and decreasing wave heights and decreasing (at 8 m and 13 m) or increasing (at 8 m and 5 m) mean currents.

CHAPTER 4

EVALUATING PROFILE DATA AND DEPTH OF CLOSURE WITH SONAR ALTIMETRY

Introduction

Establishing the climatology of the shoreface sediment prism is critical for understanding coastal evolution and nearshore sediment budgets for sandy coastal environments. One important engineering parameter, the seaward limit of *significant* net sediment transport, or the depth of closure, D_c, has traditionally been determined by comparing cross-shore profiles to locate the point beyond which negligible vertical change has occurred. Although D_c is expected to vary with environmental conditions and time scales, the depth limitations of most beach and nearshore profiling methods do not permit estimation of D_c for all events (Nicholls et al., 1998; Birkemeier et al., 1999).

Numerous studies have analyzed beach profile data sets for the impacts of storms (Lee et al., 1998; Birkemeier et al., 1999), D_c limits for event-dependent and time-interval cases (Nicholls et al., 1998), and seasonal patterns of cross-shore sediment movement (Aubrey, 1979; Larson and Kraus, 1994). Extensive beach/nearshore profile data spanning almost 20 years have been collected at sites such as the US Army Corps of Engineer's Field Research Facility (FRF) in Duck, NC. Analyses of these data indicate that seabed elevation changes occur rapidly during storms. Although post-storm recovery

can occur quickly on the inner profile, recovery on the upper shoreface (> 5 m depth) occurs very slowly (Birkemeier et al., 1999).

Due to physical limitations of survey equipment and personnel, beach profiles are surveyed pre-storm and during some stage of the post-storm beach recovery process when hydrodynamic and meteorological conditions permit. By comparing pre- and post-storm surveys, *integrated* effects of storms on beach profiles and D_c can be assessed. These surveys do not document the absolute timing or magnitude of sediment erosion and accretion during storms (Pilkey et al., 1993). Additional measurements of seabed elevation changes are required to define the shoreface erosion and recovery process. To incorporate seabed elevation changes throughout storms and extend observations to 13 m depth, we use continuous data from downward-looking sonar altimeters to evaluate the seabed elevation changes measured by less frequent beach profiles.

First, we describe the long-term field deployment during which our data were collected. Next, we describe the method for establishing the chronology of seabed elevations with beach profiles and remotely sensed acoustic seabed elevation data at 3 cross-shore locations. Finally, we present our results that document traditional beach profile measurements of D_c for a particular event do not fully resolve seabed elevation variability during storms.

Seabed Elevation Data

Study Area

The US Army Engineer Field Research Facility (FRF) is located on the Atlantic Ocean in Duck, NC, near the middle of Currituck Spit along a 100 km stretch of shoreline. Offshore contours (Fig. 4.1) are relatively straight to 13 m depth with some

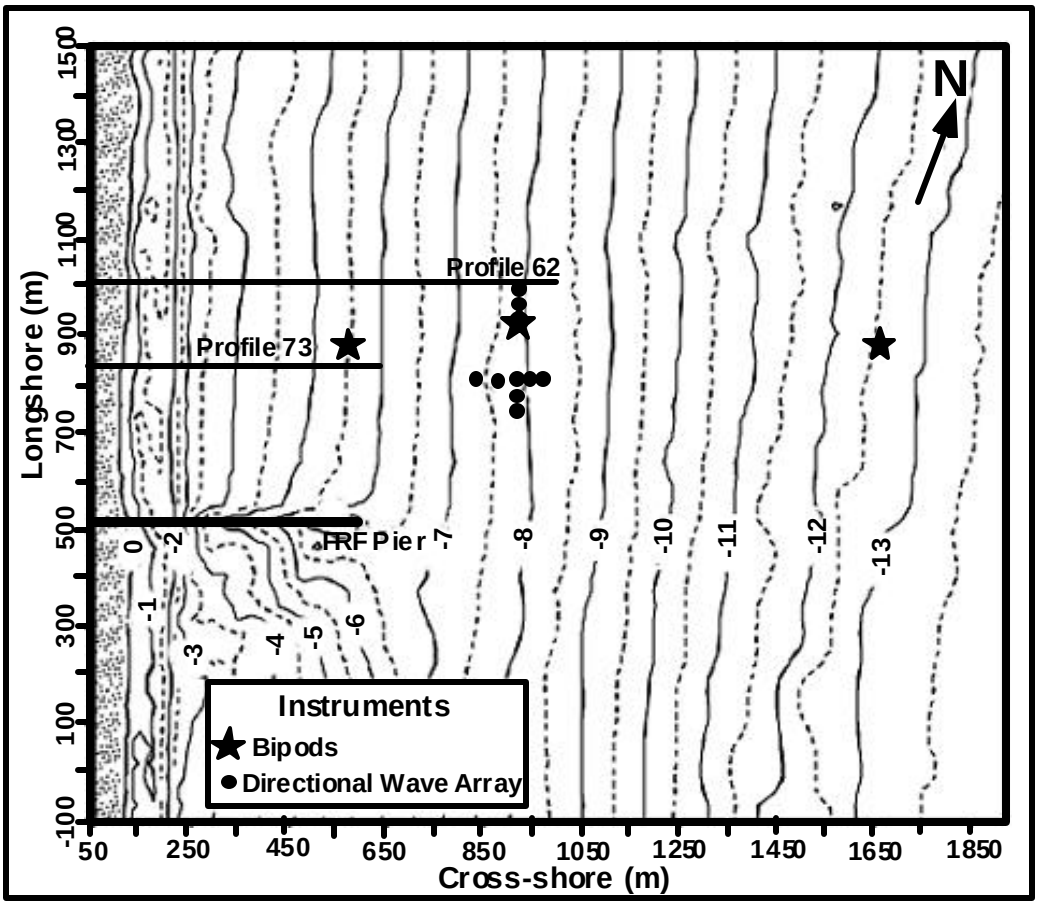

Figure 4.1. Location of bipod instrumentation and Profiles 62 and 73 at the Field Research Facility. Contours are in meters.

irregularities adjacent to the research pier. One or two nearshore sandbars are usually present (Lippmann and Holman, 1990). Sediments consist primarily of quartz sand, with a secondary component of rock-fragment and shell gravel (Meisburger and Judge, 1989). In the outer littoral zone where D_c is often observed (Nicholls et al., 1998), sediments become finer offshore to 13 m depth (Schwartz et al., 1997) and are well-sorted fine to very fine sands (0.21 to 0.07 mm or 2.3 to 3.8 ϕ).

Tides are semi-diurnal and have a mean range of approximately 1 m. Average annual significant wave height is 1.0 $\pm$ 0.6 m (1980-1991) with a mean peak spectral period of 8.3 $\pm$ 2.6 s (Leffler et al., 1993). Extratropical northeasters are the most common significant storms with increased incidence in fall, winter and early spring months. Tropical storms and hurricanes can occur from July to October but are not as common.

Beach Profile Data

Beach profiles to 8 m depth are collected biweekly and after storms when wave heights are less than 2 m. Profiles are surveyed with the Coastal Research Amphibious Buggy (CRAB), a 10-m tall amphibious vehicle. Offshore distances are measured relative to a shore parallel baseline located behind the frontal dune. Elevation data are referenced to the 1929 National Geodetic Vertical Datum (NGVD). Horizontal and vertical accuracy of the CRAB survey system is approximately $\pm$ 3 cm.

Survey data from July 1981 to July 1993 were used by Nicholls et al. (1998) to evaluate D_c. They found that beach surveys to 8 m are occasionally of insufficient length to document D_c for the largest events. In a recent study of these data collected between 1981 and 1991, Lee et al. (1998) examined the cross-shore movement of sediments and the importance of storms and storm groups on nearshore morphology. Extending this study through 1998, Birkemeier et al. (1999) found that the deepest, most significant changes resulted from sequences of two or more storms occurring within a period of less than 40 days with each storm having root-mean-square wave heights >3.15 m.

Bipod Instrumentation

The need for continuous seabed observations across and beyond the nominal surveying limit of 8 m motivated the deployment of seabed monitoring instruments. Instrument packages to monitor waves, currents, and seabed elevation changes were deployed in 5.5 and 13 m water depths in September and October 1994 (Fig. 4.1). In May 1995, a third instrument package was deployed in 8 m water depth.

Instrument packages are secured on 'bipod' frames (Fig. 4.2) designed to sleeve over two 6.4 m long pipes jetted vertically 4 m into the seabed. Power and communications are provided from shore via armored multi-conductor cables. Except for sensor repairs or replacement, these instrument packages have been collecting data since fall 1994. During August - December 1995, all 3 bipods were continuously monitoring conditions in 5.5, 8, and 13 m depths.

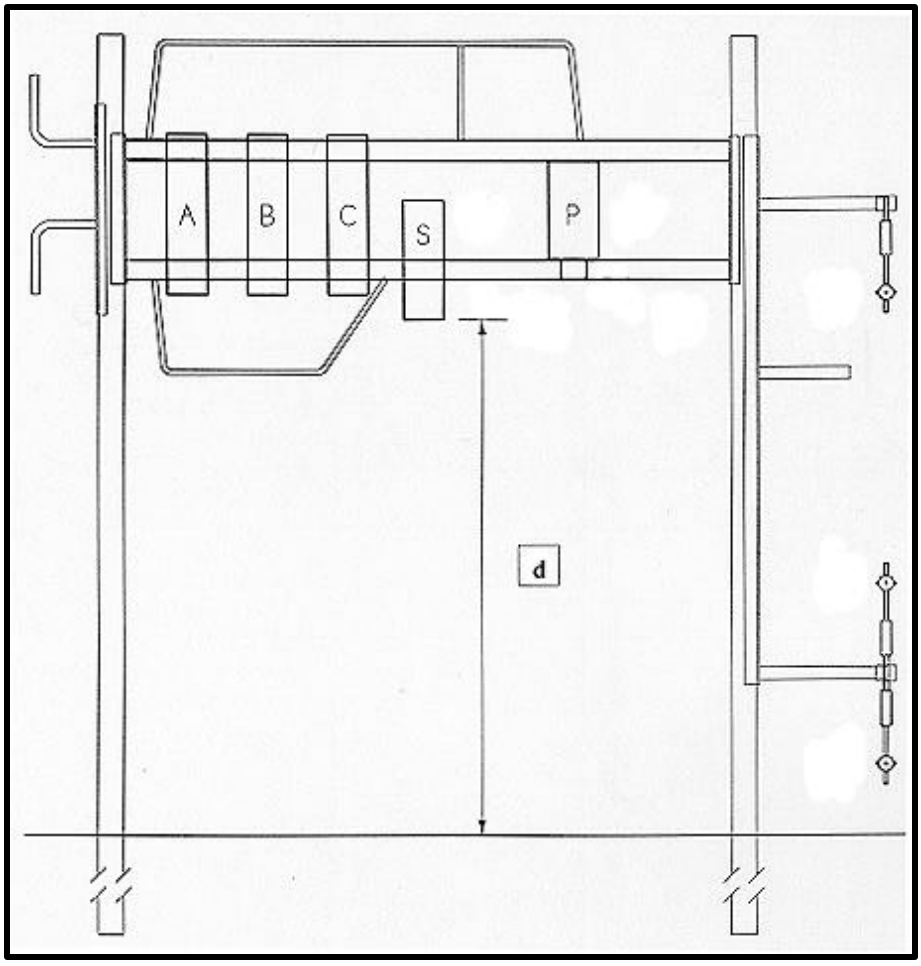

Figure 4.2. Bipod instrumentation.

Each bipod (Fig. 4.2) included 3 Marsh-McBirney electromagnetic current meters located on the offshore end of the frame. This end of the frame was deployed to the southeast so the current meters would be upstream of vertical support posts during northeast waves. Current meters were initially deployed at nominal elevations of 0.2, 0.55, and 1.5 m above the seabed to permit calculation of bed shear stresses associated with different flows by the velocity profile method (Drake and Cacchione, 1992). With a

shoreline orientation of approximately N20W, longshore currents flow toward 340° (i.e. northward) or toward 160° (i.e. southward). Similarly, cross-shore currents are either onshore at 250° (westward) or offshore at 70° (eastward).

A sonar altimeter (Fig. 4.2, S), pressure sensor (P), and electronics housings (A, B, and C) are secured to the frame crossbeams. Sensometric strain gauges (P) measure pressure fluctuations to determine wave height, wave period, and water elevations. Current meters and Sensometric strain gauges were sampled at 2 Hz.

The Datasonics altimeter (Fig. 4.2, S) transmits a 210 kHz acoustic pulse once per second (1 Hz) with 'bottom' return echoes detected after each pulse. Returns are range-binned for 34 minutes. The bin with the maximum number of returns is recorded as the seabed elevation during that 34-minute period. In laboratory tests, the mean distance to the bottom (Fig. 4.2, d) measured with the altimeter was accurate to $\pm$ 1 cm of an independent distance measurement. The altimeter transducer beamwidth is approximately 10° and results in an approximately 20 cm diameter footprint at 1 m range. The footprint of the sonar altimeter is too large to define short wavelength (1-5 cm) ripples (Gallagher et al., 1996); instead, larger scale patterns of erosion and deposition are resolved.

Sonar Altimetry vs. Beach Profiles

During August - December 1995, 8 surveys to 8 m depth were collected along Profile 62, and 4 surveys to 7 m depth were completed along Profile 73 (Fig. 4.1). Cross-shore coordinates of 580 m on Profile 73 and 920 m on Profile 62 are most proximal to the sonar altimeters located on the 5.5 and 8 m bipods respectively (Fig. 4.1). Surveyed

seabed elevations at these cross-shore coordinates were plotted with the corresponding sonar altimeter data (Figs. 4.3a and b).

Surveyed seabed elevations (Fig. 4.3a and b, open circles) are within 8 $\pm$ 4 cm of continuous sonar altimeter measurements (Fig. 4.3, x) during August – December 1995. This correlation between sites that are separated by <70 m in the longshore direction is not surprising and provides a basis from which to evaluate storm-induced bed elevation changes and D_c.

Even with the correspondence of bed elevation measurements on the days beach profiles were surveyed, surveys do not document the entire range of seabed elevations during storms and fair weather conditions. The range of seabed elevations decreased with depth along surveyed profiles (25 $\pm$ 6 cm range at 5.5 m and a 10 $\pm$ 6 cm range at 8 m). Even though sonar altimeters measured a decreased range of seabed elevations with increasing depth, this decrease was much smaller. At all 3 bipod locations, the range of seabed elevations was approximately 40 cm (45 $\pm$ 2 cm at 5.5 m, 38 $\pm$ 2 cm at 8 m, and 36 $\pm$ 2 cm at 13 m).

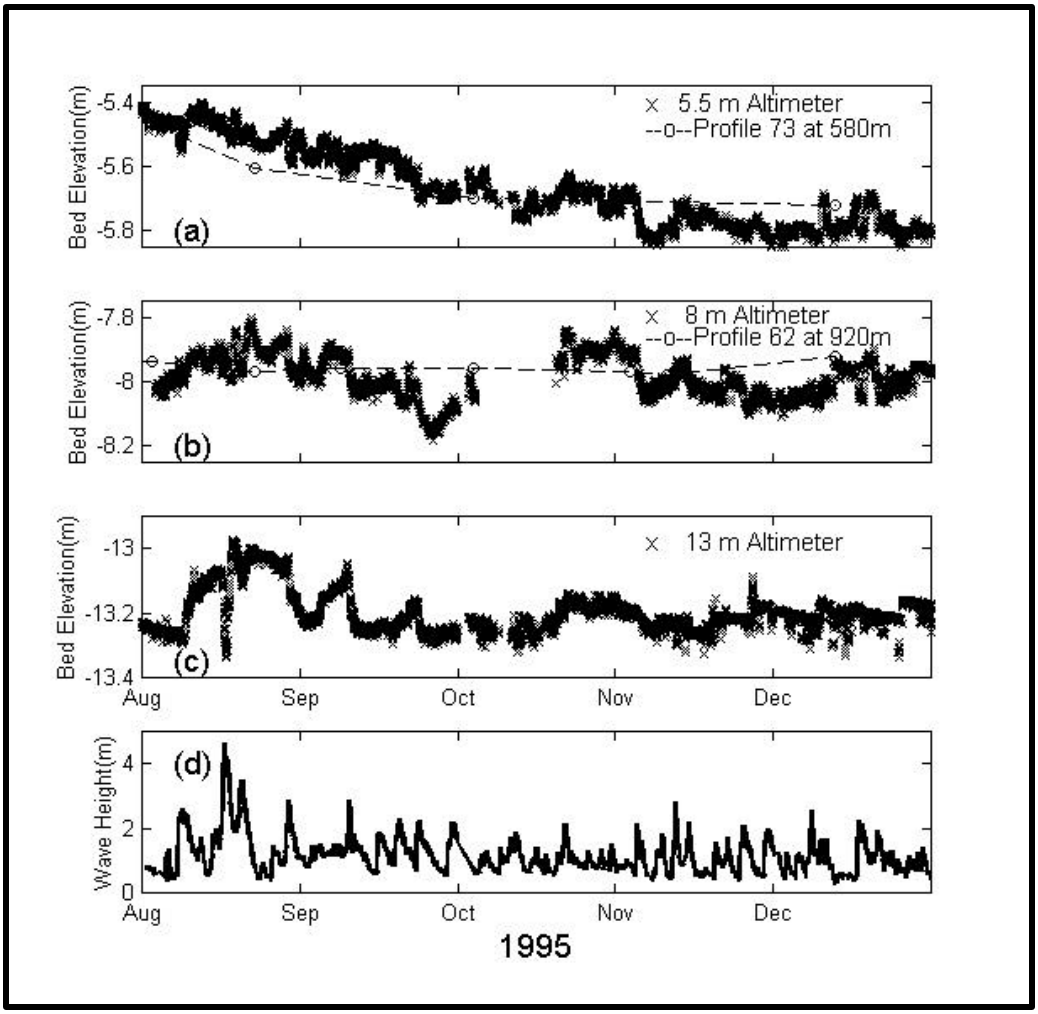

Figure 4.3. Seabed elevations collected by sonar altimeters and beach profiles (a-c) and offshore wave heights (H_{mo}) (d) during August-December 1995.

This approximately 40 cm range in seabed elevations recorded by the sonar altimeters is not an artifact of sound velocity variations in the water column, scour around instrument frame pipes, or settling of the instrument frame. The most significant evidence to support this variability in seabed elevation is a suite of over 100 boxcores collected

near deployed altimeters during 1994 to1997. Comparison of pre- and post-storm cores, which are 15 cm wide x 30 cm deep, verify the magnitude of events in altimeter data (Fig. 4.3), since downcore depths to erosion surfaces in post-storm cores correspond remarkably well with sonar altimeter erosion maxima occurring during storm events (Beavers et al., 1997b). During 1994 to 1997, individual storm deposits ranged from <1 cm to >25 cm thick in 5.5, 8, and 13 m depths (Beavers et al., 1998).

From August – December 1995, the 5.5 m site experienced net erosion, while the 8 and 13 m locations did not. The longer-term elevation changes at these sites can be placed in context by evaluating longer-term sonar altimeter records (1994-present), beach profile records (Birkemeier et al., 1999), and sand bar observations (Lippmann and Holman, 1990).

Preliminary analyses of the impact of increased hydrodynamic forcing during storm events, represented by wave heights (Fig. 4.3d), on nearshore seabed elevations reveal seabed elevations measured by sonar altimeters (Fig. 4.3a-c) do not coincide at all 3 depths for every event. In fact, during August 1995, the range of bed elevation changes (20 ± 2 cm at 5.5 m, 25 ± 2 cm at 8 m, and 36 ± 2 cm at 13 m) increases with increasing water depth. A major influence on the hydrodynamic forcing during August 1995 was Hurricane Felix. This hurricane produced the maximum wave heights recorded during August-December 1995.

Hurricane Felix - August 1995

Hurricane Felix developed in the mid-Atlantic and moved northwest, then westerly on August 15, putting North Carolina on alert for hurricane landfall. Felix stalled when interacting with a high pressure system about 300 km west of Cape Hatteras, turned northeast, and was downgraded from a category 3 to a category 1 hurricane (on the Saffir/Simpson Hurricane Scale) (Baron et al., 1995). By early August 17, Hurricane Felix moved northward away from the North Carolina coast and never made landfall. Maximum southerly winds reached 17 m/s at 1816 Eastern Standard Time (EST) on August 16. Maximum wave height (H_{mo}) at an offshore Waverider buoy reached 4.6 m at 0208 EST on August 16 (Fig. 4.4d). The peak wave period (T_p) was 15.1 s.

As Hurricane Felix approached the North Carolina coast, the 13 m site eroded 26 $\pm$ 2 cm during the 24 hours preceding 1516 EST on August 16. During this interval, maximum H_{mo} reached 4.6 m at 0208 EST, and mean currents at 13 m (Fig. 4.5) were directed southward (24 cm/s at 1300 EST) and onshore (9 cm/s at 0316 EST). Further inshore, longshore and cross-shore currents reached maximum northward (62 cm/s) and offshore (50 cm/s) velocities at 0242 EST at 5.5 m before reversing to flow southward and onshore like 13 m. Onshore flows at 13 m and offshore flows at 5.5 and 8 m on the morning of August 16 indicate flow convergence on the shoreface between 8 and 13 m. This reversal in current directions at inshore locations preceded the erosion maxima recorded at 1516 EST at 13 m.

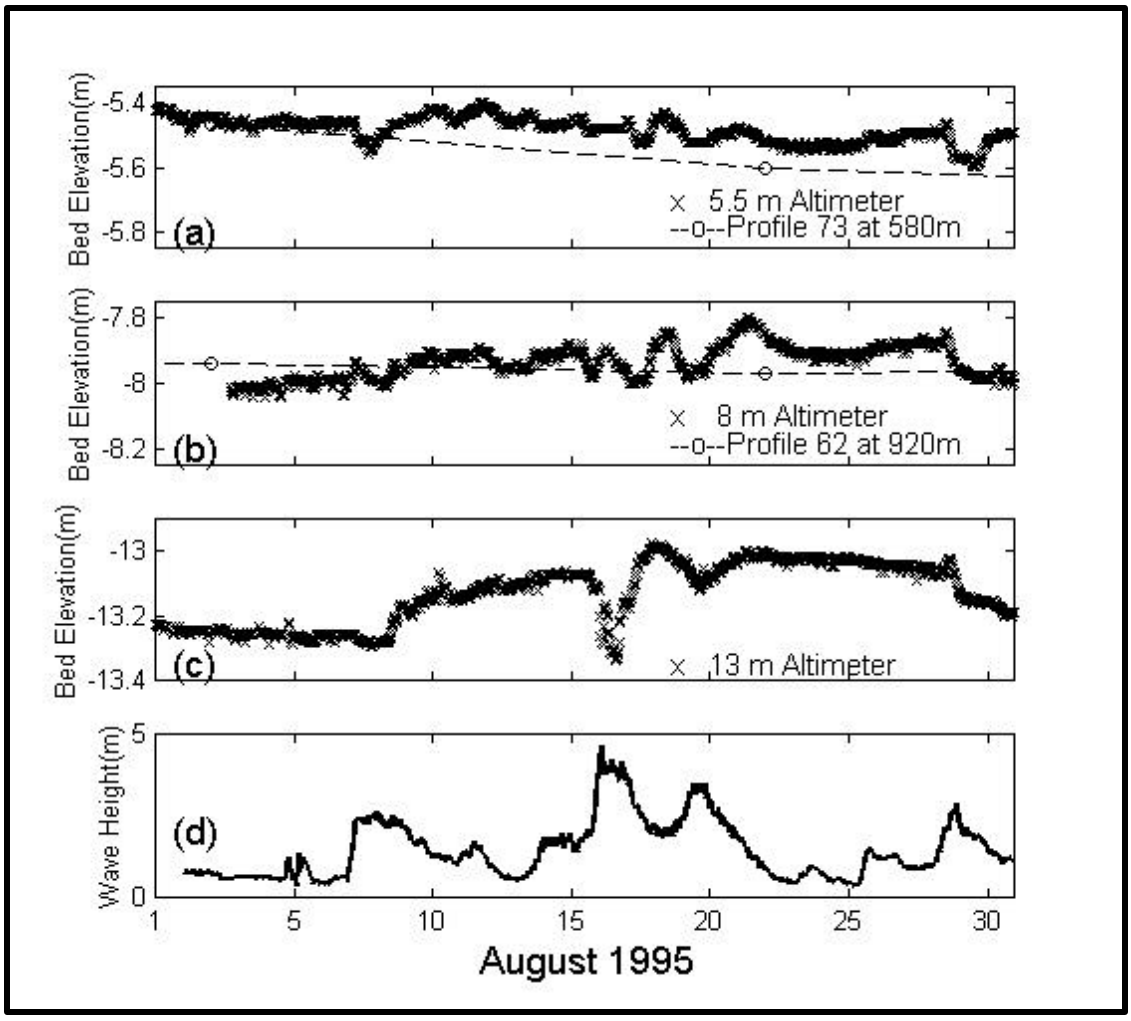

Figure 4.4. August 1995 seabed elevations (a-c) and offshore wave heights (H_{mo}) (d).

For the next 35 hours, until 0016 EST on August 18, 36 $\pm$ 2 cm of sediment were deposited at 13 m. H_{mo} decreased as Hurricane Felix veered away from the North Carolina coast, and southward (63 cm/s at 0316 EST at 8 m) and onshore (23 cm/s at 0134 EST at 8 m) flows reached peak velocities at all locations and then decreased (Fig. 4.5). Deposition occurred at 13 m during onshore flows and may be due to a shoreward

flux of sediment. Sediments were also advected by southward currents, but longshore fluxes of sediment were not constrained by this cross-shore array.

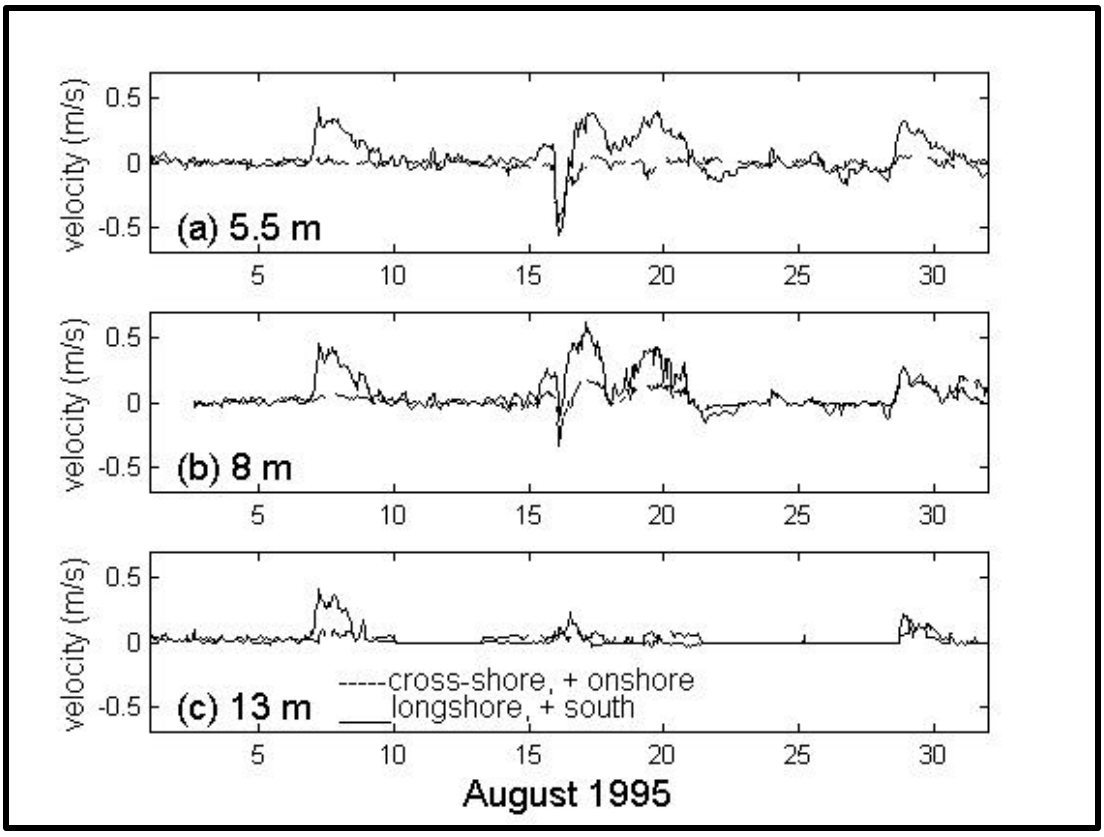

Figure 4.5. Longshore and cross-shore mean currents measured approximately 20 cm above the seabed at the 5.5, 8, and 13 m bipods.

Somewhat surprisingly, the 5.5 and 8 m depths (Fig. 4.4a and b) experienced a more limited range of bed elevation changes during Hurricane Felix. The 8 m site experienced a 16 $\pm$ 2 cm range, and timing of these changes did not coincide exactly with changes in 13 m. In 5.5 m, the 10 $\pm$ 2 cm range of bed elevation changes was even smaller. Evaluating small- scale seabed elevation fluctuations in sonar altimeter data is

limited by the resolution of the data (± 1 cm) and must consider the presence of bedforms (Hay and Wilson, 1994; Gallagher et al., 1998).

Northeaster storm events on August 7-8, 18-20, and 28 had wave heights at the Waverider buoy which exceeded 2.0 m (Fig. 4.4d) and southward longshore currents (Fig. 4.5). Although none of these northeaster storms produced bed elevation changes approaching the 36 ± 2 cm of accretion measured at 13 m during Hurricane Felix, the storm on August 7-8 was associated with net accretion at all 3 depths. When combined with Hurricane Felix on August 15-18, the storm on August 18-20 sustained H_{mo} near or above 2.0 m for 5 days and also affected the profile morphology that was surveyed on August 22.

Closure Depth

Figure 4.6 shows the profile surveys before and after Hurricane Felix including changes caused by 2 smaller storms on August 7-8 and 18-20. Using a 6 cm change criteria between surveys to determine the most landward point of observed closure (Nicholls et al., 1998), the event-dependent depth of closure (D_c) is only –4.0 m NGVD (-3.6 m Mean Low Water). This observed D_c is well under the predicted D_c for Hurricane Felix of -8.3 m based on 12-hour exceeded wave height (Hallermeier, 1977).

Between surveys, the sandbar moved approximately 40 m offshore, and this movement is quantified by event-dependent D_c. By comparison, the impact of Hurricane

Felix along the outer profile appears minimal when viewed at the entire profile scale (Fig. 4.6). From August 2 to 22 (Fig. 4.4), surveyed elevations at 5.5 m and 8 m experienced 14 $\pm$ 6 cm and 3 $\pm$ 6 cm of erosion respectively. Sonar altimetry recorded a comparable 11 $\pm$ 2 cm of erosion at 5.5 m but documented a contrasting 11 $\pm$ 2 cm of *accretion* at 8 m. These comparable measurements at 5.5 m bode well for event-dependent D_c calculations that designate the innermost profile depth with limited change, but discrepancies at 8 m depth represent potential errors for shoreface sediment budget calculations.

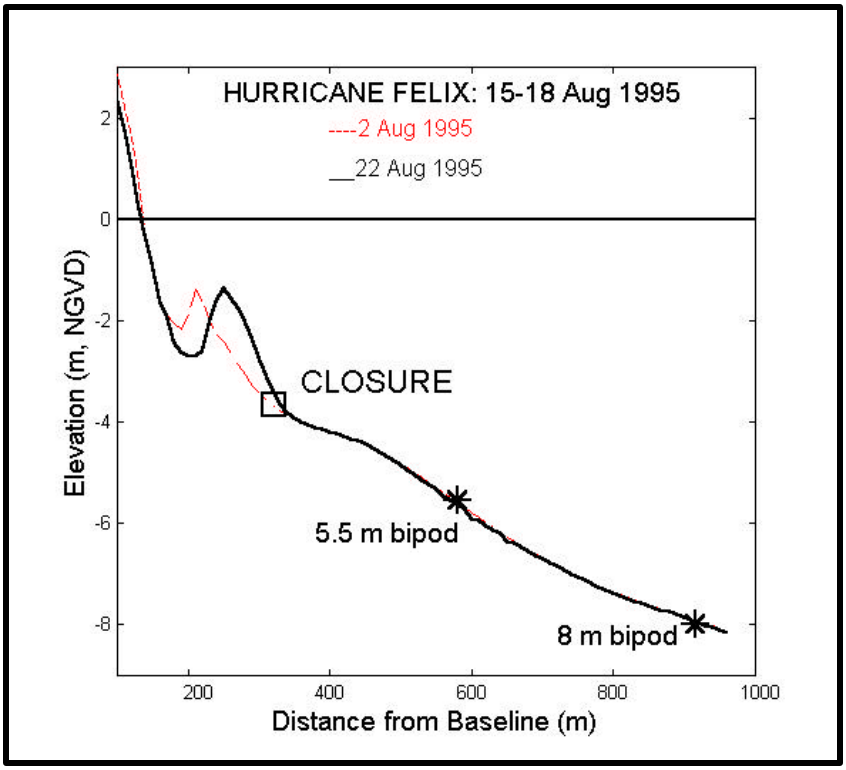

Figure 4.6. Elevation change along Profile 62 during August 1995.

Discussion

Sonar altimeter data complement beach and nearshore profile data while raising new questions. During August – December 1995, seabed elevations measured by both methods are within 8 $\pm$ 4 cm in 5.5 and 8 m depth (Figs. 4.3a and b). By establishing this relationship during non-storm conditions, storm-induced seabed elevation changes measured by sonar altimeters can be used to refine our understanding of profile dynamics.

As expected from previous analyses of profile data, the range of seabed elevations decreased with increasing depth along surveyed profiles. Although the range of continuously measured seabed elevations decreased slightly from 5.5 to 13 m depth, the range at all locations was approximately 40 cm. By encompassing seabed elevation changes during storms, we have documented that sediments seaward of event-dependent D_c are highly mobile. In fact, the seabed at 13 m experienced a greater range of elevation changes than either 5.5 or 8 m depths during Hurricane Felix (Fig. 4.4).

Potential reasons for this increase in seabed mobility at 13 m during August 1995 include minor changes in sediment grain size and composition, particularly silt and clay content. Bioturbation of sediments by polychaetes (worms) and sanddollars has been documented at all locations (Beavers et al., 1998). Since bioturbation rates are generally higher at offshore sites and in warmer waters (Diaz et al., 1994), increased seabed mobility at 13 m during August 1995 may be due to higher rates of bioturbation.

During Hurricane Felix, sediments were deposited in 13 m depth during onshore flows, indicating a shoreward flux of sediment. Even though event-dependent D_c (-4.0 m

NGVD) defined the offshore movement of the sandbar, discrepancies between bed elevation measurements at 8 m depth represent potential errors for shoreface sediment budget calculations. Additional studies have also documented accretion beyond surveyed profile depths during onshore flows. Observations by Wright et al. (1994a) offshore of Duck, NC in 14 m depth documented 18 cm of seabed accretion. This accretion occurred after the passage of a mild storm event in October 1992 and at a time when net sediment flux was observed to be directed shoreward (Wright et al., 1994a). These rapid large-scale sediment accretion events, including the 36 $\pm$ 2 cm of sediment deposited at 13 m during Hurricane Felix, often create distinct storms deposits (Beavers et al., 1998). Since the altimeter record of storm events can be verified by sediment cores, incorporating measurements of seabed variability during storms is necessary to address some lingering questions about shoreface dynamics. A few of these questions include:

- Given that D_c may be identified as the most landward point of negligible post-storm profile change, does a range of seabed elevation changes of approximately 40 cm in 5.5, 8, and 13 m depths indicate another quantifiable index of shoreface variability?
- What hydrodynamic processes are responsible for the timing and magnitude of nearshore seabed elevation changes during storms?
- How do sequences of storm events affect seabed elevation changes?

Conclusions

Results of these analyses of field measurements collected during August – December 1995 at the FRF in Duck, NC may be summarized as follows:

1. Surveyed profile data and sonar altimetry measurements of seabed elevations were within 8 $\pm$ 4 cm in 5.5 and 8 m depths.
2. Continuous sonar altimeter measurements were collected during storm events and span a range of seabed elevations of approximately 40 cm in 5.5, 8, and 13 m water depths. Biweekly and post-storm profiles recorded a range of only 25 $\pm$ 6 cm at 5.5 m depth and 10 $\pm$ 6 cm at 8 m depth.
3. During Hurricane Felix, sediments were deposited in 13 m depth during onshore flows, and may be due to a shoreward flux of sediment.
4. Event-dependent closure depth (D_c) may be in error depending on the extent of profile adjustment which occurs before post-storm surveys are completed.
5. Sediment budgets must account for additional cross-shore fluxes of sediment beyond D_c.

CHAPTER 5

CONCLUSIONS

This study presents the first field results of outer surf zone and inner continental shelf cores collected where the seabed elevation and hydrodynamic forcing are continuously measured by instrumentation during storms. Sonar altimeter measurements of seabed elevation changes throughout storms have been used to define net erosion or accretion patterns for northeaster storms and hurricanes (Chapter 2), the chronology of sediments preserved in post-storm cores (Chapter 3), and seabed variability during storms that is not captured in fairweather nearshore surveys (Chapter 4).

In Chapter 2, comparison of sonar altimeter measurements of seabed elevation changes during 1994-1997 for 5 hurricanes and 6 northeasters storms produced some expected and unexpected results. Both northeaster storms and hurricanes resulted in maximum values of net seabed accretion at locations in the outer surf zone. As expected, net seabed erosion and accretion diminished with distance offshore of the edge of the surf zone. This inverse relationship between net seabed elevation change and distance offshore of the surf zone indicates linking sedimentation processes across time scales and surf zone and inner shelf environments must incorporate analyses of the transition in fluid motions from the inner shelf to the surf zone.

A somewhat unexpected result emphasizes that not all storms are alike. At surf zone and inner shelf locations, northeaster storms are more likely to cause net accretion than no net change in seabed elevation or net deposition, whereas hurricanes are almost as likely to cause net erosion as net deposition. Given the constraints that these analyses are based on a small number of storms with variable duration, maximum wave heights, and wave periods, these data indicate hurricanes and northeaster storms have different impacts on the seabed at surf zone and inner shelf locations.

In Chapter 3, the combination of deployed instrumentation and diver-operated cores proved successful in documenting sedimentary strata created by a northeaster storm. Sediment deposits that are approximately 20 cm thick have been attributed to storms in other coastal areas (Morton, 1988), but this is the first study to conclusively document the thickness, deposition rate, primary structures, and associated hydrodynamic regime of a nearshore storm deposit. Storm deposits from the surf zone and inner continental shelf reached maximum thickness of 25 cm at all locations, but sampled storm deposits are not as thick due to post-deposition erosion by subsequent seabed activity. Detailed analyses of sonar altimeter data and the adjacent cores reveal storm sediments accreted in 2 or more phases that totaled 4-20 hours. Initial deposition rates may have been fast as 5 cm/hr, but all deposition rates exceed 1 cm/hr.

Primary sediment structures created by a northeaster storm include parallel to sub parallel laminations, hummocky and ripple cross-stratification, shell and gravel lags, and basal erosion contacts. Laminae were 1-4 mm thick and were deposited during increasing

and decreasing wave heights and decreasing (at 8 m and 13 m) or increasing (at 8 m and 5 m) mean currents.

Measuring seabed elevation changes during storms eliminates the need to interpret nearshore cores on the basis of preserved signatures alone. However, interpreting paleonearshore conditions on the basis of preserved signatures alone will benefit from additional field studies to document what portion of storm events and non-storm conditions erode and deposit sediments in modern nearshore environments.

During August-December 1995, surveyed profile data and sonar altimetry measurements of seabed elevations were within 8 $\pm$ 4 cm in 5.5 and 8 m depths. Continuous sonar altimeter measurements were collected during storm events and span a range of seabed elevations of approximately 40 cm in 5.5, 8, and 13 m water depths. Since profile measurements are not collected during storms, event-dependent closure depth (D_c) may be in error depending on the extent of profile adjustment which occurs before post-storm surveys are completed.

During Hurricane Felix, sediments were deposited in 13 m depth during onshore flows, indicating a shoreward flux of sediment. Even though event-dependent D_c (-4.0 m NGVD) defined the offshore movement of the sandbar, discrepancies between bed elevation measurements at 8 m depth represent potential errors for shoreface sediment budget calculations. This research provides results that suggest additional measures of cross-shore fluxes of sediment beyond D_c should be used to quantify nearshore sediment budgets.

APPENDIX 1

BOXCORE COLLECTION

Introduction

Boxcoring is an easily executed method for obtaining shallow sediment cores. These boxcorers are modified Klovan style boxcorers (Greenwood et al., 1984) and are useful both on land and in water. First, the boxcorer is described. Next, logistics and equipment that greatly increase diver safety while obtaining cores in shallow waters are presented.

Diver-operated Boxcorer

The stainless steel boxcorers used in this work are 15 cm wide x 10 cm deep x 30 cm long and have a removable slide hammer and angled sliding door (Fig. A.1). Grooves along the open side of the corer guide the removable sliding door down the open face once the corer is in place in the sediment. This angled sliding door eliminates the need to excavate and expose the lower surface of the corer to install a lower plate as was required in previous versions of diver-collected 'box' cores.

One diver easily manipulates this corer. The primary component is the wedge shaped box that has a hollow pipe handle that can be threaded to the top of the corer. The hammer is comprised of a sliding sleeve on the pipe handle. The sliding door has a handle of wood, synthetic polymer, or metal to enable pushing the door into place.

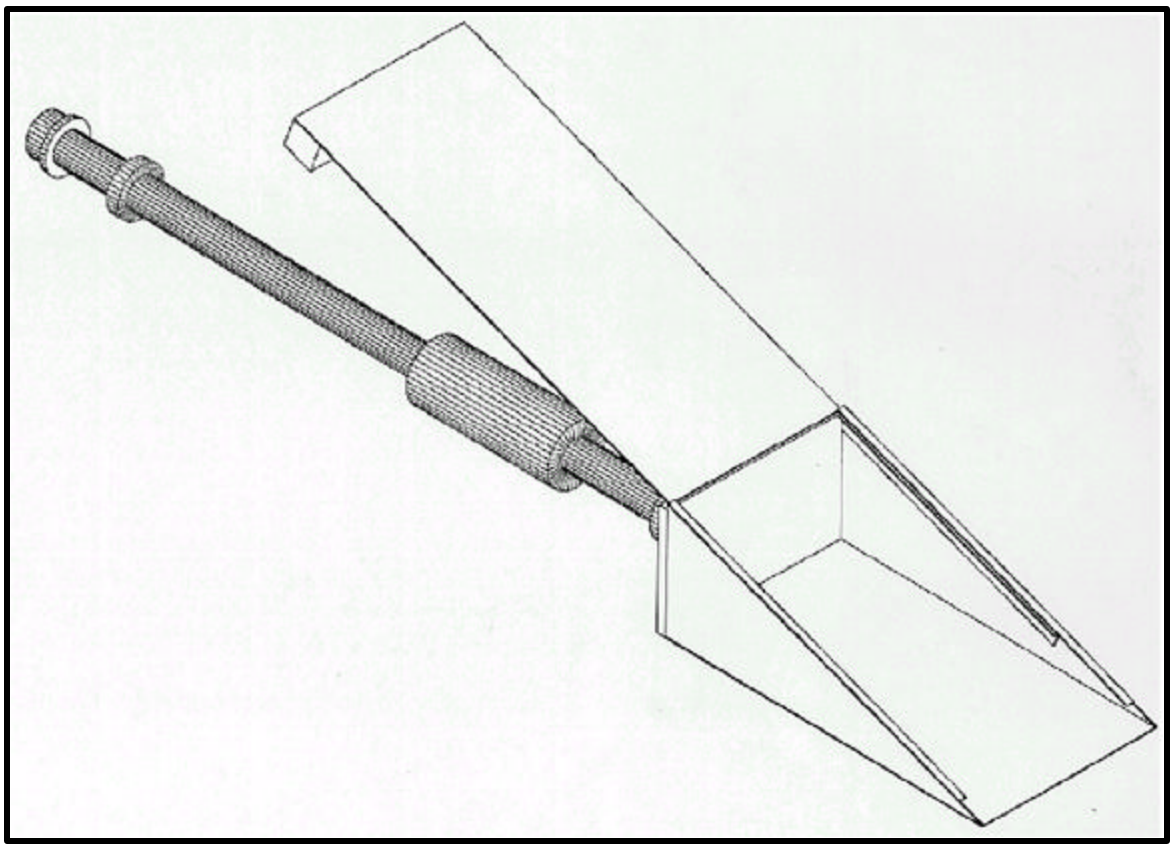

Figure A.1. Stainless steel boxcorer with slide hammer and removable door.

Nearshore Boxcoring

To commence coring in waters deeper than 2 m, a diver descends along a down line with a lift box containing 1-3 corers and a 50 lb. lift bag (Fig. A.2). The second diver carries the slide hammer attached to an additional corer should 4 cores be planned. The use of a lift box equipped with a lift bag allows 2 divers to descend and ascend along a down line with minimal equipment. Our lift box is a plastic container with ¼ inch holes drilled in the base and lid to allow the closed box to fill with water. Lines attached to each side of the box provide a bridle to attach to a lift bag.

Figure A.2. Boxcoring equipment: (left to right) lift box on its side with 50 lb. lift bag clipped to bridle, tag line with clips on each end, boxcorer with removable sliding door and hammer, filled boxcore with door removed, clear tray, and metal slide used to extract core from boxcorer.

Once on the seabed, divers proceed to the coring site (Fig. A.3) along a known bearing and a set distance from the instrument frame. In low visibility conditions, a tag

line (Fig. A.2) is clipped to the instrument frame. The lift box can also be secured to the instrument frame during coring activity.

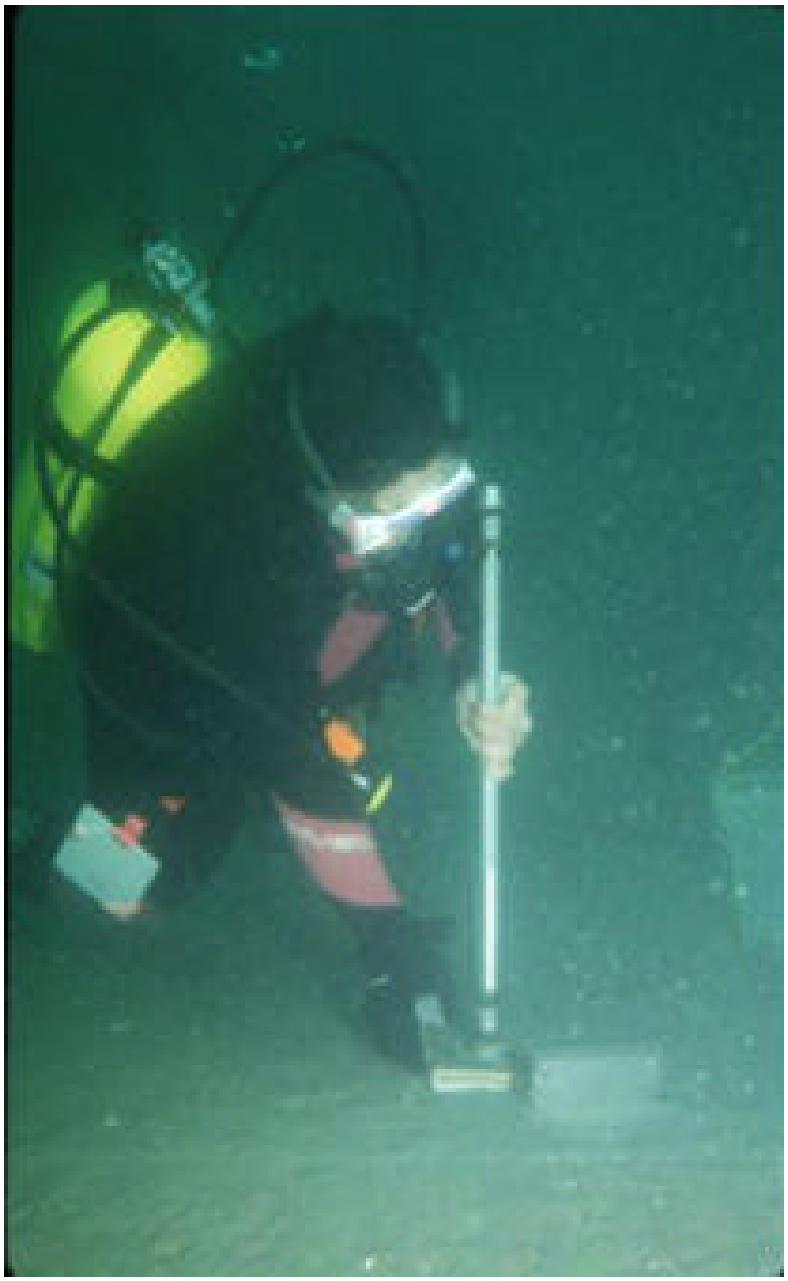

Figure A.3. Diver sliding door into second of an orthogonal pair of boxcores.

A boxcorer with slide hammer attached is held perpendicular to the sediment surface and oriented with the diver's compass. Light to moderate force with the sliding hammer is used to drive the corer into the sediment. Forceful pounding of the hammer can drive target sediment away from the corer. In very fine sands, the corer can be driven level with the sediment surface in 1-2 minutes. In fine to medium sands, especially sediments compacted by wave action, the coring may take 3-5 minutes per corer. Once the corer top is flush with the sediment surface, the corer is full. The sliding door is aligned with the guide grooves and slid into the sediment until it reaches the base of the corer (Fig. A.3).

The second corer is then placed orthogonal to or in series with the first corer. The process of hammering in the corer, inserting the sliding door, removing the hammer, and readying a new corer is continued until finished at a particular location. The cores can be extracted by pulling on the slide hammer or pulling the corer from the sediment without the hammer in place.

To minimally disturb the cores, the extracted cores are placed in the lift box. Elevating the base of the filled corers in the lift box helps to prevent sediment draining from the bottom of the corer. Once the cores are secured in the lift box, a 50 lb. lift bag is attached to the lift box bridle, inflated, and facilitates transport of cores to the water surface. If the cores are not transported in a lift box, tilting the base of the core slightly above horizontal prevents loss of sediment from the base of the core.

Figure A.4. Boxcorer filled with sediment. Core top is to the left. Scale is in cm.

In the lab, the boxcorer door is removed (Fig. A.4), and the sediment is allowed to dry for 4-24 hours. Methods for extracting the core, making sediment relief peels, and developing xrays of core sediments are contained in the following appendix.

Applications

The unique application of this method of core collection near deployed acoustic altimeters has allowed us to document individual storm event beds in the sediment record. Depth downcore to changes in sediment structures or type corresponds

remarkably well with erosional maxima documented during storm events by sonar altimeters (Beavers et al., 1997b). While conditions prevent diving during storms, a deployed altimeter and post-storm diver-collected boxcores can be combined to document the sediment record from storm events.

This boxcorer can be effectively used in muddy to gravely sands. Although diver-collected boxcores work well in numerous sediment types, they cannot penetrate large rocks or shells. These boxcorers have been used to collect a transect of cores extending below the waterline to subaerial portions of a sandy spit near Beaufort, NC. This transect of cores was able to document hurricane overwash deposits.

With an operational range that includes subaerial and subaqueous sediments, instruction on the coring procedure can be demonstrated to scientific divers on land before they enter the water to collect boxcores. When fundamentals of this technique, including core orientation, use of the slide hammer, and aligning the sliding door, are practiced and mastered on land, in-water core collection can proceed more efficiently.

APPENDIX 2

BOXCORE PROCESSING

Core Extraction

1) Collect boxcore.
2) Remove boxcore door and allow sediments to dry. If sediments are very wet, the base of the core may be elevated 5-10 cm to prevent sediments draining from the core. Process the core while the sediments are still moist but not saturated. If you cannot process the core within 48 hours, keep the door on the boxcore until you are ready to process the core.
3) Remove uppermost sediments from corer with 4" putty knife.
4) Subsample core for grain size and composition analyses.
5) Leave a level 2 cm thick slab of sediment. Remove 1 cm or less of sediment from the sides of the boxcore to allow a 13 cm x 30 cm plexiglass tray with 1 cm molded sides to securely cover the core sediments. Be careful not to make the slab too thin. The core should never be less than 1 cm thick.
6) Label sides and base of plexiglass tray with top and bottom of core, orientation (note: when core is flipped, the orientation with respect to observer will change), and core label (e.g.-971013-8).

7) Invert plexiglass tray on top of sediments. Place 14 cm x 30 cm metal slide between the sample and boxcore. Maintain pressure on the metal slide to keep it flush against the boxcore, particularly near the top of the core.
8) Keeping a light pressure on the tray and metal slide, lift the sediments from the corer. Invert or 'flip' the sample so the boxcore sediments now rest in the tray. Note that orientation of the sediment has changed.
9) 'Slide' the metal slide off the sediment surface. Shave the surface of the tray sediments in the direction of the bedding until the thickness of the sediment is even with the height of the tray. Shave around gravel or shell fragments that originate in the lower 1 cm of sediment.

Core Logging

1) Place scale next to core.
2) Describe primary sedimentary features (grain size, grading, bedding, etc.) and secondary sedimentary features (e.g.-bioturbation).
3) Photograph and digital image core.

Xrays

Operating Instructions for the Vet-Ray VR8020LBC

1) Prepare core sample.
2) Wear radiation detection badge.

3) Securely mount the portable Vet-Ray unit on the stand. Connect the unit to an electrical outlet. Insert the exposure hand switch plug into the connector.
4) Turn on the light beam collimator lamp and adjust the beam to highlight the approximate area to be exposed.
5) Turn on the LV (line switch) and gradually increase the settings until the LV pointer is in line with the red diamond.
6) Set distance from xray unit to film. Recommended settings are in Table A.1.
7) Set the exposure time.
8) Select the proper Kv/Ma setting. Higher Kv (kilivolts) increase penetration, and higher Ma (miliamps) produce better contrast. Proper exposures of core sediments may require a high Kv and low Ma.
9) When changing parameters, change distance (6), time (7), and Kv/Ma (8), in that order. The ideal xray is low penetration (Kv), high contrast (Ma), and a short distance. Increasing Kv/Ma decreases the required exposure time.
    - With polariods (which give positive prints) increase time to lighten, and decrease time to darken.
    - With Dupont Cronex film (which give negative prints) increase time to darken, and decrease time to lighten.
10) Place film under xray unit. Position the core on top of the film.
11) Place lead letters and numbers for the sample name and an arrow with ON indicating onshore on left side of sample. Place letters BOT on left side at the base of the core. It is often easier to secure lead letters on duct tape, and place near the sample.

12) Direct and center the xray emission port (collimator cross mark) on the sample.

13) Confirm the film to tube focus distance with tape measure.

14) Stand behind a radiation barrier.

15) Start the exposure by pressing and holding the exposure hand switch. During the exposure, the exposure light will illuminate. The Ma meter shows the actual Ma. Amperage of the xray unit changes from 17 to 26 amps. A 20 amp breaker will work, but it is recommended to increase amperage of breaker to 30 amp.

16) Turn the line switch off.

17) Allow the xray unit to cool between xrays for 2 minutes for every second of xray.

18) Mark the yellow paper cover of industrex film with the core identification. Place film in cover and archive.

Table A.1. Recommended settings for core xrays.

Material	**Sand boxcore**	**Silt boxcore**	**Epoxy peel**
Sample thickness	w/ 1/8" plexi-glass 1.27cm (1/2")	w/ 1/8" plexi-glass 1.27 cm	1.27 cm
Height of camera	53 cm	53 cm	53 cm
Kv/Ma	60/20	70/15	70/15
Exposure time	2.5 s	3.5 s	2.4 s
Developer time	2.5 min	2.5 min	2.5 min
Fixer time	2.5 min	2.5 min	2.5 min
Film size	8" x 10"	8" x 10"	8" x 10"

<u>Developing Kodak Industrex film</u>

- Order the smallest containers of developer and fixer that will use in 1-2 day interval, otherwise the remainder of a larger container will oxidize and spoil.

- Premixed solutions are only effective for a limited time (i.e. a few weeks).
- The developer is too old to use when it has turned brown.
- Kodak industrex film is single emulsion (side with dull gray color). Kodak Technical Customer Service is (800) 242-2424 (Ask for Health Science); Kodak Government Sales (800) 828-6203
- Wear gloves and eye protection when developing film, mixing chemicals, or handling the xray film.

1) Place developer, fixer, and water in plastic bins. Place separate "drip" bins for excess developer, fixer, and water near the respective bins.
2) Seal off all light coming into the room, and turn on the red darkroom lights.

In darkroom

3) Remove film from the film envelope.
4) Place the film in the developer bin. There should be enough solution to completely submerge the film. Do not place more than one film in the developer solution simultaneously. Developing time will vary according to the temperature of the solution that is a function of the temperature of the room. The temperature of the xray room (behind Mr. Scarborough's office at the FRF) is 72°. Develop for 3 minutes at 72° or 75°, 5 minutes at 68° (preferred), and 7 minutes at 62°.
5) Agitate the solution every 30 seconds for 5 seconds.

6) Before placing film in the fixer, let the excess developer drip from the film into the drip bin.
7) Repeat steps 4-6 for the fixer bath with the exception that you can place more than one film in the fixer at the same time.
8) Before placing film in the water bin, let the excess fixer drip off the film into the drip bin.
9) Place the film in the water bin for a minimum of 20 minutes. At this point, the lights may be turned on. Change the water often.
10) Frequently agitate the film in the water to rinse chemicals from the film.
11) Before hanging the film to dry for 24 hours, let the excess drip off film in the drip bin.

Relief Peels

1) Process and xray boxcore.
2) Cut cheesecloth into 18 cm x 35 cm pieces. Place 3 layers of cheesecloth over 1 cm thick core in plexiglass tray.
3) In a sturdy container, mix resin and hardener in the following ratios:

- 3 pumps epoxy resin and 3 pumps hardener for 30 cm of core. WestSystem epoxy resin is recommended.
- 3 oz polyester resin and hardener for 30 cm of core

4) Use a disposable paintbrush to paint resin on cheesecloth until the cheesecloth and uppermost core sediments are saturated. The thickness of the peel should be 3-8 mm thick, so avoid applying too much resin.

5) Place labels for core identification and orientation on cheesecloth and affix with resin.
6) Allow the peel to harden.
7) Remove the peel from the Plexiglas tray. It may be necessary to use a spatula or other utensil to pry the peel from the tray. Be careful not to break or crack the tray or peel.
8) Remove excess sediments from the peel with running water (a garden hose is great for robust peels) or knock the side of the peel against a hard surface.
9) Trim excess cheesecloth from peel edges with scissors. Affix the peel to a labeled masonite board with additional resin.

REFERENCES

Aagaard, T. and Greenwood, B., 1994. Suspended sediment transport and the role of infragravity waves in a barred surf zone. Marine Geology, 118: 23-48.

Amos, C.L., Bowen, A.J., Huntley, D.A., Judge, J.T. and Li, M.Z., 1999. Ripple migration and sand transport under quasi-orthogonal combined flows on the Scotian Shelf. Journal of Coastal Research, 15(1): 1-14.

Arnott, R.W. and Southard, J.B., 1990. Exploratory flow-duct experiments on combined-flow bed configurations, and some implications for interpreting storm-event stratification. Journal of Sedimentary Petrology, 60(2): 211-219.

Aubrey, D.G., 1979. Seasonal patterns of onshore/offshore sediment movement. Journal of Geophysical Research, 84(C10): 6347-6354.

Barnes, J., 1998. North Carolina's Hurricane History. The University of North Carolina Press, Chapel Hill, 256 pp.

Baron, C. et al., 1995. Preliminary data summary for August 1995, CERC Field Research Facility, U.S. Army Corps of Engineers, Waterways Experiment Station, Vicksburg, MS.

Battisto, G.M., Friedrichs, C.T., de Kruif, A. and Rijks, D.C., 1998. Data Report: Pump sampling and sediment analysis in support of the Sensor Insertion System, Duck, N.C., April and October, 1997. 56, VIMS.

Battisto, G.M., Friedrichs, C.T., Miller, H.C. and Resio, D.T., 1999. Response of OBS to mixed grain-size suspensions during SandyDuck'97, Coastal Sediments '99. ASCE Press, Long Island, NY.

Beach, R.A. and Sternburg, R.W., 1996. Suspended-sediment transport in the surf zone: response to breaking waves. Continental Shelf Research, 16(15): 1989-2003.

Beavers, R., Boynton, T. and Howd, P., 1997a. Documenting storm sedimentation with diver-collected boxcores and acoustic altimeters offshore of Duck, NC. In: E.J. Maney, Jr. and C.H. Ellis, Jr. (Editors), Diving for Science...1997; Proceedings of the American Academy of Underwater Sciences, Boston, Massachusetts.

Beavers, R.L., Howd, P.A., Birkemeier, W.A. and Hathaway, K.K., 1999. Evaluating profile change and depth of closure with sonar altimetry, Coastal Sediments '99. ASCE Press, Long Island, NY.

Beavers, R.L., Howd, P.A. and Hathaway, K.K., 1997b. Documenting storm sedimentation with diver-operated boxcores and acoustic altimeters offshore of Duck, NC, EOS, Transactions, American Geophysical Union, pp. 335.

Beavers, R.L., Howd, P.A., Hay, A.E., Wilson, D.J. and Hathaway, K.K., 1998. Nearshore sedimentary strata created during SandyDuck97 storms, EOS, Transactions, American Geophysical Union, pp. 445.

Birkemeier, W.A., Nicholls, R.J. and Lee, G., 1999. Storms, storm groups and nearshore morphologic change, Coastal Sediments '99. ASCE Press, Long Island, NY.

Bridge, J.S. and Best, J., 1997. Preservation of planar laminae due to migration of low-relief bed waves over aggrading upper-stage plane beds: comparison of experimental data with theory. Sedimentology, 44: 253-262.

Burns, R.F., 1998. SandyDuck 97. Sea Technology, 39(1): 51-59.

Cacchione, D.A. and Drake, D.E., 1982. Measurements of storm-generated bottom stresses on the continental shelf. Journal of Geophysical Research, 87(C3): 1952-1960.

Cacchione, D.A., Drake, D.E., Ferreira, J.T. and Tate, G.B., 1994. Bottom stress estimates and sand transport on northern California inner continental shelf. Continental Shelf Research, 14(10-11): 1273-1289.

Clifton, H.E., 1976. Wave-formed sedimentary structures; a conceptual model, Beach and nearshore sedimentation. SEPM (Society for Sedimentary Geology), Tulsa, OK, pp. 126-148.

Clifton, H.E., Hunter, R.E. and Phillips, R.L., 1971. Depositional structures and processes in the non-barred high-energy nearshore. Journal of Sedimentary Petrology, 41(3): 651-670.

Cox, M.O., Howd, P.A. and Kirby, J.T., 1995. Shoreface geologic control of nearshore wave energy, Geological Society of America Abstracts with Programs, pp. 79.

Davidson-Arnott, R.G.D. and Greenwood, B., 1976. Facies relationships on a barred coast, Kouchibouguac Bay, New Brunswick, Canada, Beach and Nearshore Sedimentation. SEPM Special Publication, pp. 149-168.

Davis, R.A., Jr., 1965. Underwater study of ripples, southeastern Lake Michigan. Journal of Sedimentary Petrology, 35(4): 857-866.

Davis, R.A., Jr., 1992. Depositional Systems. Prentice-Hall, Englewood Cliffs, NJ, 604 pp.

Diaz, R.J., Cutter, G.R. and Rhoads, D.C., 1994. The importance of bioturbation to continental slope sediment structure and benthic processes off Cape Hatteras, North Carolina. Deep Sea Research II, 41(4-6): 719-734.

Dolan, R. and Davis, R.E., 1992. An intensity scale for Atlantic coast Northeast Storms. Journal of Coastal Research, 8(4): 840-853.

Dott, R.H., Jr., 1996. Episodic event deposits versus stratigraphic sequences-shall the twain never meet? Sedimentary Geology, 104: 243-247.

Drake, D.E. and Cacchione, D.A., 1992. Wave-current interaction in the bottom boundary layer during storm and non-storm conditions: observations and model predictions. Continental Shelf Research, 12(12): 1331-1352.

Duke, W.L., Arnott, R.W.C. and Cheel, R.J., 1991. Shelf sandstones and hummocky cross-stratification: new insights on an old debate. Geology, 19: 625-628.

Elgar, S., Freilich, M.H. and Guza, R.T., 1990. Model-data comparisons of moments of nonbreaking shoaling surface gravity waves. Journal of Geophysical Research, 95(C9): 16055-16063.

Field, M., Berne, S., Colella, A., Nittrouer, C. and Trincardi, F., 1999. Conference stresses relevance of marine strata to today's issues. EOS, Transactions, American Geophysical Union, 80(12): 135.

Field, M.E. and Duane, D.B., 1976. Post-Pleistocene history of the United States inner continental shelf: significance to origin of barrier islands. Geological Society of America Bulletin, 86: 691-702.

Foster, D.L., Beach, R.A. and Holman, R.A., 1994. Phase relationships within the bottom boundary layer as measured during the Duck94 field experiment, EOS, Transactions, American Geophysical Union, pp. 335.

FRF, 1999. Wind and wave database, http://frf.usace.army.mil/data.html. US Army Corps of Engineers, Field Research Facility.

Gallagher, E.L., Boyd, W., Elgar, S., Guza, R.T. and Woodward, B., 1996. Performance of a sonar altimeter in the nearshore. Marine Geology, 133(3-4): 241-248.

Gallagher, E.L., Elgar, S. and Thornton, E.B., 1998. Megaripple migration in a natural surf zone. Nature, 394(6689): 165-168.

Greenwood, B., Davidson-Arnott, R.G.D., Hale, P.B. and Mittler, P.R., 1984. A Klovan-type box corer for use with SCUBA. Geo-Marine Letters, 4: 59-62.

Greenwood, B. and Mittler, P.R., 1979. Structural indices of sediment transport in a straight, wave-formed, nearshore bar. Marine Geology, 32: 191-203.

Haines, J.W. and Sallenger, A.H., Jr., 1994. Vertical structure of mean cross-shore currents across a barred surf zone. Journal of Geophysical Research, 99(C7): 14223-14242.

Hallermeier, R.J., 1977. Calculating a yearly limit depth to the active beach profile. Technical Paper 77-9, US Army Corps of Engineers, Coastal Engineering Research Center, Fort Belvoir, VA.

Hanes, D.M., Alymov, V., Thosteson, E.D., Chang, Y.-S. and Vincent, C.E., 1998. Local seabed morphology and small scale sedimentation processes during SandyDuck97, EOS, Transactions, American Geophysical Union, pp. 444.

Hay, A.E. and Bowen, A.J., 1993. Spatially correlated depth changes in the nearshore zone during autumn storms. Journal of Geophysical Research, 98(C7): 12387-12404.

Hay, A.E. and Wilson, D.J., 1994. Rotary sidescan images of nearshore bedform evolution during a storm. Marine Geology, 119: 57-65.

Howd, P.A., Beavers, R.L. and Hathaway, K.K., 1994. Shoreface morphodynamics I: Cross-shore scales of fluid flows, EOS, Transactions, American Geophysical Union, pp. 339.

Hubertz, J.M., 1986. Observations of local wind effects on longshore currents. Coastal Engineering, 10: 275-288.

Hunter, R., E., Clifton, H.E. and Phillips, R.L., 1979. Depositional processes, sedimentary structures, and predicted vertical sequences in barred nearshore systems, southern Oregon coast. Journal of Sedimentary Petrology, 49(3): 711-726.

Jette, C.D. and Hanes, D.M., 1997. High-resolution seabed imaging: an acoustic multiple transducer array. Measurement Science and Technology, 8: 787-792.

Larson, M. and Kraus, N.C., 1994. Temporal and spatial scales of beach profile change, Duck, North Carolina. Marine Geology, 117: 75-94.

Lee, G., Nicholls, R.J. and Birkemeier, W.A., 1998. Storm-driven variability of the beach-nearshore profile at Duck, North Carolina, USA, 1981-1991. Marine Geology, 148: 163-177.

Leffler, M.W., Baron, C.F., Scarborough, B.L., Hathaway, K.K. and Hayes, R.T., 1993. Annual data summary for 1991, CERC Field Research Facility. Tech. Rep. CERC-93-3, U.S. Army Corps of Engineers, Waterways Experiment Station, Vicksburg, MS.

Lippmann, T.C. and Holman, R.A., 1990. The spatial and temporal variability of sand bar morphology. Journal of Geophysical Research, 95(C7): 11575-11590.

List, J.H. and Farris, A.S., 1999. Large scale shoreline response to storms and fair weather, Coastal Sediments '99. ASCE Press, Long Island, NY.

Longuet-Higgins, M.S. and Stewart, R.W., 1964. Radiation stresses in water waves; a physical discussion, with applications. Deep-Sea Research, 11: 529-562.

Lyne, V.D., Butman, B. and Grant, W.D., 1990. Sediment movement along the U.S. east coast continental shelf- I. Estimates of bottom stress using the Grant-Madsen model and near-bottom wave and current measurements. Continental Shelf Research, 10(5): 397-428.

Maa, J.P.-Y., Lee, C.-H. and Chen, F.J., 1995. Bed shear stress measurements for VIMS Sea Carousel. Marine Geology, 129: 129-136.

Madsen, O.S., Wright, L.D., Boon, J.D. and Chisholm, T.A., 1993. Wind stress, bed roughness, and sediment suspension on the inner shelf during an extreme storm event. Continental Shelf Research, 13(11): 1303-1324.

Meisburger, E.P. and Judge, C., 1989. Physiographic and geologic setting of the Coastal Engineering Research Center's Field Research Facility. CERC-89-9, US Army Corps of Engineers, Waterways Experiment Station, Vicksburg, MS.

Morton, R.A., 1988. Nearshore responses to great storms. In: H.E. Clifton (Editor), Sedimentologic consequences of convulsive geologic events. Geological Society of America, Orlando, FL, pp. 7-22.

Myrow, P.M. and Southard, J.B., 1991. Combined-flow model for vertical stratification sequences in shallow marine storm-deposited beds. Journal of Sedimentary Petrology, 61(2): 202-210.

Nicholls, R.J., Birkemeier, W.A. and Lee, G., 1998. Evaluation of depth of closure using data from Duck, NC. Marine Geology, 148: 179-201.

Osborne, P.D. and Vincent, C.E., 1996. Vertical and horizontal structure in suspended sand concentrations and wave-induced fluxes over bedforms. Marine Geology, 131(3-4): 195-208.

Pilkey, O.H. et al., 1993. The concept of shoreface profile of equilibrium: A critical review. Journal of Coastal Research, 9(1): 255-278.

Reineck, H.-E. and Singh, I.B., 1980. Depositional Sedimentary Environments. Springer-Verlag, Berlin, 551 pp.

Rice, T.M., Beavers, R.L. and Snyder, S.W., 1998. Preliminary geologic framework of the inner continental shelf offshore Duck, North Carolina, USA. Journal of Coastal Research, SI(26): 219-225.

Riggs, S.R., Cleary, W., J. and Snyder, S.W., 1995. Influence of inherited geologic framework on barrier shoreface morphology and dynamics. Marine Geology, 126: 213-234.

Riggs, S.R., York, L.L., Wehmiller, J.F. and Snyder, S.W., 1992. Depositional patterns resulting from high-frequency Quaternary sea-level fluctuations in northeastern North Carolina. In: C.H. Fletcher and J.F. Wehmiller (Editors), Quaternary Coasts of the United States. SEPM (Society for Sedimentary Geology), pp. 141-154.

Roelvink, J.A. and Stive, M.J.F., 1989. Bar generating cross-shore flow mechanisms on a beach. Journal of Geophysical Research, 94(C4): 4785-4800.

Sallenger, A.H., Jr. and Holman, R.A., 1985. Wave energy saturation on a natural beach of variable slope. Journal of Geophysical Research, 90(C6): 11939-11944.

Schwartz, R.K., Cooper, D.W. and Etheridge, P.H., 1997. Sedimentologic architecture of the shoreface prism, relationship to profile dynamics, and relevance to engineering concerns: Duck, North Carolina. Technical Report CHL-97-19, U.S. Army Corps of Engineers.

Sherman, D.J. and Greenwood, B., 1984. Boundary roughness and bedforms in the surf zone. Marine Geology, 60: 199-218.

Smith, J.B., Drake, T.G., Gallagher, E.L. and Elgar, S., 1995. Do detailed hydrodynamic and sedimentologic data aid prediction of nearshore stratigraphy?, Geological Society of America Abstracts with Programs, pp. 79.

Stive, M.J.F. and Wind, H.G., 1986. Cross-shore mean flow in the surf zone. Coastal Engineering, 19: 325-340.

Thornton, E.B. and Guza, R.T., 1983. Transformation of wave height distribution. Journal of Geophysical Research, 88(C10): 5925-5938.

Thornton, E.B. and Guza, R.T., 1986. Surf zone longshore currents and random waves: field data and models. Journal of Physical Oceanography, 16(7): 1165-1178.

Thornton, E.B., Humiston, R.T. and Birkemeier, W., 1996. Bar/trough generation on a natural beach. Journal of Geophysical Research, 101(C5): 12097-12110.

Thornton, E.B., Swayne, J.L. and Dingler, J.R., 1998. Small-scale morphology across the surf zone. Marine Geology, 145: 173-196.

Trowbridge, J. and Young, D., 1989. Sand transport by unbroken water waves under sheet flow conditions. Journal of Geophysical Research, 94(C8): 10971-10991.

Trowbridge, J.H. and Agrawal, Y.C., 1995. Glimpses of a wave boundary layer. Journal of Geophysical Research, 100(C10): 20729-20743.

Vincent, C.E. and Downing, A., 1994. Variability of suspended sand concentrations, transport and eddy diffusivity under non-breaking waves on the shoreface. Continental Shelf Research, 14(2-3): 223-250.

Vincent, C.E., Hanes, D.M. and Bowen, A.J., 1991. Acoustic measurements of suspended sand on the shoreface, and the control of concentration by bed roughness. Marine Geology, 96: 1-18.

Whitford, D.J. and Thornton, E.B., 1993. Comparison of wind and wave forcing of longshore currents. Continental Shelf Research, 13(11): 1205-1218.

Wiberg, P. and Smith, J.D., 1983. A comparison of field data and theoretical models for wave-current interactions at the bed on the continental shelf. Continental Shelf Research, 2(2-3): 147-162.

Wiberg, P.L. and Harris, C.K., 1994. Ripple geometry in wave-dominated environments. Journal of Geophysical Research, 99(C1): 775-789.

Wright, L.D., 1995. Morphodynamics of Inner Continental Shelves. CRC Press, Boca Raton, FL, 241 pp.

Wright, L.D., Boon, J.D., III, Green, M.O. and List, J.H., 1986. Response of the mid shoreface of the southern Mid Atlantic Bight to a "Northeaster". Geo-Marine Letters, 6: 153-160.

Wright, L.D., Boon, J.D., Kim, S.C. and List, J.H., 1991. Modes of cross-shore sediment transport on the shoreface of the Middle Atlantic Bight. Marine Geology, 96: 19-51.

Wright, L.D., Madsen, O.S., Chisholm, T.A. and Xu, J.P., 1994a. Inner continental shelf transport processes: the Middle Atlantic Bight, Coastal Dynamics'94. Waterways, Port, Coastal and Ocean Division, ASCE, Barcelona, Spain, pp. 867-878.

Wright, L.D., Xu, J.P. and Madsen, O.S., 1994b. Across-shelf benthic transports on the inner shelf of the Middle Atlantic Bight during the "Halloween storm" of 1991. Marine Geology, 118: 61-77.